Chapter

4

Dielectric Relaxation Study of Binary Mixtures (n-Hexanol+ N, N-Dimethylformamide)

Contents

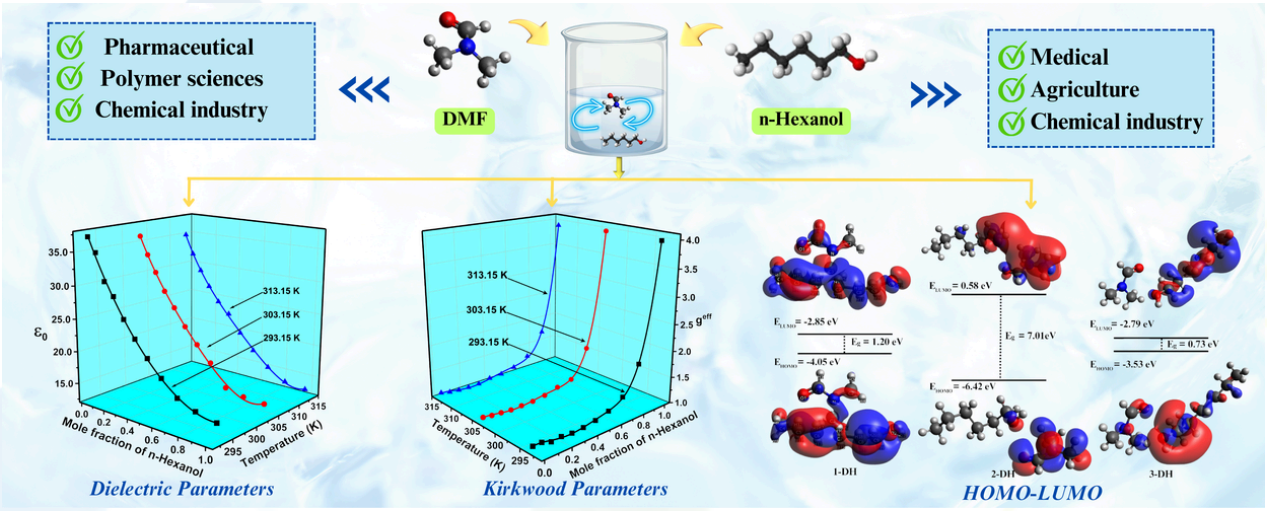

4.1 Introduction

In order to probe the intermolecular structures of liquid mixtures and investigate their molecular dynamics, dielectric spectroscopy is a powerful technique widely used in the field. The dielectric spectroscopy involves analysis of the complex permittivity spectra measured by varying the frequencies of the electrical signals at varying temperatures or at a fixed temperature [1]. The dynamic electric and dielectric behaviour of molecules present within a weakly conducting dipolar liquid system are easily studied using this experimental method. It has been a difficult task to study the dielectric properties of conducting materials for the research community. Some special technical measures need to be taken for getting reliable data from the experiments in such cases [2]. Various investigations on weakly conducting dipolar solvents have concluded that these solvents can be thermally activated through ionic impurities. However, this phenomenon is observed only at frequencies lower than that of the molecular reorientation relaxation frequency, usually lying below the microwave region [2–6]. In recent years, there has been a tremendous attention from the scientific community towards dielectric relaxation spectroscopy (DRS) studies on the dipolar liquids within static permittivity region, encompassing frequencies from a few Hertz to a few megahertz [2, 7–10]. Within this region, dielectric relaxation resulting due to dipolar rotation of molecules is absent, and the relaxation mechanism is mainly governed by the electrode polarization and ionic conductivity processes. In this frequency range, the polar liquids exhibit changes in their dielectric properties due to the ionic conduction processes and the electrode polarization. These changes are the result of the volatile ionic impurities or added ions in the liquid mixtures. Several researchers have concluded that even in their pure forms, highly polar liquids show presence of these impurities [7, 9, 11–13]. The combined effects of ionic conduction processes and electrode polarization (EP) shape the dielectric spectrum of polar liquids in the lower-middle frequency regions. The values of the complex dielectric function of such liquids are determined on these two phenomena [2, 14]. Due to the accumulation of ions at the interface between the electrode and dielectric, electric double layer (EDL) is formed resulting in the electrode polarization (EP). On the other hand, the transition from the direct current (DC) to alternating current (AC) for the transportation of the ions in the liquids results in the well-known ionic conduction process [4, 5, 14]. Moreover, the thickness (Debye length) of the ion layer at the

electrode surface can be determined from the low-frequency complex permittivity data which is often influenced by electrode polarization [2, 10].

Alcohols and amides are the center of interest among the protic and aprotic solvents. Due to their ability of forming hydrogen bonds, the alcohols play a crucial role in all the scientific felds such as chemistry and biology. Alcohols, which are self-associated liquids, constitute a three-dimensional network of hydrogen bond due to which they can interact with other chemical groups having some degree of polar attractions. Hence, alcohols have demanded a noteworthy attention from many researchers due to its complex and interesting nature [1, 15–17]. Within the chemical industry, amides are an important class of solvents owing to their high polarity and strong solvating power. Because of its long-chained molecule and its wide use in petrochemical, agricultural and pharmaceutical industries [18], we have chosen n-Hexanol as one of the components of the binary liquid system to be investigated. The other component of the binary liquid mixture is DMF belonging to the amide group. A considerable interest has been subjected towards the study of various properties of DMF due to its association to the proteins and peptides [19-21].

Broad-frequency and temperature-dependent complex permittivity spectra (CPS) measurements are crucial for various engineering applications [22,23]. Studies on low-frequency dielectric dispersion in liquids offer detailed insights into charge dynamics and electrical conduction mechanisms, which are closely related to dielectric polarization strength and molecular structure [24]. In this chapter, dielectric and electrical properties of the binary mixtures of n-Hexanol and N, N-Dimethylformamide have been studied in the frequency range 20 Hz to 2 MHz at various temperature. Different electrical parameters such as electrical modulus (M*(f)), electrical conductivity (σ*(f)) and complex impedance (Z*(f)) were derived from the complex permittivity spectra (ε*(f)). Ionic polarization relaxation time (τ_σ) and DC conductivity (σ_{dc}) were calculated from different dielectric and electrical formalism.

Complex permittivity spectra for binary mixtures of n-Hexanol, N, N-Dimethylformamide (DMF) with varying concentrations (0.0 → 1.0) were also obtained in the higher frequency range of 200 MHz to 20 GHz. Dielectric relaxation studies on binary mixtures of polar molecules across different compositions aid in developing accurate models for liquid relaxation and provide valuable insights into relaxation processes within these mixtures [25]. The microwave frequency dependence

of the complex permittivity for many polar liquids is commonly described by the Debye equation [22,26]. However, some liquids show an experimental broadening in their dielectric response over the frequency domain that the single-relaxation-time Debye (DB) model cannot fully capture. To address this, empirical modifications such as the Cole–Cole (CC) and Cole–Davidson (CD) expressions are often used, as they account for a distribution of relaxation processes within the material [22,27-28]. These models are widely applied to identify mechanisms of dielectric relaxation [29]. In this study, the frequency dependence of the complex permittivity for binary mixtures of n-Hexanol and DMF was analyzed using the Debye (DB), Cole-Cole (CC), and Cole-Davidson (CD) dielectric models through complex nonlinear least squares (CNLS) fitting techniques. Comparing the dielectric spectra from each model enabled the identification of the best-fit relaxation model and allowed for the derivation of key dielectric relaxation parameters, such as dielectric strength ($\Delta\varepsilon$), dielectric relaxation time (τd), and distribution parameters for relaxation processes within the mixtures. A detailed comparison of the dielectric spectra from each model determined the best-fit relaxation model for evaluating dielectric parameters, including the static dielectric permittivity (ε_0) and permittivity at optical frequency (ε_∞) for studied binary mixtures (n-Hexanol +DMF) at various temperatures. From these values, the excess static permittivity $(\varepsilon_0)^E$ and excess permittivity at optical frequency $(\varepsilon_\infty)^E$ were calculated and fitted to the Redlich-Kister equation. Effective correction factor (g^{eff}) and corrective correlation factor (g^f) were derived from the modified Kirkwood equation, while static permittivity data were fitted to the modified Bruggman equation to obtain the Bruggman factor (F_B). The variation in these parameters was analyzed in terms of molecular structure, intermolecular forces, and dipole-dipole interactions. Additionally, the relaxation times determined at different temperatures were used to calculate thermodynamic parameters, which were then interpreted based on the molecular hindrance forces and the orientational behavior of molecules within the liquid mixtures.

4.2 Materials, Experimental Details

n-Hexanol and N, N-Dimethylformamide (DMF) of analytical reagent (AR) grade were procured from Loba Chemie (India) and utilized without any further purification. Binary mixtures of this system (n-Hexanol+DMF) were prepared at eleven different concentrations based on volume fraction (0.0→1.0). These volume fractions were then converted into the mole fraction of n-Hexanol using Equation (3.1) [30].

An Agilent E4980A precision LCR meter, along with a four-terminal liquid dielectric test fixture (Agilent 16452A), was used to measure capacitance and resistance in the frequency range of 20 Hz to 2 MHz with a standard uncertainty of 0.04 [31]. The test fixture was calibrated following standard procedures as described in reference [31].

For accurate complex permittivity measurements of the samples, a Vector Network Analyzer (VNA) (Anritsu model MS46322A) with a DAK-3.5 (SPEAG) open-ended dielectric probe was used, covering a frequency range of 200 MHz to 20 GHz. The SPEAG DAK software helped determine the complex permittivity values. The dielectric probe was calibrated with three standard materials - open, short, and load - using the steps described in reference [32]. Air, a copper strip, and distilled water served as the open, short, and load standards, respectively, ensuring accurate calibration and correction for signal reflections [32]. During measurements, the probe and cable were kept still to prevent any variations in signal phase and amplitude.

Measurements for capacitance and resistance were done from 20 Hz to 2 MHz, while complex permittivity measurements were performed from 200 MHz to 20 GHz. These tests were carried out at four temperatures (293.15, 303.15, and 313.15 K), with the sample temperatures controlled by a water bath accurate to ±0.1 K. The experimental values of static permittivity (ε_0) of both pure compounds (n-Hexanol and DMF) at different temperatures are tabulated in Table 4.1. In order to confirm the purity of compounds used in present investigation, the experimental values are compared with the literature values in the same table. The experimental values of ε_0 for pure compounds are found in good agreement with the literature value [20-21,33-36].

Table 4.1 Comparison of static permittivity (ε_0) of pure compounds (n-Hexanol and DMF) with literature data at different temperatures.

		Temperatures (K)		
Compounds	**Static Permittivity (ε_0)**	**293.15**	**303.15**	**313.15**
n-Hexanol	Experimental	14.64	14.10	13.27
	Literature	13.05 [33]	12.80 [34]	12.15 [35]
DMF	Experimental	37.00	36.22	34.75
	Literature	37.69 [36]	36.65 [20]	35.09 [21]

4.3 Results and Discussion

- The results and discussion section is organized into two main parts.
  - I. Dielectric spectroscopy in the lower Frequency Range 20 Hz to 2 MHz (Using LCR Study).
  - II. Dielectric relaxation spectroscopy in the Higher Frequency Range 200 MHz to 20 GHz (Using VNA Study).

4.3.1 Dielectric spectroscopy in the lower Frequency Range 20 Hz to 2 MHz.

4.3.1.1 Complex Dielectric Spectra

Figures 4.1 (A), (B) and (C) and 4.2(A), (B) and (C) present the real (ε') and imaginary (ε") parts of the complex dielectric function, ε*(f), plotted on a log-log scale, illustrating their dependence on frequency and concentration at various temperatures (293.15 K, 303.15 K, 313.15K). It can be seen from the figure 4.1 that the permittivity spectra ε′ are divided into two different regions (i) In terms higher frequency region (frequency independent plateau region) and (ii) lower frequency region (frequency dependent nonlinear region).

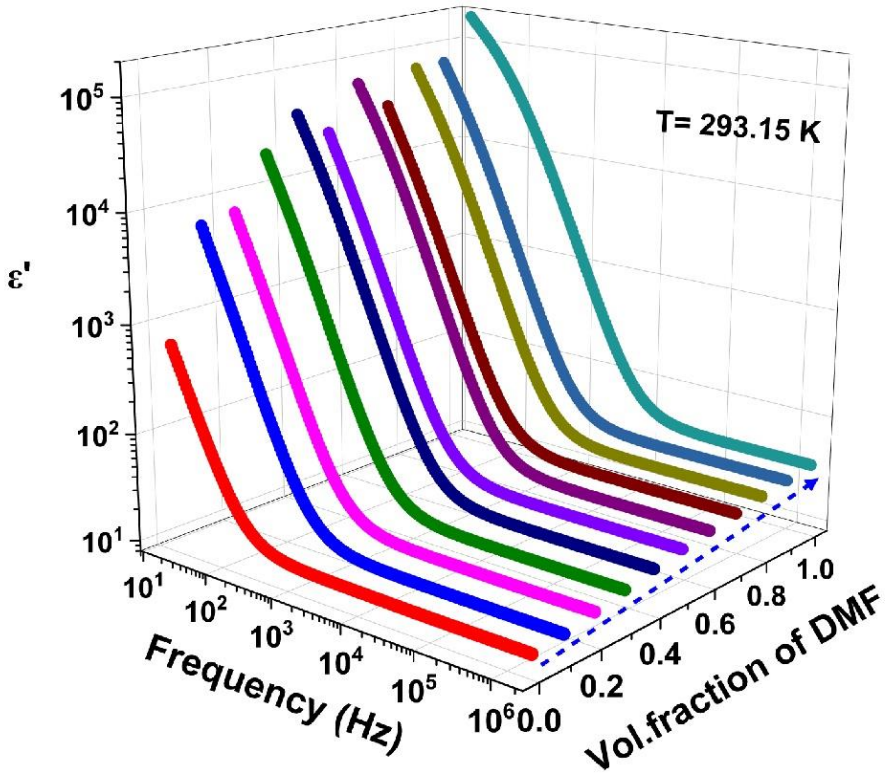

Fig. 4.1 (A) Plots of real part of complex dielectric permittivity (ε') as function of frequency and concentration of n-Hexanol in DMF at 293.15 K.

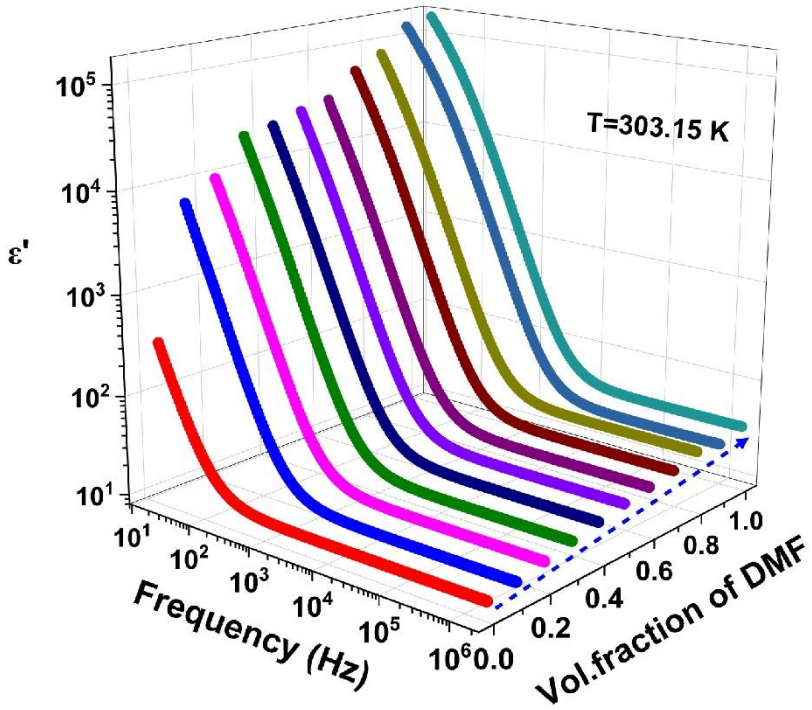

Fig. 4.1 (B) Plots of real part of complex dielectric permittivity (ε') as function of frequency and concentration of n-Hexanol in DMF at 303.15 K.

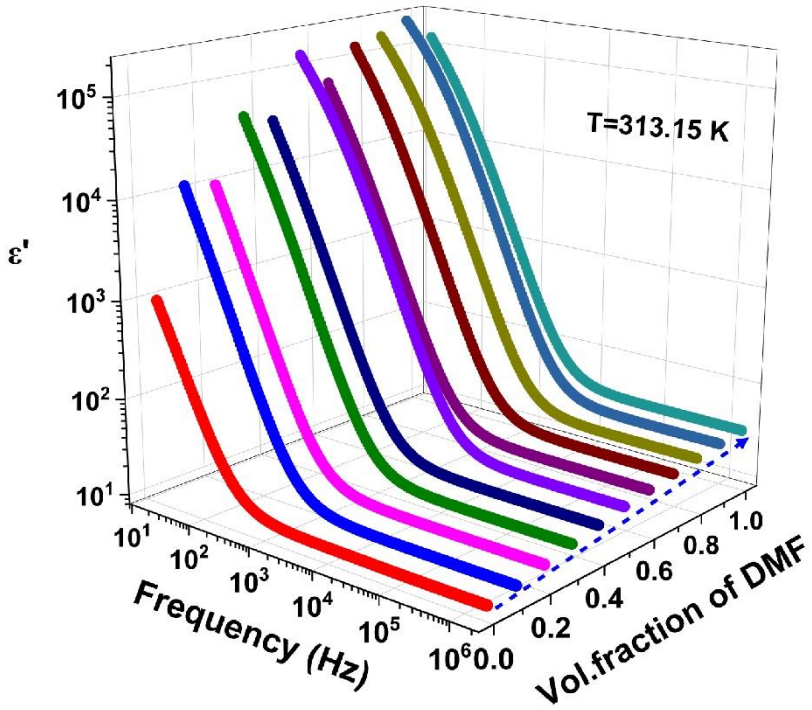

Fig. 4.1 (C) Plots of real part of complex dielectric permittivity (ε') as function of frequency and concentration of n-Hexanol in DMF at 313.15.

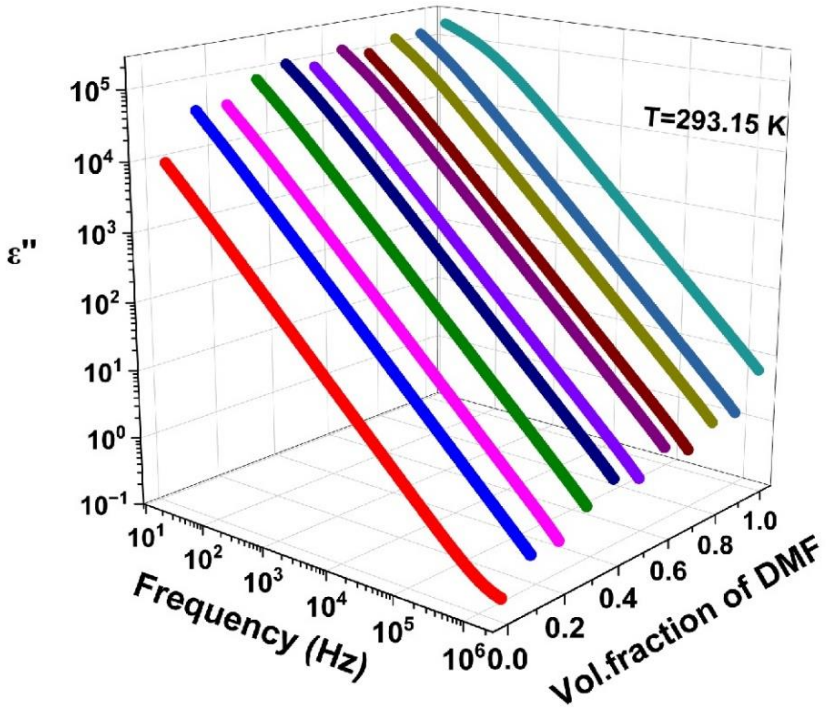

Fig. 4.2 (A) Plots of imaginary part of complex dielectric permittivity (ε") as function of frequency and concentration of n-Hexanol in DMF at 293.15 K.

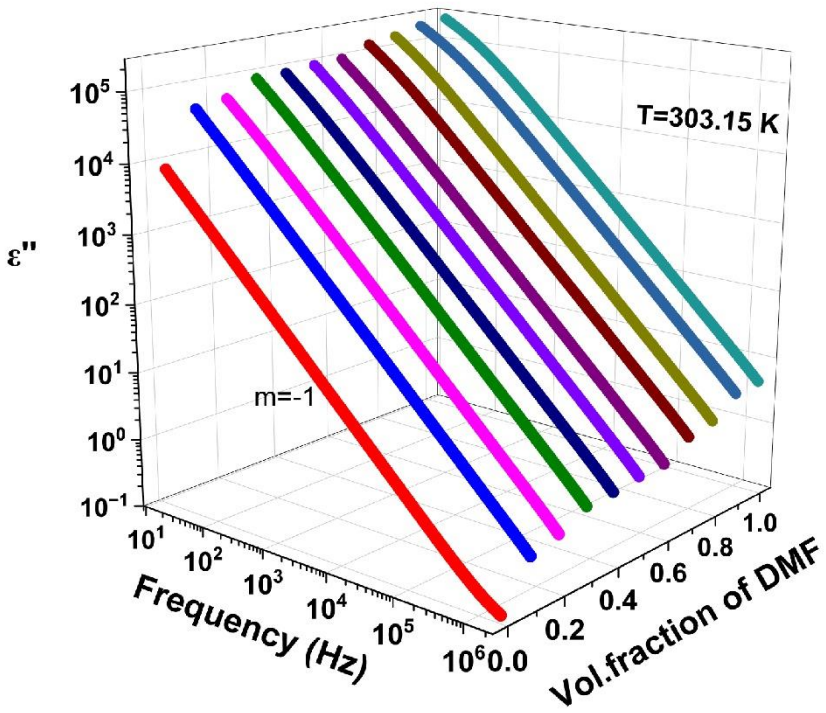

Fig. 4.2 (B) Plots of imaginary part of complex dielectric permittivity (ε") as function of frequency and concentration of n-Hexanol in DMF at 303.15 K.

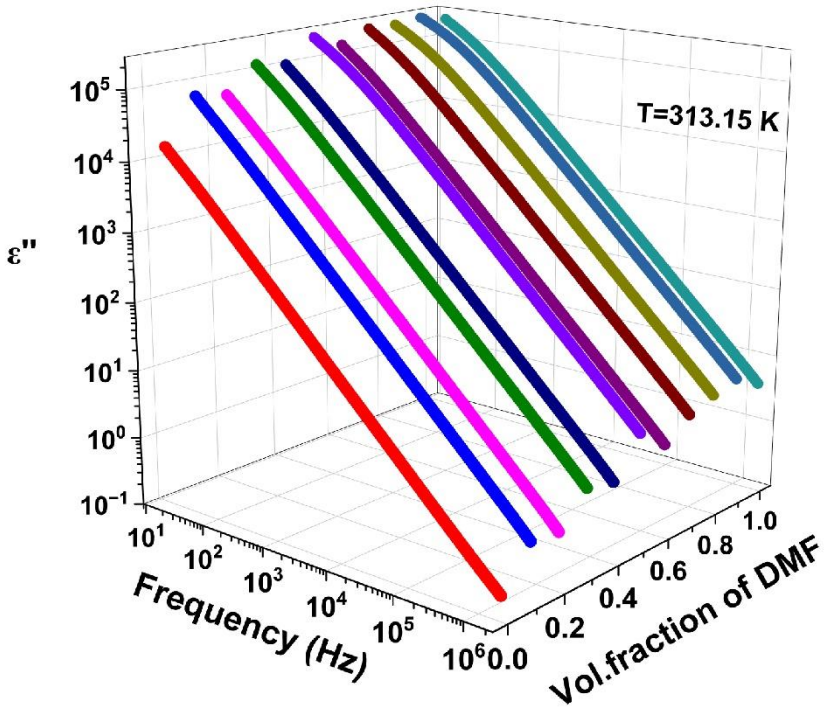

Fig. 4.2 (C) Plots of imaginary part of complex dielectric permittivity (ε'') as function of frequency and concentration of n-Hexanol in DMF at 313.15 K.

In the higher frequency region above 10^4 Hz, the real part of permittivity spectra is independent of the frequency, providing static value of dielectric constant. In the lower frequency region below 10^4 Hz, there is an observed increase in the real part (ε') value with an increase in the volume fraction of DMF with an increase in frequency. High values of real part of permittivity (ε') observed at low frequencies regions are attributed to the EP (electron polarization) effect [5]. In Fig. 4.1(A), (B) and (C) indicates that static permittivity (ε_0) rises with an increase in DMF concentration at different temperatures particularly at the spectral endpoints. At these frequencies, pure DMF exhibits a higher real part of the dielectric function ε' compared to pure n-Hexanol, pointing to an enhanced molecular polarization strength in the DMF system. In terms of variation in frequency: The value of ε′ is highest at the lowest frequency (20 Hz) and decreases rapidly with an increase in frequency. For higher frequencies (above a few tens of kHz), it remains constant for all mixtures. The significant increase in ε′values in the low-frequency regime is a result of the electrode polarization (EP) effect. This effect represents the formation of electric double layer (EDL) capacitance, where charges are trapped at the interface between the electrode and bulk material surfaces. When a DC electric field is applied, ions are distributed in a double layer. Under an AC field, the

ions in the material respond to changes at the electrodes, hindered by their drag force from the liquid medium. The EDL is sensitive to the frequency of the applied field because the oscillations at the electrodes can become faster than the ion movements. At high frequencies, the ions cannot move quickly enough to form the EDL, causing the ε′ values to stabilize, approaching the static permittivity (ε_0) [1]. The magnitude of the EP effect depends on the fractal structure of the electrode surface and the materials used to fabricate the electrodes [5]. Similar results were observed by Sengwa et al. [7] in the binary mixtures of formamide and 2-aminoethanol. The presence of ionic impurity charge carriers in the system is reflected in the imaginary part of the dielectric function (ε′′), which shows losses due to the ionic current induced by an applied electric field [37].

Figure 4.2 (A), (B) and (C) shows the imaginary part (ε") for varying volume fractions of DMF within the n-Hexanol mixtures which reveal a strikingly consistent linear frequency dependence on log-log scale, with a slope of -1.00 (±0.02) for all mixture concentrations (0.0→1.0) at different temperatures (293.15 K, 303.15 K and 313.15 K), in accordance with the equation $\varepsilon'' = \frac{\sigma_{dc}}{\omega\varepsilon_0}$. This logarithmic scale slope underscores the manifestation of an Ohmic-type ionic conduction mechanism intrinsic to these liquid dielectric mixtures. This empirical behavior aligns with established patterns observed in diverse dipolar liquids and their binary compositions [5]. Notably, the ε′′ values for n-HxOH-DMF mixtures, initially in the order of six logarithmic magnitudes at 20 Hz, exhibit a systematic linear decline with increasing frequency, suggesting an asymptotic approach to zero at higher frequencies, surpassing the experimental ceiling of 2 MHz at different temperatures. Very large values of imaginary part (ε") at low frequency is due to ionic conduction loss. The dielectric constant, dielectric loss values, and AC conductivity at 303.15 K for n-Hexanol and DMF at various frequency points are presented in Table 4.2. This outcome verifies that n-Hexanol possesses a higher concentration of ionic impurities compared to DMF.

Table 4.2 Values of dielectric constant (ε′), dielectric loss (ε″), and AC conductivity (σ′) of n-Hexanol and DMF at different frequencies at 303.15 K temperature.

Frequency (Hz)	n-Hexanol			DMF		
	(ε′)	(ε″)	(σ)	(ε′)	(ε″)	(σ)
20	3.50E+02	8.75E+03	9.73E-06	1.56E+05	2.26E+05	2.52E-04
100	3.49E+01	1.77E+03	9.84E-06	2.46E+04	7.96E+04	4.44E-04
1000	1.29E+01	1.78E+02	9.93E-06	5.59E+02	9.67E+03	5.39E-04
10 K	1.24E+01	1.80E+01	1.00E-05	4.39E+01	9.93E+02	5.53E-04
50 K	1.23E+01	3.61E+00	1.01E-05	3.65E+01	2.00E+02	5.57E-04
100 K	1.23E+01	1.82E+00	1.01E-05	3.62E+01	1.00E+02	5.59E-04
500 K	1.23E+01	3.80E-01	1.06E-05	3.61E+01	2.01E+01	5.60E-04
1 M	1.23E+01	2.08E-01	1.16E-05	3.61E+01	1.00E+01	5.60E-04
1.5 M	1.24E+01	1.50E-01	1.30E-05	3.61E+01	6.27E+00	5.54E-04
2 M	1.24E+01	1.31E-01	1.45E-05	3.62E+01	4.93E+00	5.48E-04

The experimentally obtained complex permittivity data in the frequency range (below 10^4 Hz) for the studied mixtures are influenced by the electrode polarization (EP) effect. To model this effect, we employed the Cole–Cole model [38] and utilized the Havriliak–Negami (HN) [39] equation, which is given by

$$\varepsilon^*(f) = \varepsilon_\infty + \frac{\Delta\varepsilon_{EP}}{[1+(i\omega\tau_{EP})^{\alpha}]^{\beta}} \quad (4.1)$$

Where $\Delta\varepsilon_{EP} = \varepsilon_{0(EP)} - \varepsilon_0$, $\varepsilon_0$is indicate the static dielectric constant, $\varepsilon_{0\,(EP)}$= low-frequency dielectric constant in the presence of EP and τ_{EP} = is the electrode polarization relaxation, α and β = the asymmetry and broadness parameters of the dielectric loss peaks. A complex nonlinear least squares (CNLS) fitting procedure, as outlined in reference [40], was performed to fit the experimental data to Equation (4.1). In this process, $\Delta\varepsilon_{EP}$, ε_0, and τ_{EP} were selected as the fitting parameters. The resulting plots of the complex dielectric spectra (ε*(f)) fitted to the Cole–Cole model (using Equation (4.1) with β=1) for a volume fraction of DMF at X_A = 0.5 at different temperatures, along with their corresponding experimental values, are presented in Figure 4.3 (A) (B) and (C). The Cole–Cole model shows excellent agreement with the experimental results. Similar fitting outcomes were achieved across the entire concentration range of $0.0 \leq X_A \leq 1.0$. The best-fit values of the fitting parameters for all concentrations (0.0→1.0) are summarized in Table 4.3, revealing that the static

permittivity increases with the rising volume fraction of DMF. Additionally, the electrode polarization relaxation time exhibits an anomalous variation with increasing concentration of the mixture at different temperatures.

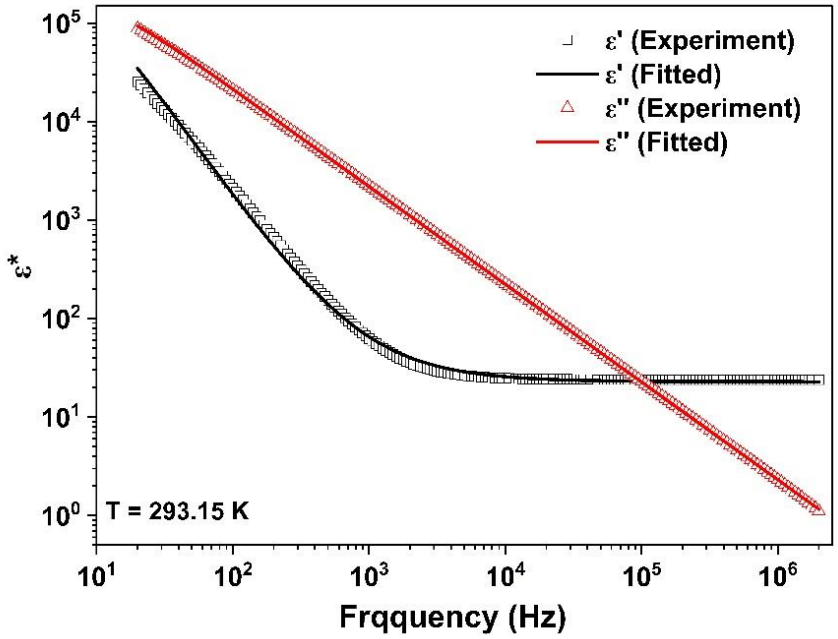

Fig. 4.3 (A) Shows the experimental and fitted complex dielectric function (ε*) data to the Cole–Cole model using CNLS for the concentration range (XA =0.5) at 293.15 K.

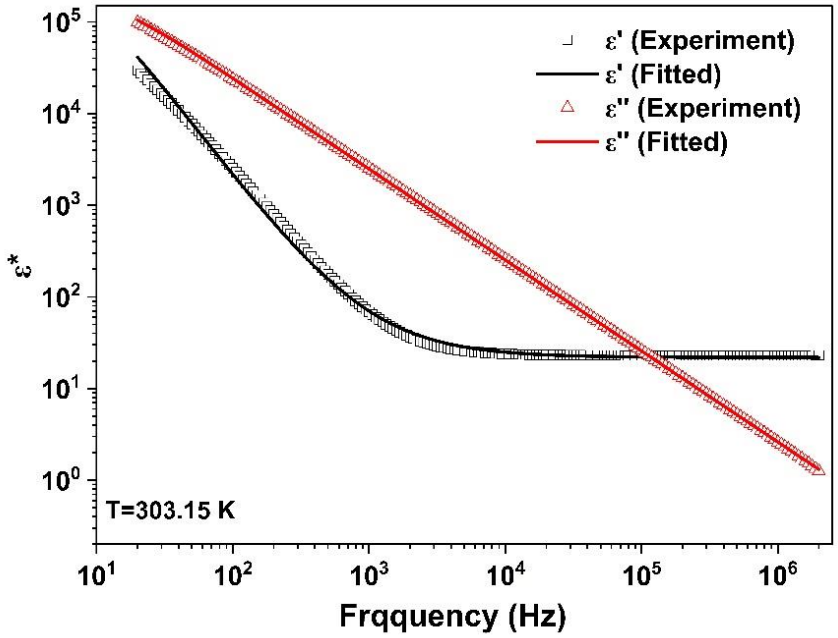

Fig. 4.3 (B) Shows the experimental and fitted complex dielectric function (ε*) data to the Cole–Cole model using CNLS for the concentration range (XA =0.5) at 303.15 K.

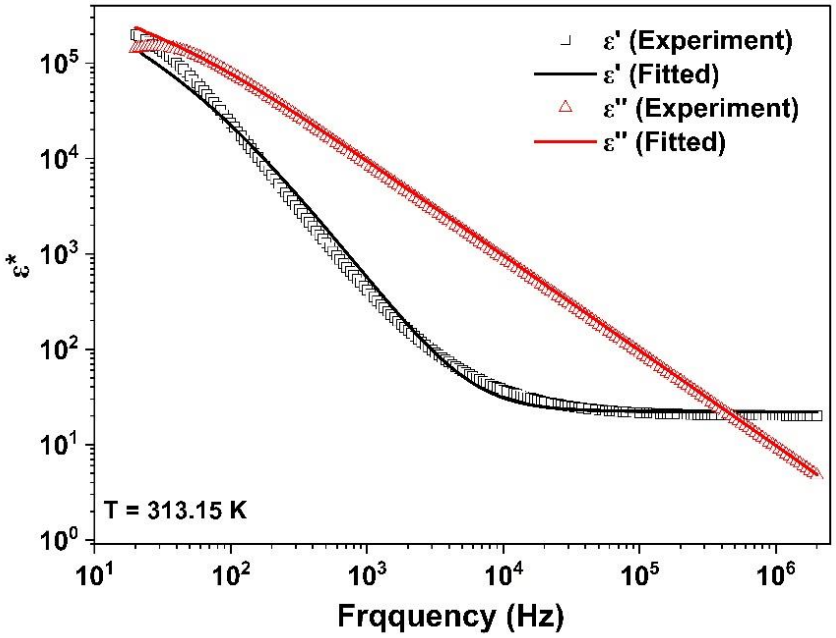

Fig. 4.3 (C) Shows the experimental and fitted complex dielectric function (ε*) data to the Cole–Cole model using CNLS for the concentration range (XA =0.5) at 313.15 K.

Table 4.3 Values of fitted parameters ε_0 (Static permittivity), $\Delta\varepsilon_{EP}$ (Relaxation strength), τ_{EP} (relaxation time), α (Shape parameter), τ'_{EP} (Electrode polarization relaxation time) ionic polarization relaxation time (τ_σ) and dc conductivity (σ_{dc}) for various concentration of DMF at different temperatures.

X_A	ε_0	$\Delta\varepsilon_{EP}$	τ_{EP} (ms)	α	τ'_{EP} (μS)	τ_σ (μS)	σ_{dc} (μS/m)
T=293.15 K							
0.0	13.05	1.86E+05	134.68	0.99	893.33	9.46	1.25E-05
0.1	13.87	2.79E+05	46.839	0.99	251.78	2.24	5.53E-05
0.2	15.63	2.56E+05	41.89	0.99	251.78	2.52	5.75E-05
0.3	17.79	2.96E+05	24.454	0.99	141.58	1.42	1.14E-04
0.4	19.99	2.92E+05	15.437	0.99	89.33	1.00	1.82E-04
0.5	22.81	2.96E+05	22.353	0.99	141.58	1.68	1.27E-04
0.6	24.86	2.54E+05	10.584	0.99	75.16	1.00	2.34E-04
0.7	27.57	2.72E+05	17.551	0.99	126.19	1.68	1.51E-04
0.8	30.07	2.65E+05	10.141	0.98	75.16	1.06	2.58E-04
0.9	32.75	2.69E+05	10.387	0.99	79.62	1.19	2.53E-04
1.0	34.24	2.21E+05	3.0096	0.98	25.18	0.45	7.41E-04

T=303.15 K							
0.0	12.20	2.53E+05	227.20	0.99	1415.83	10.62	1.01E-05
0.1	13.18	3.23E+05	50.65	0.99	266.69	2.00	5.87E-05
0.2	14.90	3.18E+05	39.24	0.99	199.99	1.78	7.73E-05
0.3	17.11	3.42E+05	26.38	0.99	141.58	1.26	1.23E-04
0.4	19.32	3.16E+05	23.55	0.99	133.66	1.42	1.29E-04
0.5	21.82	3.14E+05	20.90	0.98	126.19	1.42	1.45E-04
0.6	24.11	2.85E+05	18.46	0.98	119.13	1.50	1.49E-04
0.7	26.30	3.30E+05	13.26	0.99	79.62	1.00	2.45E-04
0.8	27.99	2.49E+05	4.90	0.99	75.16	1.00	2.94E-04
0.9	31.39	3.24E+05	10.83	0.98	35.56	0.53	5.14E-04
1.0	33.44	3.02E+05	53.72	0.99	39.90	0.56	5.59E-04
T=313.15 K							
0.0	11.23	3.34E+05	139.80	0.99	1716.39	12.15	2.28E-05
0.1	12.26	3.66E+05	38.82	0.99	456.68	3.42	8.78E-05
0.2	14.19	3.25E+05	39.18	0.99	542.76	4.57	7.81E-05
0.3	16.14	3.86E+05	18.24	0.99	228.88	2.04	2.25E-04
0.4	18.41	3.46E+05	20.20	0.99	288.14	2.88	1.65E-04
0.5	20.02	3.04E+05	5.71	0.98	81.21	0.97	5.40E-04
0.6	22.94	3.51E+05	13.44	0.99	203.99	2.29	5.27E-04
0.7	24.84	3.42E+05	7.10	0.99	108.29	1.36	4.79E-04
0.8	26.82	3.07E+05	5.04	0.98	86.02	1.08	6.37E-04
0.9	29.38	3.14E+05	3.99	0.98	72.38	0.97	7.88E-04
1.0	31.57	3.25E+05	7.01	0.98	121.51	1.72	4.79E-04

Figure 4.4 (A) (B) and (C) Shows the loss tangent (tan δ = ε''/ε') spectra at low frequencies serve as a useful tool for separating the dielectric properties of the bulk material from the frequency regime affected by electrode polarization (EP) [1,5,7,10]. The tanδ spectra has a peak value corresponding to the electrode polarization (EP) relaxation frequency f_{EP}. The tanδ plot of n-Hexanol, DMF, and n-Hexanol+DMF binary mixtures at different temperatures, illustrated in Figure 4.4, exhibit peaks in the frequency range approximately from 10^2 Hz to 10^4 Hz, representing the EP relaxation

process (EDL dynamics) at the frequency f_{EP}. The value of f_{EP} for n-Hexanol is found to be near 100 Hz, and it gradually shifts toward the higher frequency side with increasing DMF concentration in these binary mixtures. The electrode polarization relaxation time, τ'_{EP}, was calculated using the equation $\tau'_{EP} = (2\pi f'_{EP})^{-1}$, where f'_{EP} represents the electrode polarization relaxation frequency. Table 4.3 presents the electrode polarization relaxation time (τ'_{EP}) for all concentrations (0.0→1.0), revealing an unusual trend as n-Hexanol concentration increases in DMF. This relaxation time, τ'_{EP}, marks the onset of the electrode polarization effect and indicates the period required for charging or discharging the electric layer capacitance. This capacitance is linked to the dynamics of ion adsorption on the electrode surfaces under the influence of a varying electric field [41,42]. In the spectra, the loss tangent peak was observed to shift to higher frequencies, and the peak value of the loss tangent increased with rising temperature. Additionally, the values of τ'_{EP} in Table 4.3 exhibit anomalous behavior across the entire composition range (0.0→1.0) as temperature increases.

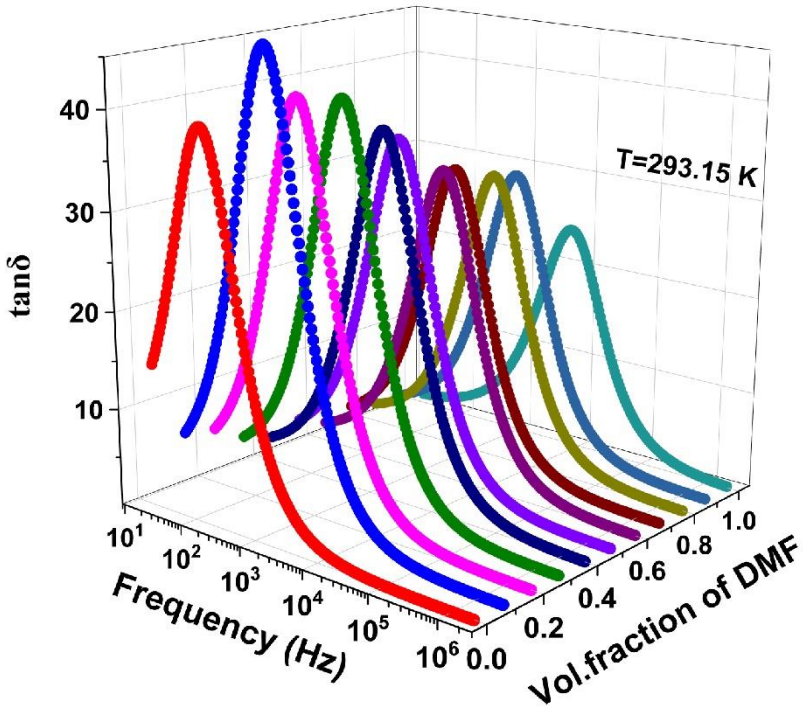

Fig. 4.4 (A) Frequency dependent response of tan δ against volume fraction of DMF at 293.15 K.

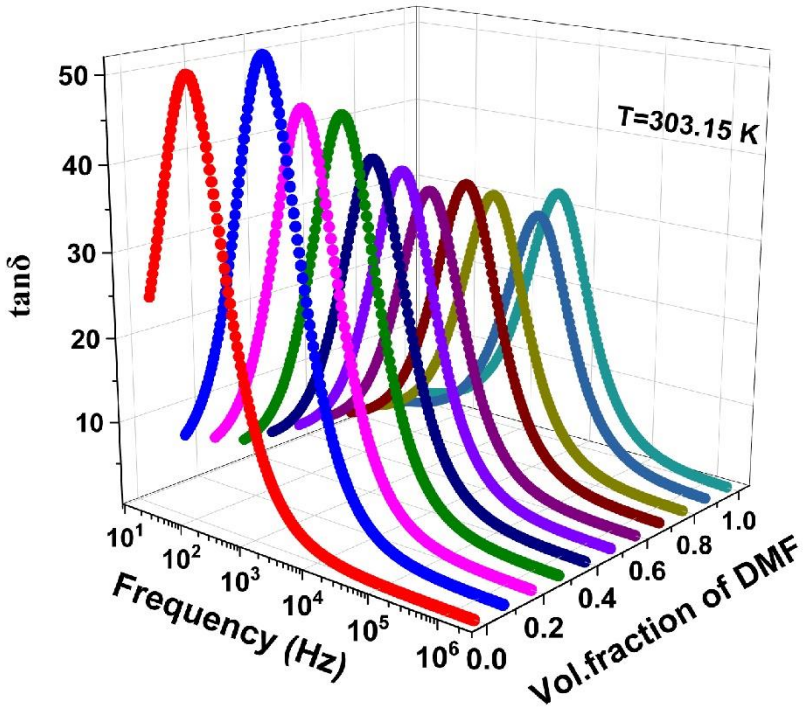

Fig. 4.4 (B) Frequency dependent response of tan δ against volume fraction of DMF at 303.15 K.

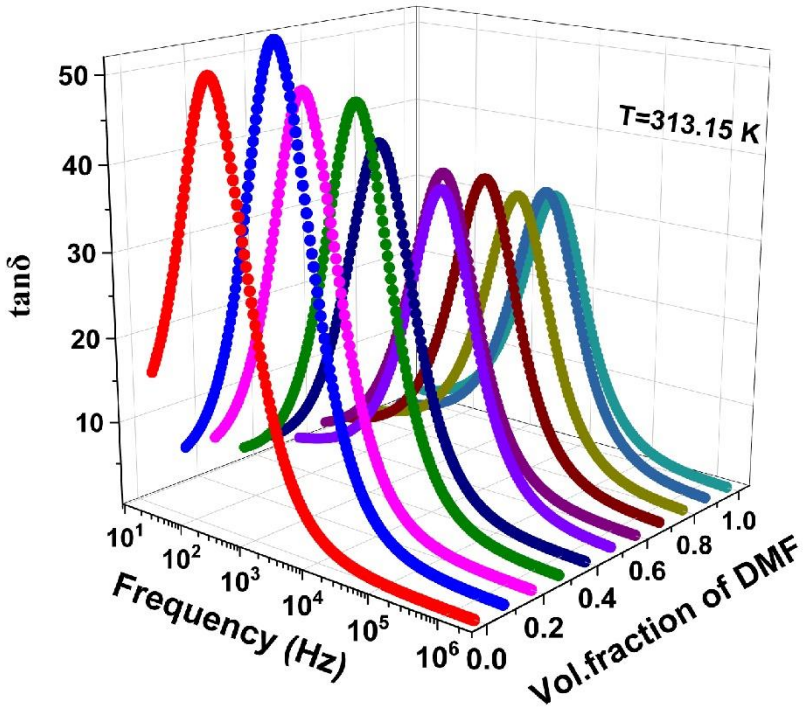

Fig. 4.4 (C) Frequency dependent response of tan δ against volume fraction of DMF at 313.15 K.

4.3.1.2 Complex Electric Modulus Spectra

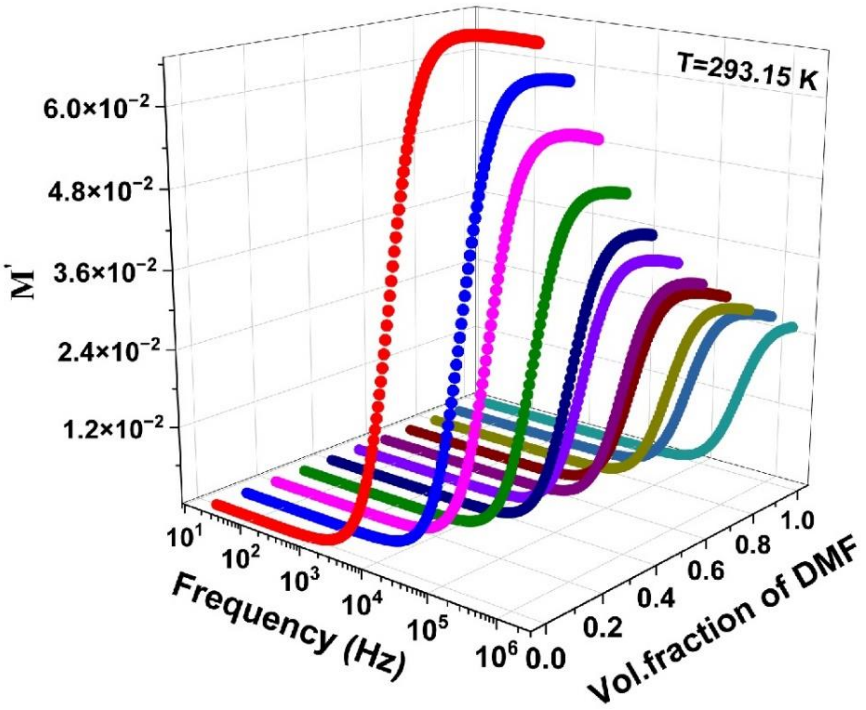

Fig. 4.5 (A) Frequency dependent response of real part of modulus (M′) against volume fraction of DMF at 293.15 K.

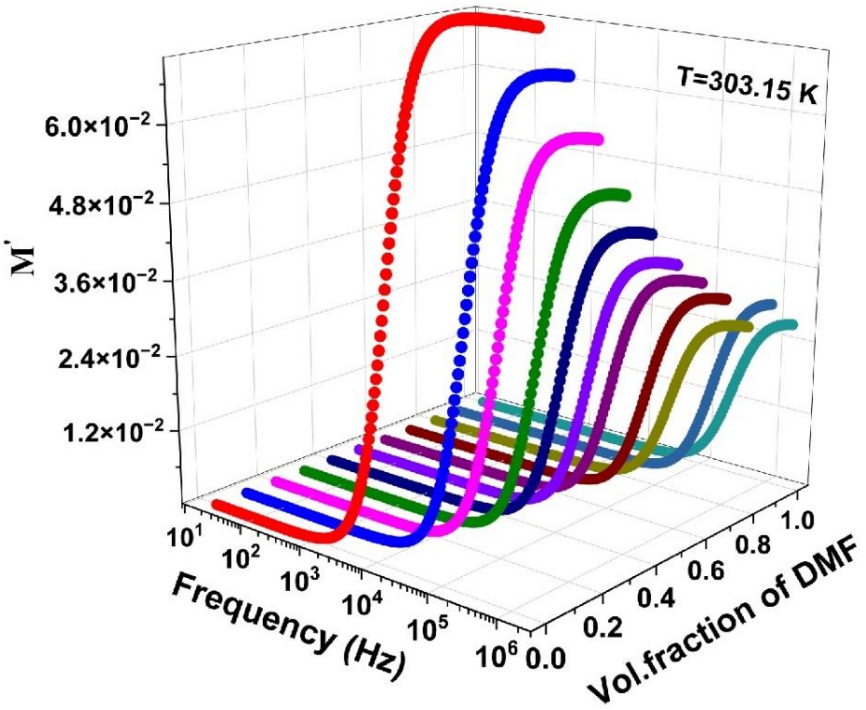

Fig. 4.5 (B) Frequency dependent response of real part of modulus (M′) against volume fraction of DMF at 303.15 K.

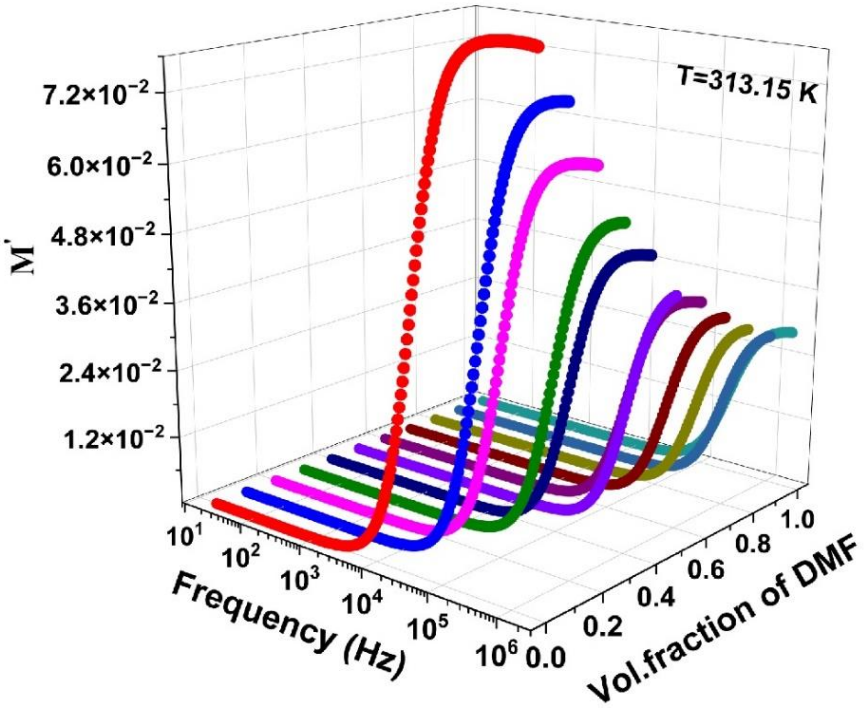

Fig. 4.5 (C) Frequency dependent response of real part of modulus (M′) against volume fraction of DMF at 313.15 K.

Converting dielectric spectra into electric modulus is a valuable approach for investigating the ionic conductivity relaxation mechanism within the bulk of binary mixtures. To validate the relaxation behavior of conductivity for any unidentified ionic impurities in the studied binary solution, electric modulus spectra were also examined. The frequency-dependent real (M') and imaginary (M") part of the electric modulus for the binary mixtures were calculated using Equation 3.7. The frequency and concentration-dependent real (M') and imaginary (M") components of the electric modulus spectra at different temperatures (293.15 K, 303.15 K and 313.15 k) are presented in Figures 4.5 (A) (B) and (C) and 4.6 (A) (B) and (C), respectively. Figure 4.5 represents 3D plot of the real part of complex electric modulus spectra for all mixtures across a range of frequencies at different temperatures. The values of M' over the EP-dominated low-frequency range (below 10^4 Hz) were found to be relatively small and nearly constant. This behavior is attributed to the suppression of high capacitance phenomena in the modulus formalism at these frequencies [10]. It has been observed that as the frequency range in which the ε' values gradually approach a steady state (as shown in Fig. 4.1), M' values exhibit dispersion. These spectra eventually reach a steady state in the higher frequency region [42,43]. In the higher frequency region, M' values exhibit an increase as the frequency increases with temperature increases. In

the mid-frequency region, for higher concentrations of DMF, the value of M' increases with an increase in frequency as temperature increases, approaching a constant level in the MHz range of frequency.

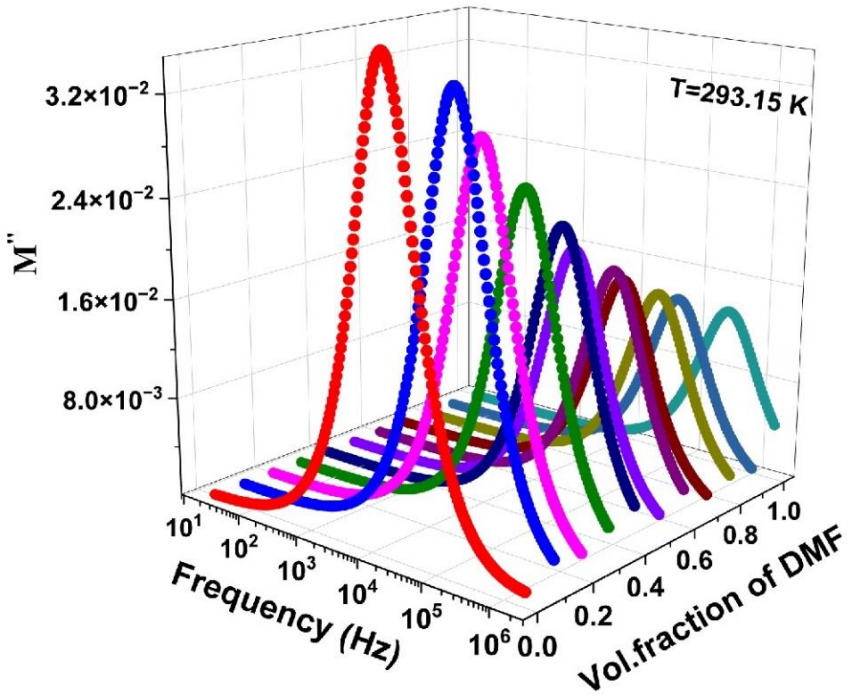

Fig. 4.6 (A) Frequency dependent response of Imaginary part of modulus (M′′) against volume fraction of DMF at 293.15 K.

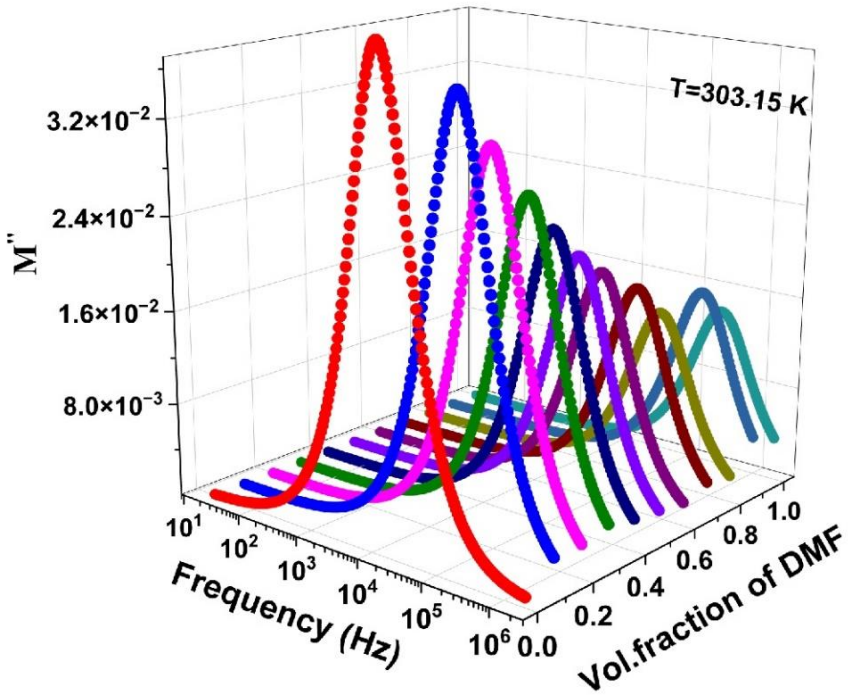

Fig. 4.6 (B) Frequency dependent response of Imaginary part of modulus (M′′) against volume fraction of DMF at 303.15 K.

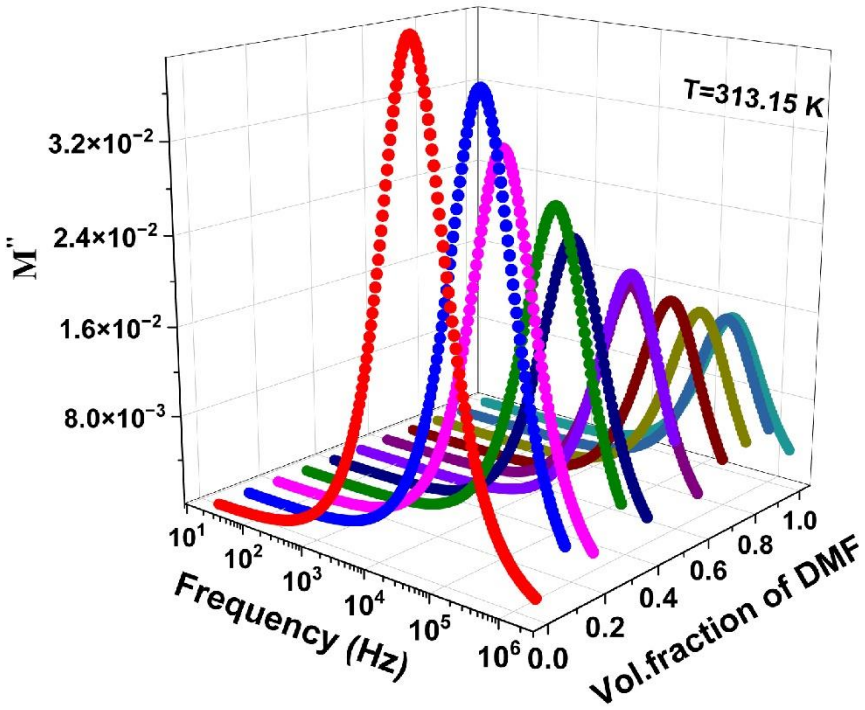

Fig. 4.6 (C) Frequency dependent response of Imaginary part of modulus (M′′) against volume fraction of DMF at 313.15 K.

Figure 4.6 (A) (B) and (C) depicts 3D plot of the M′′ for all mixtures across a range of frequencies at a different temperature. In case of higher temperature and mid concentration range of n-Hexanol in DMF, the ionic conductivity relaxation peak of M′′ spectra seem to appear above the upper limit of the experimental frequency range. The M′′ spectra exhibit dispersion in the frequency region between the frequencies f_{EP}' and fσ, which correspond to the tan δ peak and M" peak, respectively. A peak is observed for all the binary mixtures in the imaginary part of the electric modulus. The peak is observed in the higher frequency region for higher concentrations of DMF, and as the concentration of DMF decreases, the peak shifts towards lower frequencies as temperature increases. The frequency f_σ corresponding to the peak value of M" is related to the ionic conductivity relaxation time $\tau_\sigma = (2\pi f_\sigma)^{-1}$[42-44]. The values of the ionic conductivity relaxation time (τ_σ), for various concentrations are tabulated in Table 4.3. The M′′ peak value for pure n-Hexanol is significantly larger compared to its mixtures with DMF, which can be attributed to n-Hexanol lower static dielectric constant. As observed in the inset of the figure, the peak behavior in the M′′ spectra is reflected in the variation of the ionic conductivity relaxation time. At the studied temperature [293.15 K, 303.15 K and 313.15 K], an anomalous increase in the τ_σ value is observed with the increasing volume fraction of DMF. The ionic conductivity relaxation time of

pure n-Hexanol is substantially higher approximately 7.08 times greater at the studied temperature compared to pure DMF. This difference may be due to n-Hexanol's higher viscosity (4.12 mPa.s for n-Hexanol vs. 0.91 mPa.s for DMF at 313.15 K) and its larger molecular size relative to DMF. Furthermore, observed in table 4.3 concentration-dependent values of the ionic conductivity relaxation time (τ_σ) at different temperatures. The τ_σ values are two orders of magnitude lower than those of the electrode polarization relaxation time (τ_{EP}), suggesting that the electric double layer (EDL) relaxation process is considerably slower than the conductivity relaxation process [24]. The ionic conduction relaxation time (τ_σ) represents both charge carrier transport and localized molecular motions, both of which may contribute to the relaxation of the electric field [1].

Figure 4.7 (A) (B) and (C) illustrates the complex modulus plot (M′′ vs. M′) for mixtures of n-Hexanol and DMF at different temperatures, varying the volume fraction of DMF (0.0→1.0). The observed Debye-type behavior in the complex modulus plot indicates a characteristic relaxation process in the ionic conductivity [1].

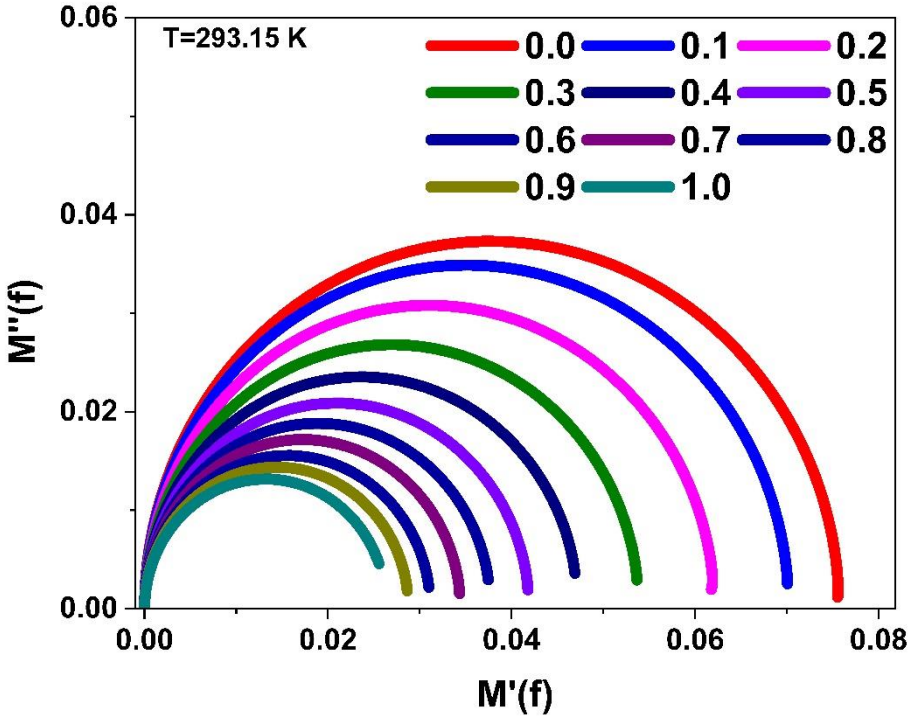

Fig. 4.7 (A) Complex electric modulus plane plots (M"(f) vs. M'(f)) for the binary mixtures of n-Hexanol and DMF at 293.15 K.

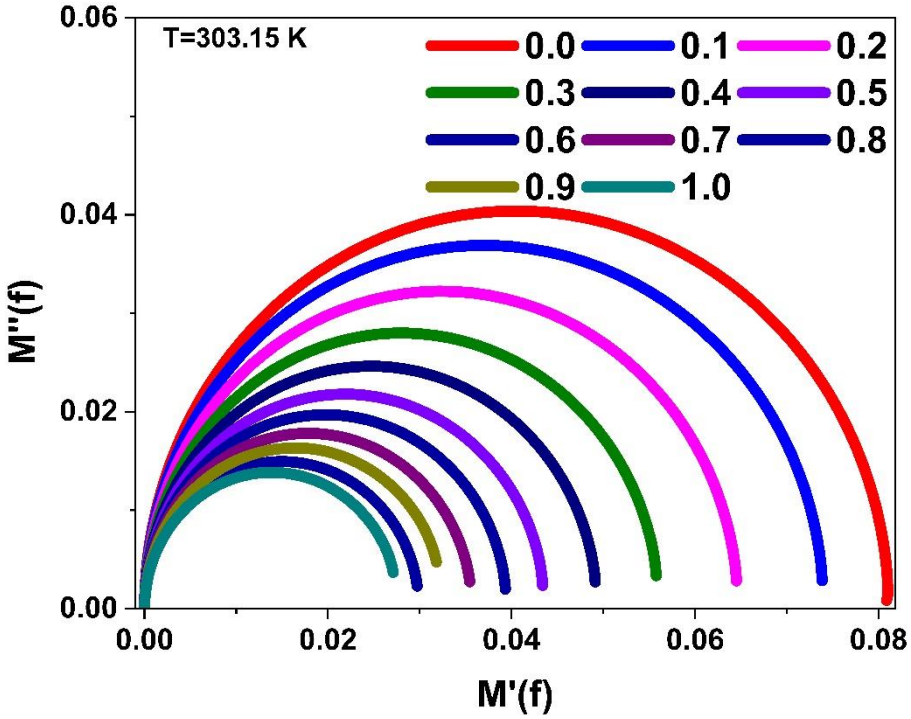

Fig. 4.7 (B) Complex electric modulus plane plots (M"(f) vs. M'(f)) for the binary mixtures of n-Hexanol and DMF at 303.15 K.

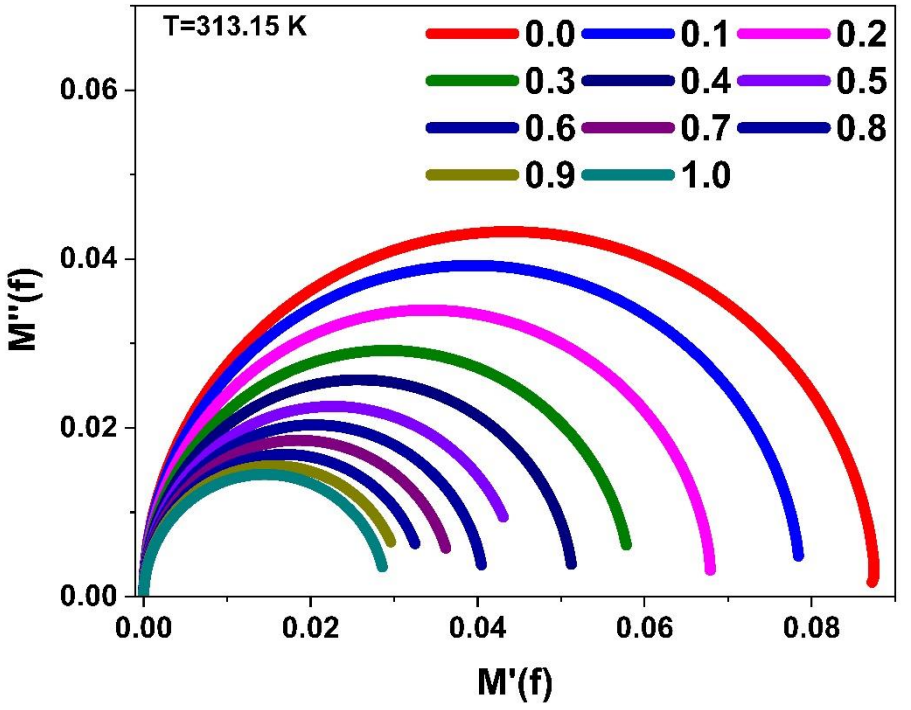

Fig. 4.7 (C) Complex electric modulus plane plots (M"(f) vs. M'(f)) for the binary mixtures of n-Hexanol and DMF at 313.15 K.

Furthermore, this behavior permits the scaling of the master curve for the electric modulus spectra in the binary system. The intercept of the M′′ versus M′ arc on the M′

axis, specifically on the higher frequency side, yields the value of static permittivity ($\varepsilon_0 = (M_\infty)^{-1}$). The determined values of the static permittivity of the mixture samples (n-Hexanol + DMF) obtained from the M″ versus M′ plots align with the static permittivity measured at a frequency of 2 MHz. The semicircular impedance plot for DMF is significantly smaller than that for n-Hexanol, reflecting their respective conductivity behaviors.

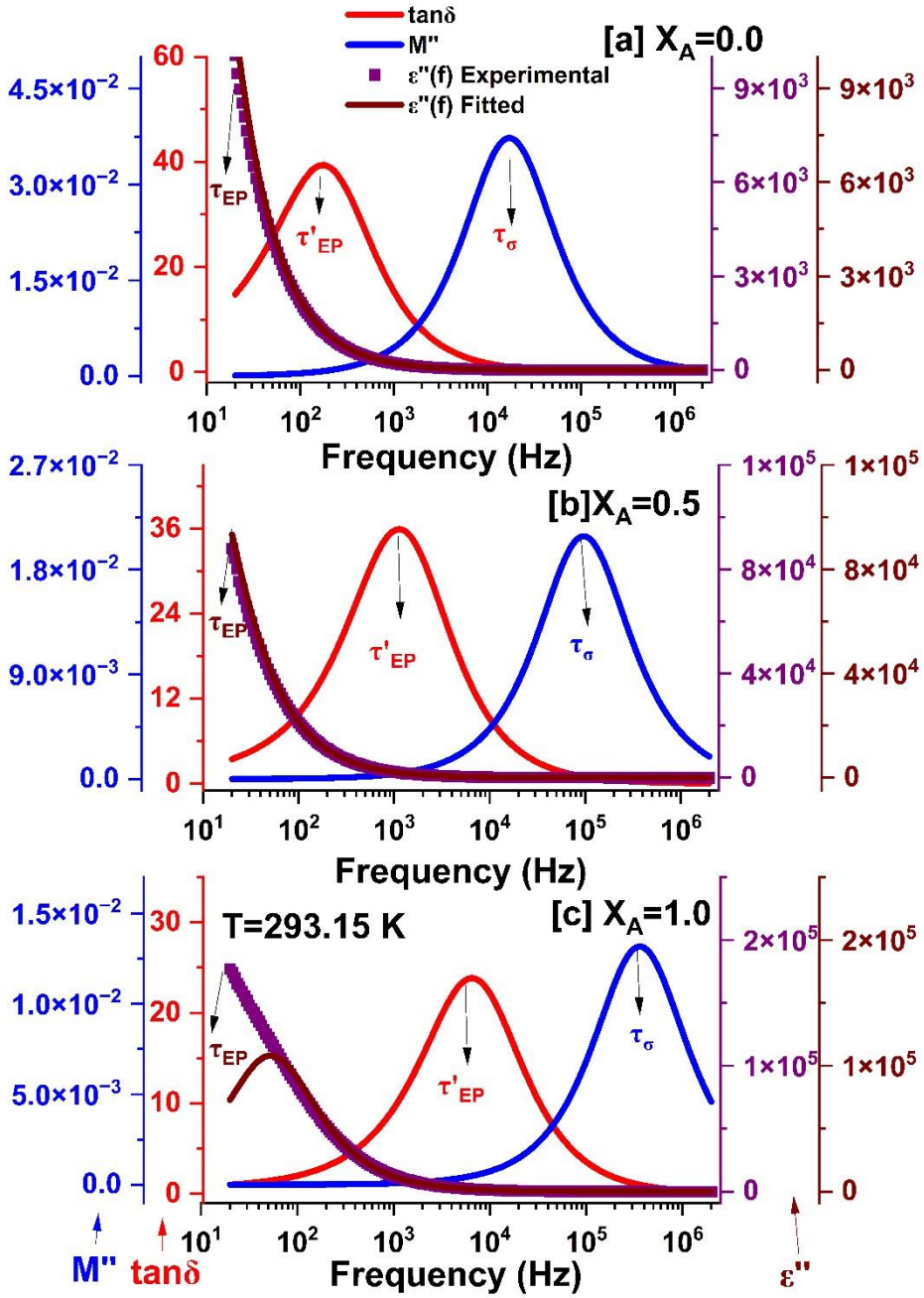

Fig.4.8. (A) Relationship between τ_{EP}, τ'_{EP} and τ_σ for X_A=0.0, X_A=0.5, and X_A=1.0 at 293.15 K.

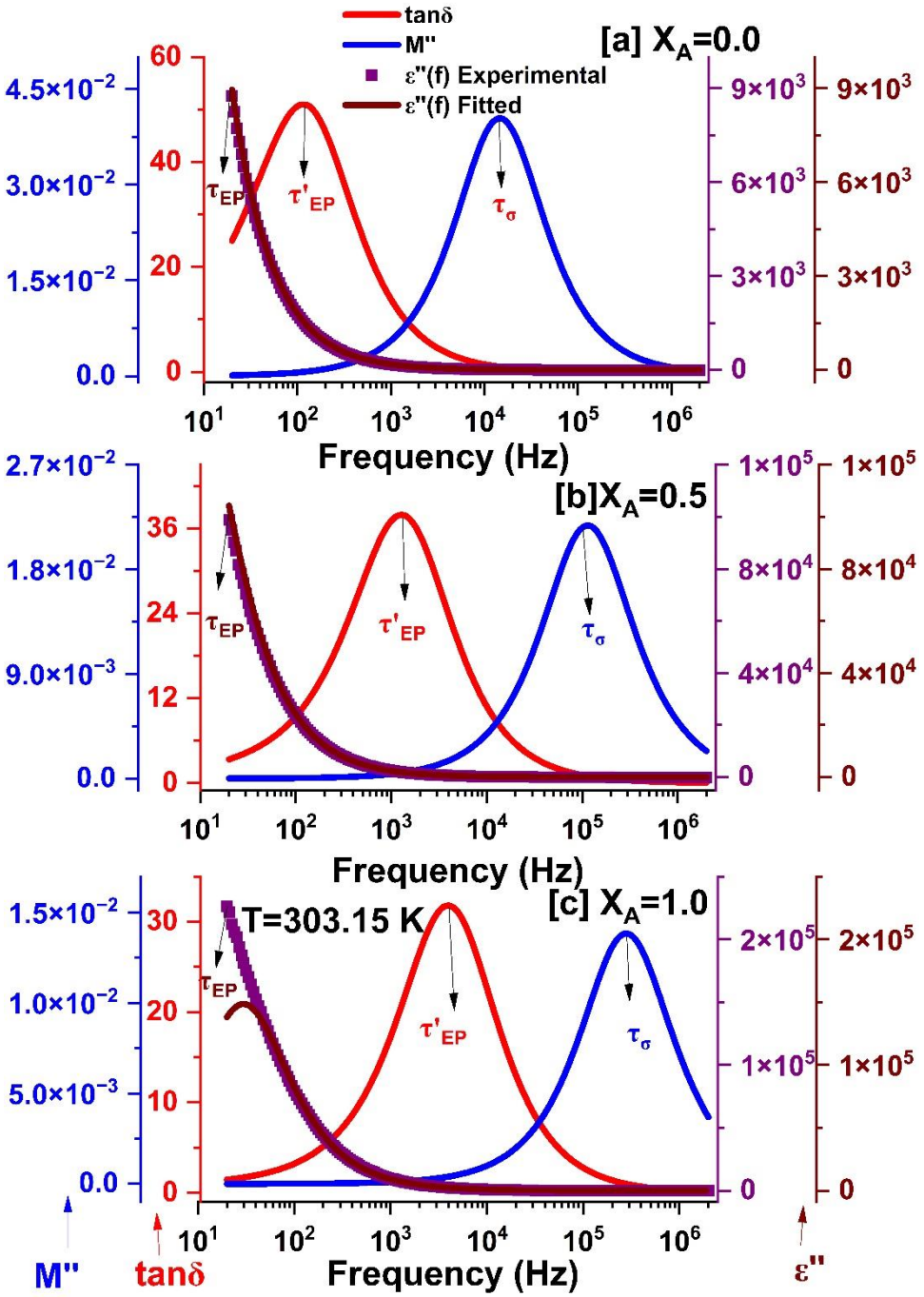

Fig.4.8. (B) Relationship between τ_{EP}, τ'_{EP} and τ_σ for for X_A=0.0, X_A=0.5, and X_A=1.0 at 303.15 K.

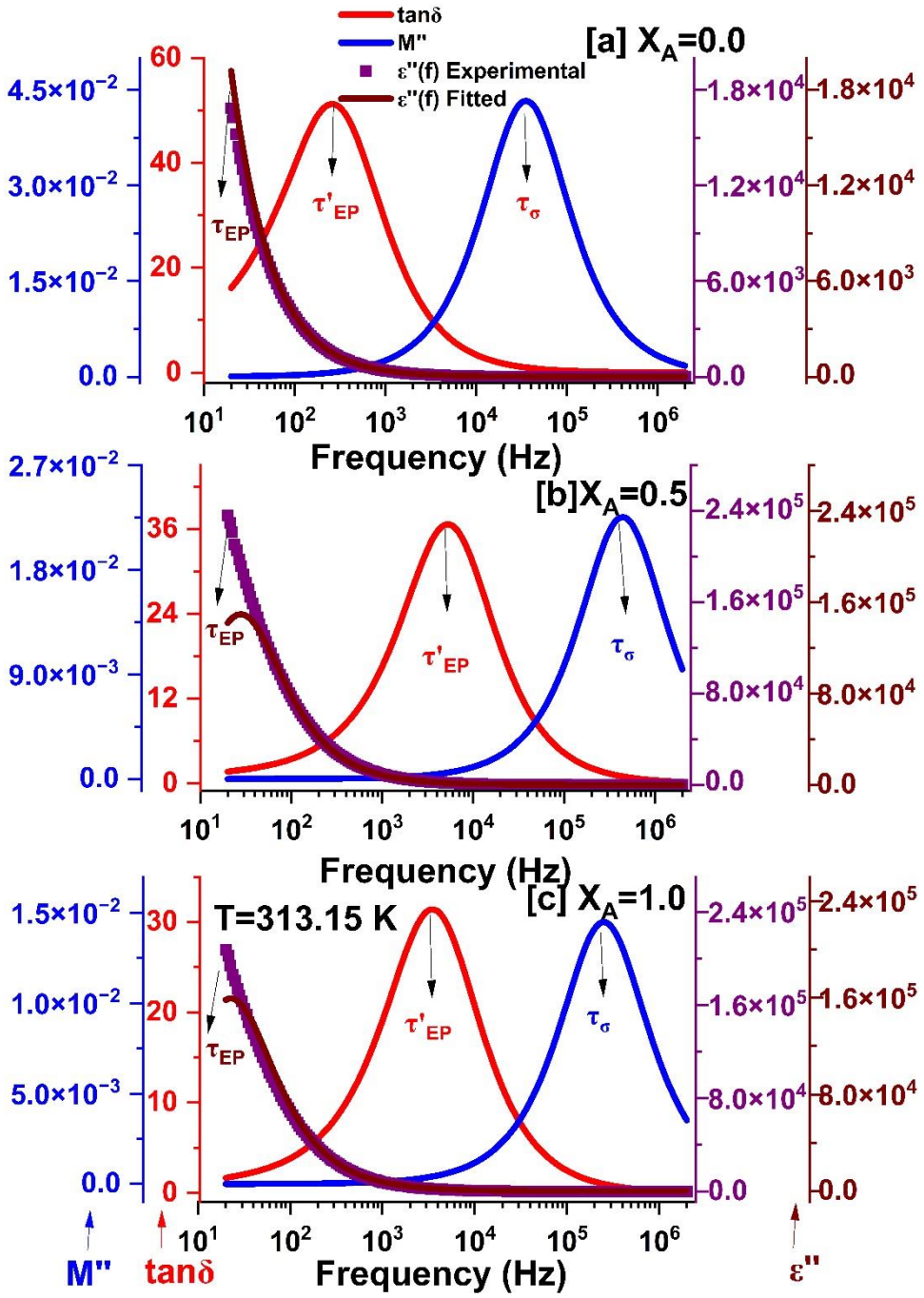

Fig.4.8. (C) Relationship between τ_{EP}, τ'_{EP} and τ_σ for X_A=0.0, X_A=0.5, and X_A=1.0 at 313.15 K.

The correlation between the three relaxation times τ_{EP}, τ'_{EP} and τ_σ presents an intriguing avenue for exploration. Figure 4.8 (A) (B) and (C) shows the frequency-dependent variations of ε" (dielectric loss), tan δ (dissipation factor), and M" (imaginary part of the complex modulus) for liquid samples at different temperatures with compositions X_A = 0.0, X_A = 0.5, and X_A = 1.0. Various relaxation time is obtained like τ_{EP} is determined by dielectric loss spectra, τ'_{EP} is determined with the tangent (tanδ) spectra

and τ_σ is evaluated with imaginary modulus (M′′) spectra and can be related by relation $\tau'_{EP} = (\tau_{EP} \times \tau_\sigma)^{\frac{1}{2}}$ [43,44]. It can be seen from the graph that for all the concentration ranges the peak is shifting towards the higher frequency region as the concentration of the mixture increases with increasing temperatures. The relaxation frequency associated with electrode polarization in the ε" plot is lower than the relaxation frequency observed in the tan δ plots. Consequently, the electrode polarization relaxation time (τ'_{EP}) has a higher value compared to the relaxation time (τ_{EP}). All different temperatures varying relaxation time values anomalous behavior is observed in Table 4.3.

4.3.1.3 Electrical ac Conductivity Spectra

The AC electrical conductivity values, encompassing both the real part (σ') and the imaginary part (σ"), are measured across a frequency range of 20 Hz to 2 MHz for binary mixtures of n-Hexanol and DMF. The real part (σ′) of the complex AC conductivity σ* (f), can be calculated using equation 3.9. Figure 4.9 (A) (B) and (C) illustrates the frequency-dependent behavior of the real component of complex AC conductivity (σ'ac) for n-Hexanol + DMF mixtures at varying temperatures (T = 293.15, 303.15, and 313.15 K). In this plot we observe two distinct regions: a dispersion part at low frequencies and a frequency-independent plateau at higher frequencies. These characteristics are noticeable within the low and mid-concentration range of DMF ($0.1 \leq X_A \leq 1.0$) at different temperatures. The observed dispersion in the low-frequency region is attributed to interfacial impedance or space charge polarization [24]. As the frequency decreases, the density of accumulated charges at the electrode and material interface gradually increases. This accumulation results in a decrease in the number of mobile ions, eventually leading to a drop in conductivity at low frequencies. In the high-frequency region, the mobility of charge carriers is high, leading to an increase in conductivity with frequency [45]. Furthermore, In Fig. 4.9, the solid line represents the DC conductivity (σ_{dc}) within the σ' spectra. Initially, σ' shows a nonlinear increase with frequency with increasing in temperature, stabilizing beyond 2 kHz. These σ_{dc} values are derived from the frequency-independent plateau region of σ' values, painted by the straight line (using DMF concentration). The values of dc electrical conductivity at different temperatures are reported in Table 4.3. Table 4.3 presents experimental σ_{dc} values for the n-Hexanol+DMF mixtures anomalous behaviour observed at different temperatures. Notably, the σ_{dc} values for pure DMF (5.59×10^{-04} μS/m) are

approximately one order of magnitude higher than those of n-HxOH (1.01×10^{-05} μS/m), consistent with the higher static dielectric constant (ε_0) of DMF (303.15 K). Figure 10 shows the σ′′ against volume fraction of DMF and their mixture in the frequency range 20 Hz to 2 MHz at constant temperature (303.15 K). Furthermore, observed in Figure 4.10, the imaginary part of conductivity shows a clear segmentation into two separate regions. Within the initial region, spanning up to 10^3 Hz, the peak of σ" exhibit a linear decline for both DMF and higher concentrations of DMF at different temperatures. In the intermediate frequency range, σ" peak values reach a minimum. The frequency at which σ" reaches its minimum matches precisely with the frequency of the peak in tan δ shown in Figure 4.4. This alignment implies that analyzing σ" spectra can provide insights into the dynamics of electric double layers (EDLs) in dipolar liquids. In the higher frequency range (second region), above 10^3 Hz, the values of σ"(ω) exhibit a linear decrease when plotted on a log-log scale for concentrations ranging from 0.0 → 1.0 at different temperature.

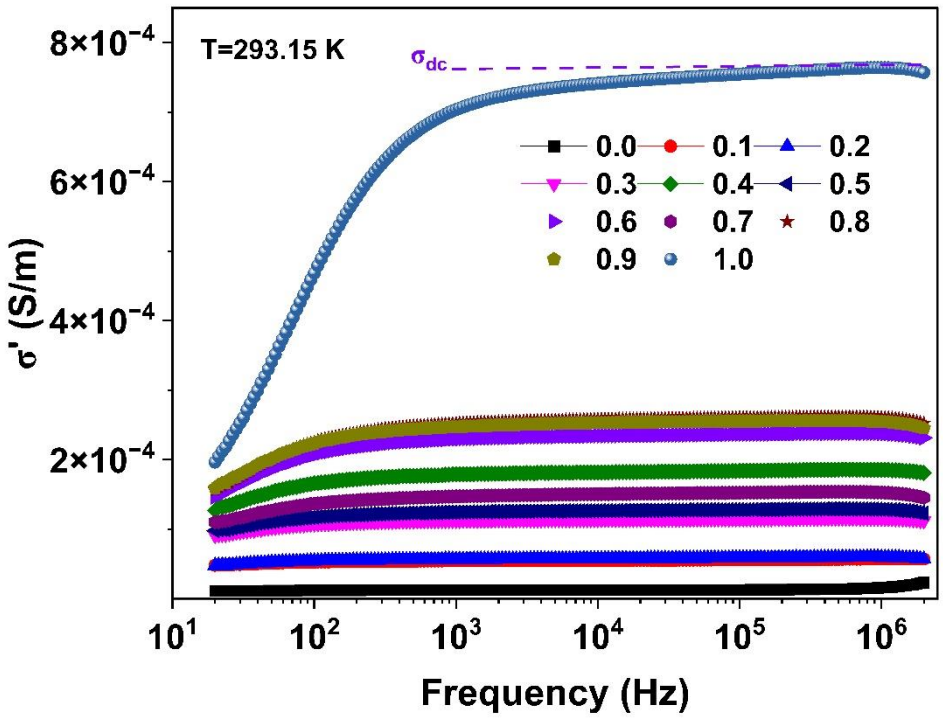

Fig.4.9. (A) Frequency dependent response of σ′ against volume fraction of DMF at 293.15 K.

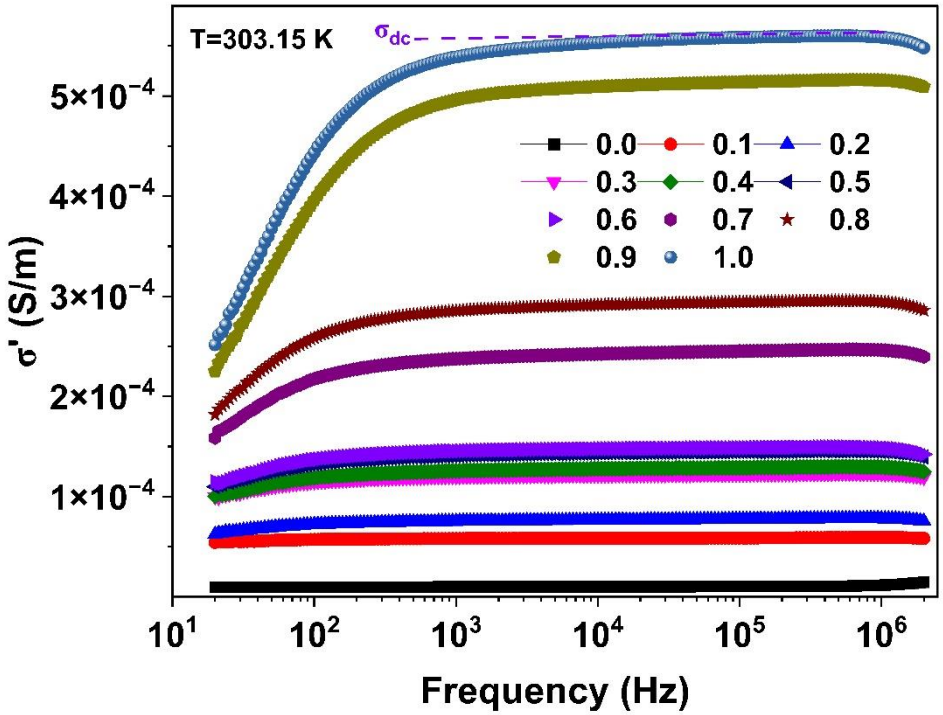

Fig.4.9. (B) Frequency dependent response of σ′ against volume fraction of DMF at 303.15 K.

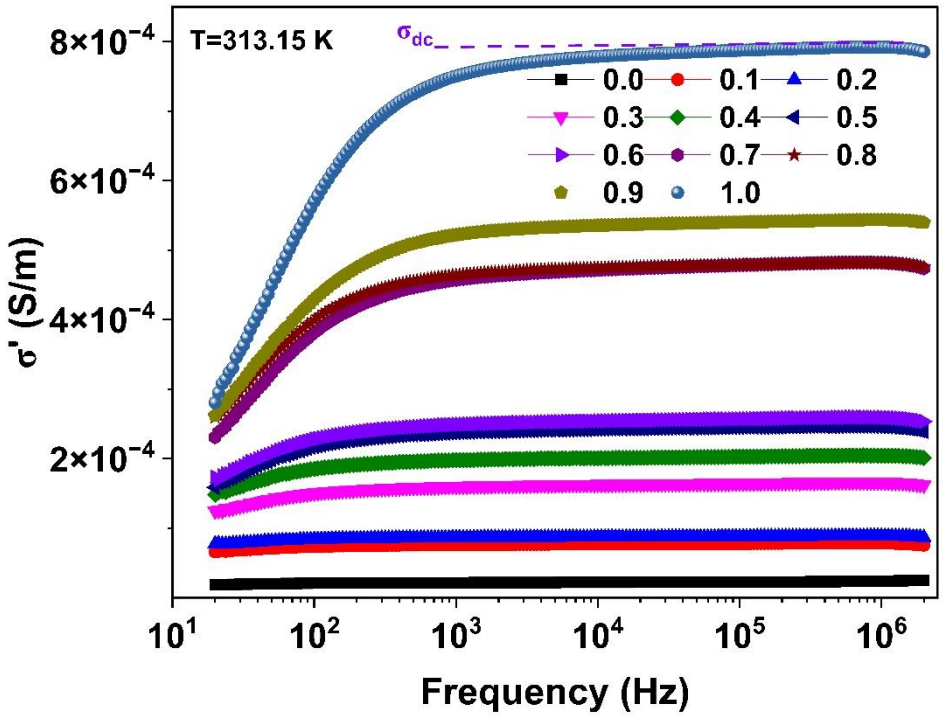

Fig.4.9. (C) Frequency dependent response of σ′ against volume fraction of DMF at 313.15 K.

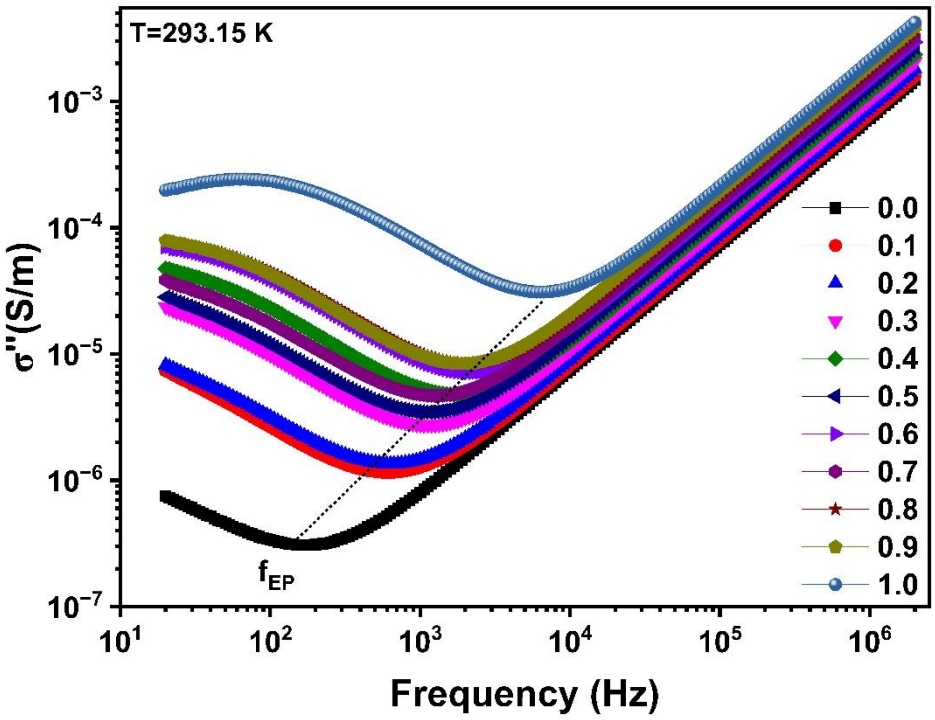

Fig.4.10. (A) Frequency dependent response of σ″ against volume fraction of DMF at 293.15 K.

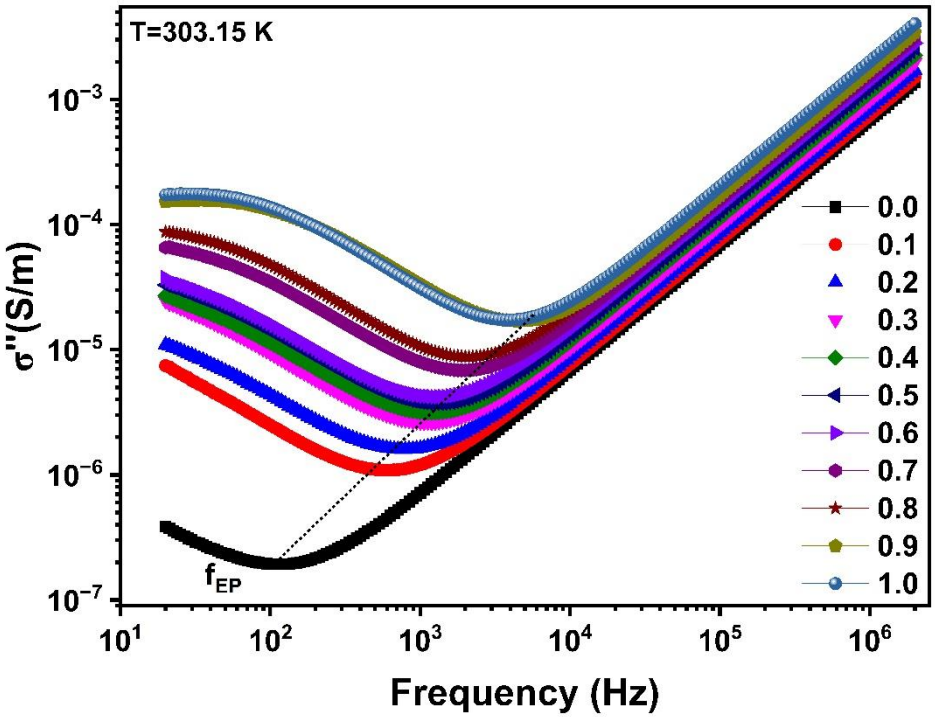

Fig.4.10. (B) Frequency dependent response of σ″ against volume fraction of DMF at 303.15 K.

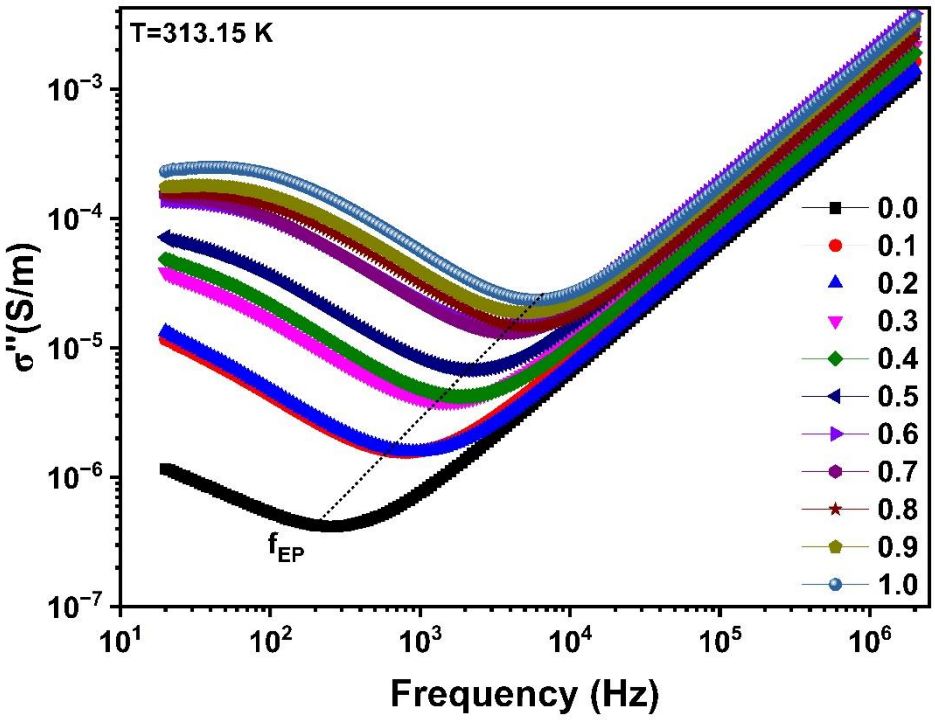

Fig.4.10. (C) Frequency dependent response of σ′′ against volume fraction of DMF at 313.15 K.

Figure 4.11 illustrates the changes in DC conductivity (σ_{dc}) and ionic conductivity relaxation time (τ_σ) for DMF, n-Hexanol, and their mixture as temperature varies. These changes follow the Arrhenius-type behavior, indicating that the dc conductivity follows an exponential relationship with temperature. The activation energy (Ea) for conductivity can be calculated using the Arrhenius equation [1].

$$\sigma_{dc} = \sigma_0 \mathrm{Exp}\left(\frac{-E_\sigma}{\mathrm{RT}}\right) \quad (4.2)$$

Where A_0 is the pre-exponential factor, is the Ea activation energy, T is the absolute temperature, and R is the gas constant. The concentration-dependent activation energy (Ea) using DC conductivity (σ_{dc}) are tabulated in Table 4.4. It has been observed table 4.3 that $E_{a\ \text{n-Hexanol}} > E_{a\ \text{DMF}}$. For the mixture concentration Ea values show the anomalous behaviour. In the n-Hexanol rich and mid-concentration (X=0.5) regions $E_{\tau\sigma}$ is higher by approximately 9 kJ/mol compared to E_{dc} . This indicates a higher energy barrier for ionic conductivity relaxation compared to DC conductivity in these regions. However, in the DMF rich region, the activation energies for DC conductivity and ionic conductivity relaxation time are approximately equal, ($E_{dc} \approx E_{\tau\sigma}$). This suggests similar energy requirements for both processes in this concentration range. From the Tolman

interpretation, activation energy is negative when the average energy of transition state is greater than the average energy of reactants [46].

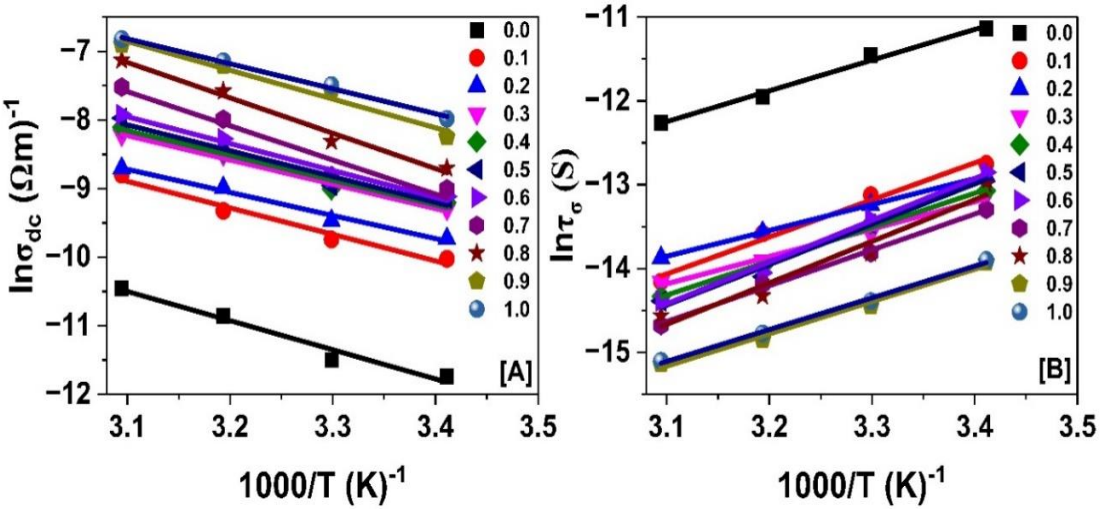

Fig. 4.11. Arrhenius plots of (a) dc conductivity (σ_{dc}) and (b) ionic conductivity relaxation time (τ_{σ}) for the binary mixture of DMF and n-Hexanol.

Table 4.4. Comparison of activation energy (Ea) of dc conductivity (E_{dc}) and ionic conductivity relaxation time ($E_{\tau\sigma}$) for the binary mixture of DMF and n-Hexanol.

X_1	E_{dc} (kJ/mol)	$E_{\tau\sigma}$ (kJ/mol)
0.0	35.34	30.49
0.1	32.14	36.76
0.2	27.97	25.72
0.3	29.46	27.10
0.4	30.01	33.68
0.5	31.33	40.09
0.6	32.59	41.42
0.7	41.38	35.57
0.8	42.92	41.22
0.9	34.88	32.04
1.0	30.24	31.49

4.3.1.4 Complex Impedance Spectra

In lower-frequency dielectric spectroscopy, polar liquid materials commonly exhibit two phenomena: electric double layer (EDL) and conductivity relaxation processes. These processes are typically identified by examining the imaginary part of the complex impedance spectra [12]. The real (Z′) and imaginary part (Z′′) of impedance plots are common methods for discerning bulk material properties and phenomena associated

with electrode surface polarization. Dielectrics with DC conductivity typically exhibit a discontinuity at the electrode/dielectric interface, characterized by distinct polarization properties compared to the bulk material. The frequency-dependent Z′ and Z″ components of the complex impedance (Z*(f)) can be determined using Equation (3.10) [42]. Figure 4.12 (A) (B) and(C) shows the real part of the complex impedance spectra Z' for n-Hexanol+DMF binary mixture at different temperature (293.15 K, 303.15 K and 313.15 K). It is observed that Z' exhibits a rapid decrease across the entire frequency range for the concentration range of $0.0 \leq X_A \leq 1.0$ at studied temperatures. The frequency-dependent Z′ values for n-Hexanol (with low static permittivity) are observed to be higher compared to those of DMF (with high static permittivity). Furthermore, the values for binary mixtures of n-Hexanol and DMF fall in between these two extremes [42]. Similar behavior has been reported by various researchers across different molecular systems [1,3,43]. Figure 4.13 depicts the Z" exhibits both minima and maxima, indicated as f'_{EP} and f_σ respectively. f'_{EP} signifies the frequency at which the static dielectric constant (ε_0) begins to increase as the frequency decreases, indicating the onset of the Electric Double Layer (EDL) relaxation process [44]. Furthermore, f_σ corresponds to the conductivity relaxation process and coincides with the peak in the imaginary part of the electric modulus (M"(f)) Fig.4.7).

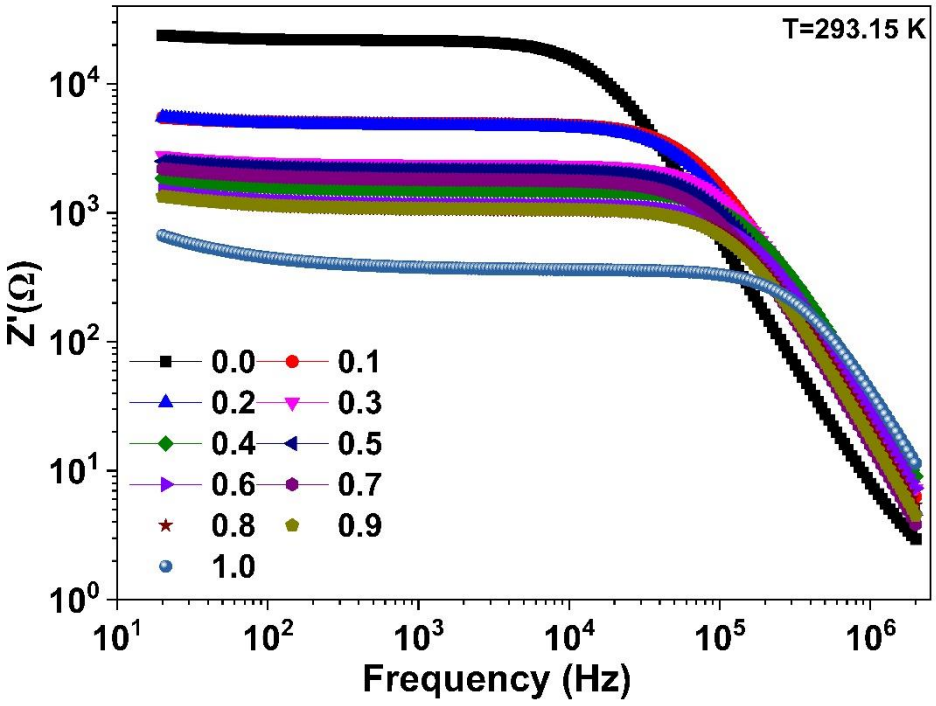

Fig. 4.12. (A) Frequency dependent response of Z′ against volume fraction of DMF at 293.15 K.

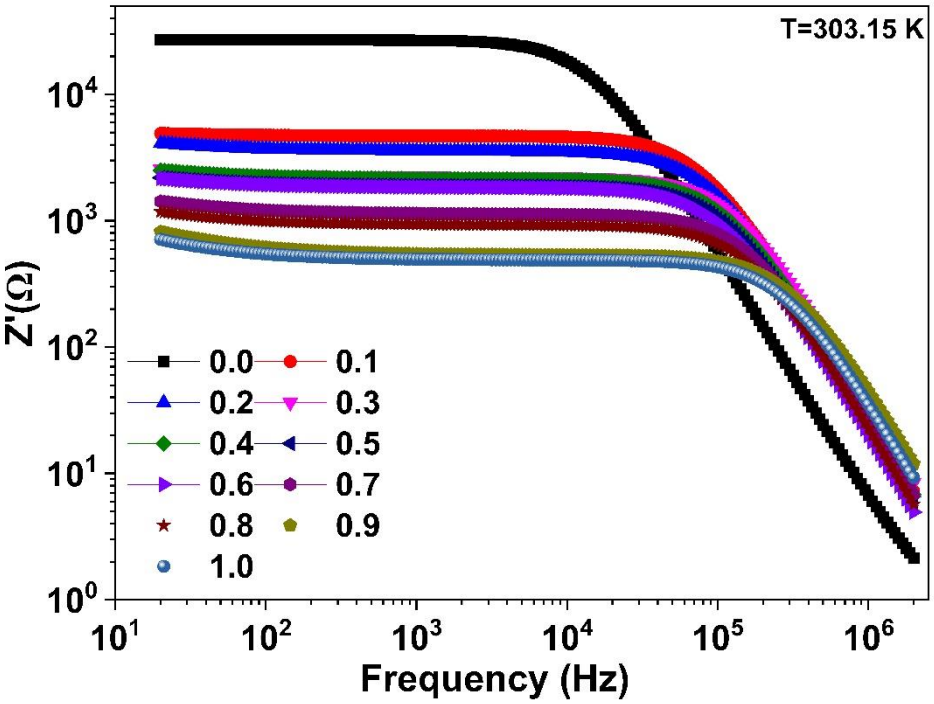

Fig. 4.12. (B) Frequency dependent response of Z′ against volume fraction of DMF at 303.15 K.

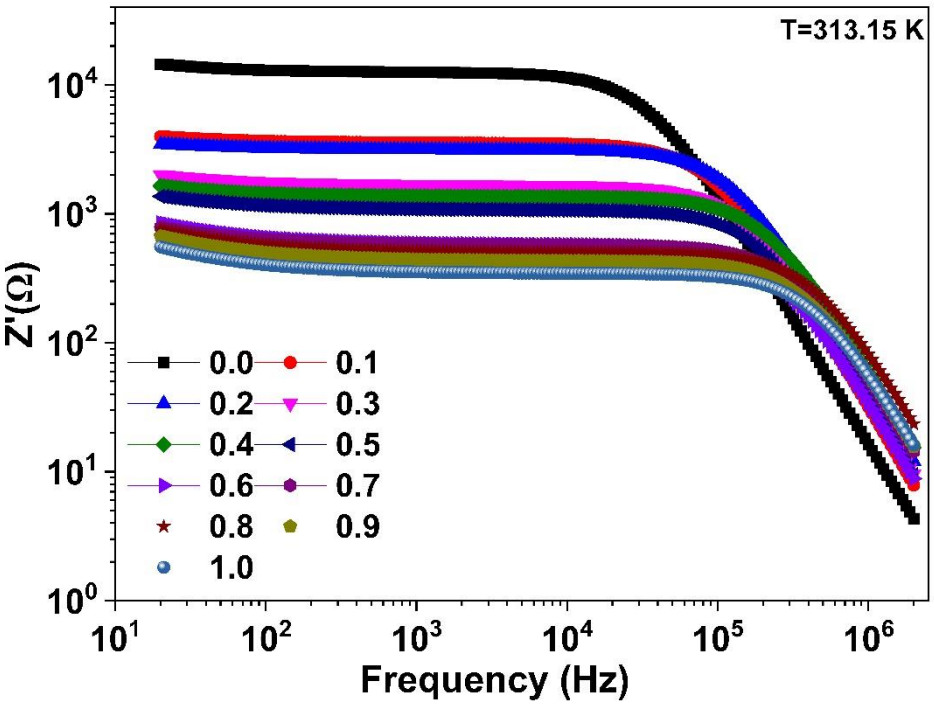

Fig. 4.12. (C) Frequency dependent response of Z′ against volume fraction of DMF at 313.15 K.

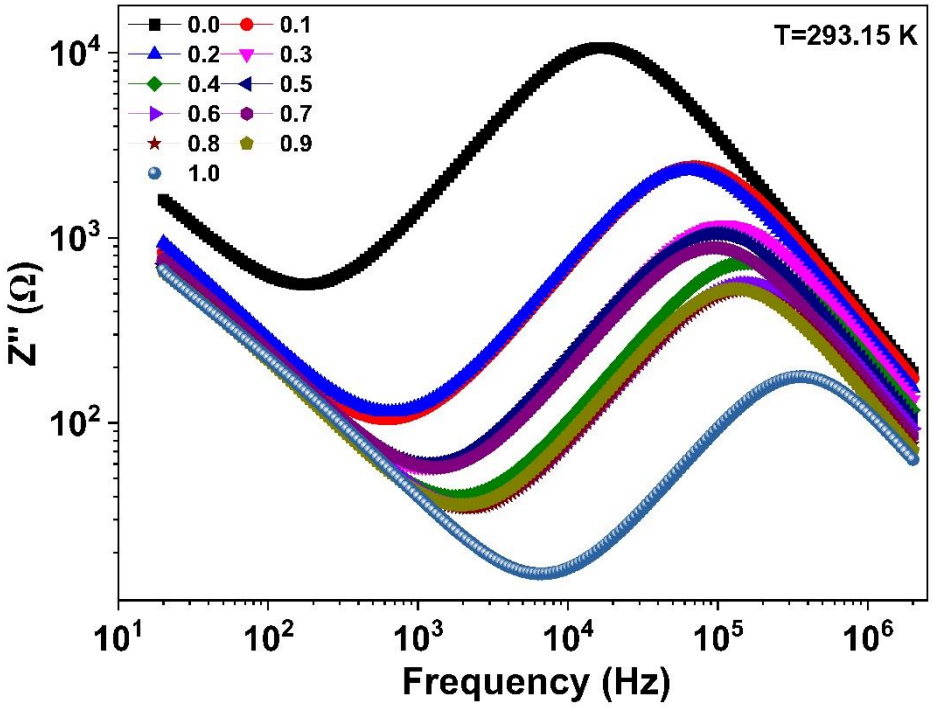

Fig. 4.13. (A) Frequency dependent response of Z″ against volume fraction of DMF at 293.15 K.

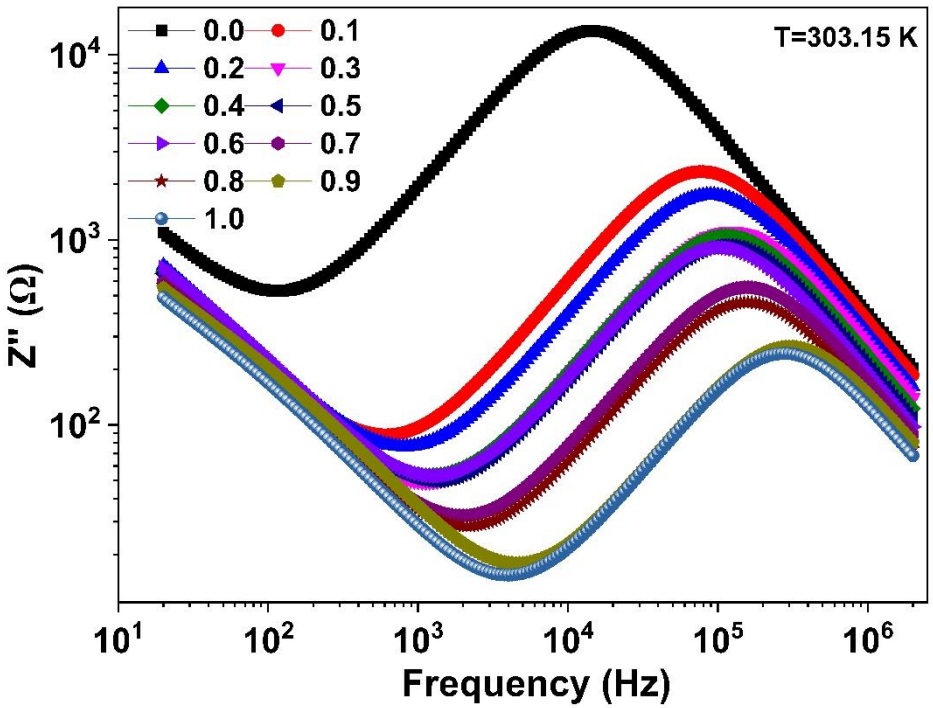

Fig. 4.13. (B) Frequency dependent response of Z″ against volume fraction of DMF at 303.15 K.

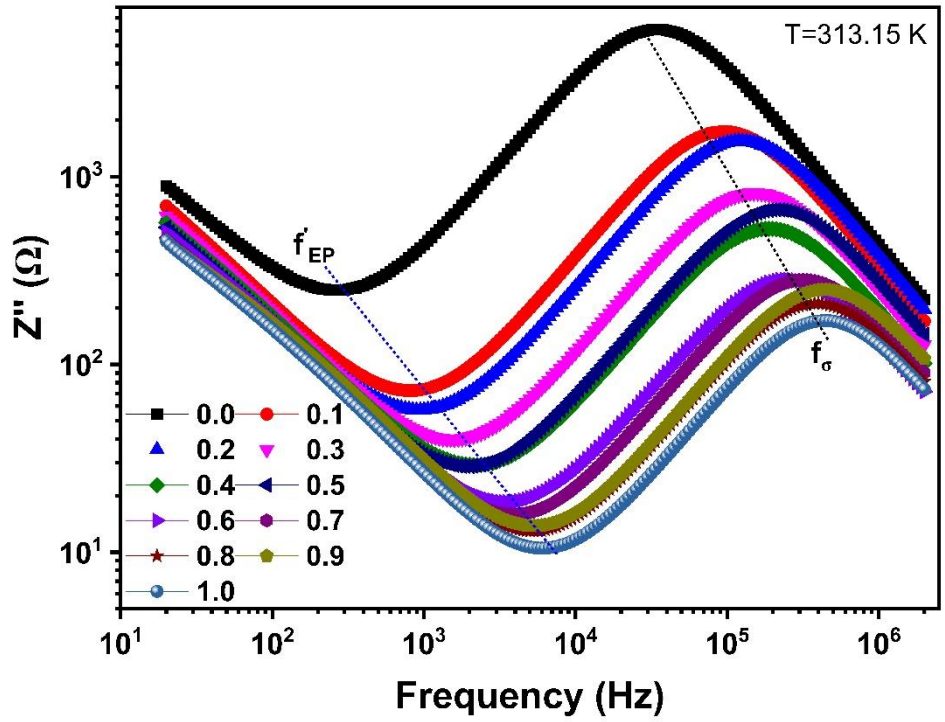

Fig. 4.13. (C) Frequency dependent response of Z″ against volume fraction of DMF at 313.15 K.

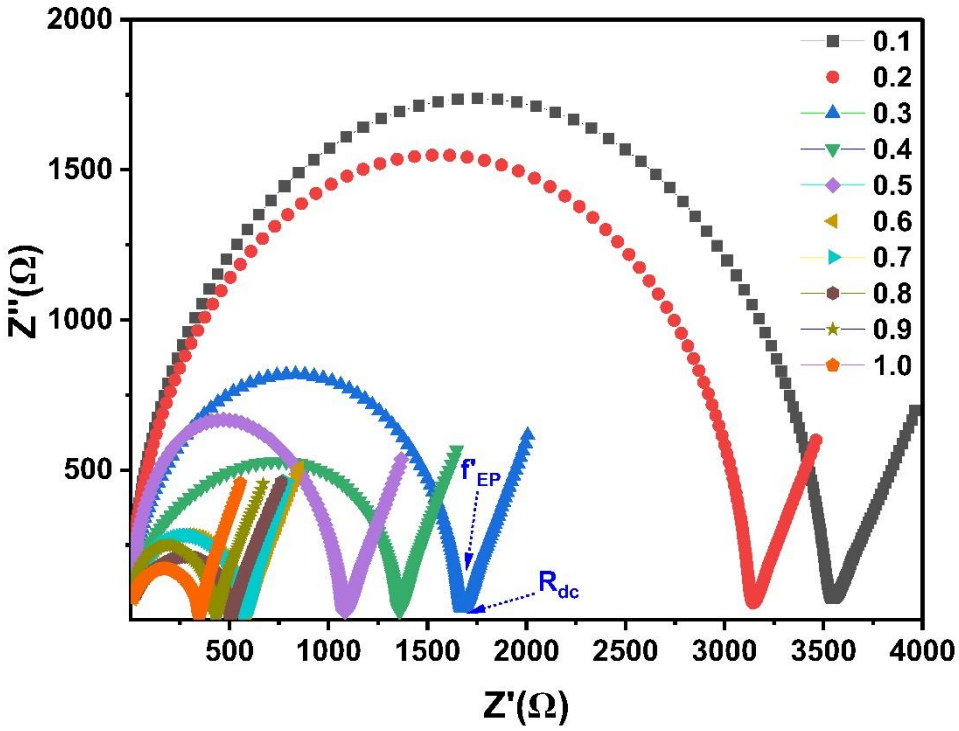

Fig.4.14 Complex impedance plot (Z"→Z') for n-Hexanol +DMF binary mixture in the frequency range 20 Hz to 2 MHz at 313.15 K.

The derived values of f'_{EP} and f_σ were utilized to compute the respective relaxation times, τ_{EP} and τ_σ, employing the general relation $\tau = \frac{1}{2\pi f}$. These calculated relaxation

times are reported in Table 4.3. In the temperature-dependent plots of complex impedance, the Z′ values decrease gradually with increasing frequency and then sharply decline at higher frequencies. An inversion effect is also noted at a specific frequency, fσ. In the temperature-dependent plot of Z″, two relaxation peaks are observed, which shift toward higher frequencies as the temperature rises, with a corresponding decrease in peak magnitude. The shift of these peaks to higher frequencies with increasing temperature indicates enhanced charge mobility within the thermally activated dielectric system [10].

Figure 4.14 shows the complex plane plots (Z″ versus Z′) for n-Hexanol+DMF mixtures at the 313.15 K temperature. The frequency of the experimental data points increases from right to left in these plots. The Debye-type semicircles in the impedance values range from a few kHz to 2 MHz, corresponding to the bulk material properties, while the spike at low frequencies indicates the dominant contribution of the electrode polarization effect. This Debye-type dispersion of impedance data over the static permittivity frequency range is characteristic of dipolar liquids [1,43]. The semicircular impedance plot for DMF is significantly smaller than that for n-Hexanol, reflecting their respective conductivity behaviors. The intercept of the semicircle and the spike on the real axis (Z′) in the impedance plot provides the DC resistance (Rdc) value of the bulk dielectric material [9]. Furthermore, observed in the Rdc of pure n-Hexanol (12715.18 Ω) is much higher, resulting in a lower conductivity compared to DMF, which has an Rdc of 580.98 Ω (313.15 K).

Complex impedance plane plots are further analyzed using Electrochemical Impedance Spectroscopy (EIS), an important technique for studying relaxation processes in liquids [3]. The impedance data of the studied samples were fitted to a six-element equivalent circuit, which represents the measuring capacitive cell. The equivalent circuit for its impedance is depicted as an inset in Figure 4.15. Experimental impedance data for all mixture concentrations were best fitted to the equivalent circuit model. Figure 4.15 presents representative plots depicting both experimental and fitted data points for concentration is X_A=0.0, X_A=0.5 and X_A=1.0 at 303.15 K.

The EC-Lab software was instrumental in identifying the components of the equivalent circuit that represents the dielectric measurement cell. By utilizing Eq. 4.3 [3] to fit experimental data points, which corresponds to the Randles Cell Circuit model, the software facilitated the analysis of complex impedances.

$$Z(f) = R_1 + \frac{R_2}{1+i\omega R_2 C_2} + \frac{R_3}{1+i\omega R_3 C_3} + \frac{\sqrt{2\sigma_4}}{\sqrt{i\omega}} \quad (4.3)$$

Here, R_1 represents the dielectric measurement cell's resistance, the second term indicates the electrode polarization effect, the third term indicates the conduction process, and σ_4 indicates the Warburg element (a constant phase element, or CPE, with a phase of 45°), which is corresponding to the Warburg impedance (W_4) in the Randles cell circuit model. The Warburg element is used to interpret the mechanism of the diffusion process in the low frequency region. Additionally, the relaxation times, including the electric double layer formation time constant (τ_{EDL}) and the geometric relaxation time constant (τ_g), are calculated using Eqs. (4.4) and (4.5) respectively for all concentrations (0.0→1.0). Table 4.5 presents the parameters obtained from fitting the equivalent circuit, providing crucial insights into the electrical behavior of the system. These parameters enable the examination of multiple relaxation behaviors for all concentrations.

$$\tau_{EDL} = R_2 C_2 \quad (4.4)$$

$$\tau_g = R_3 C_3 \quad (4.5)$$

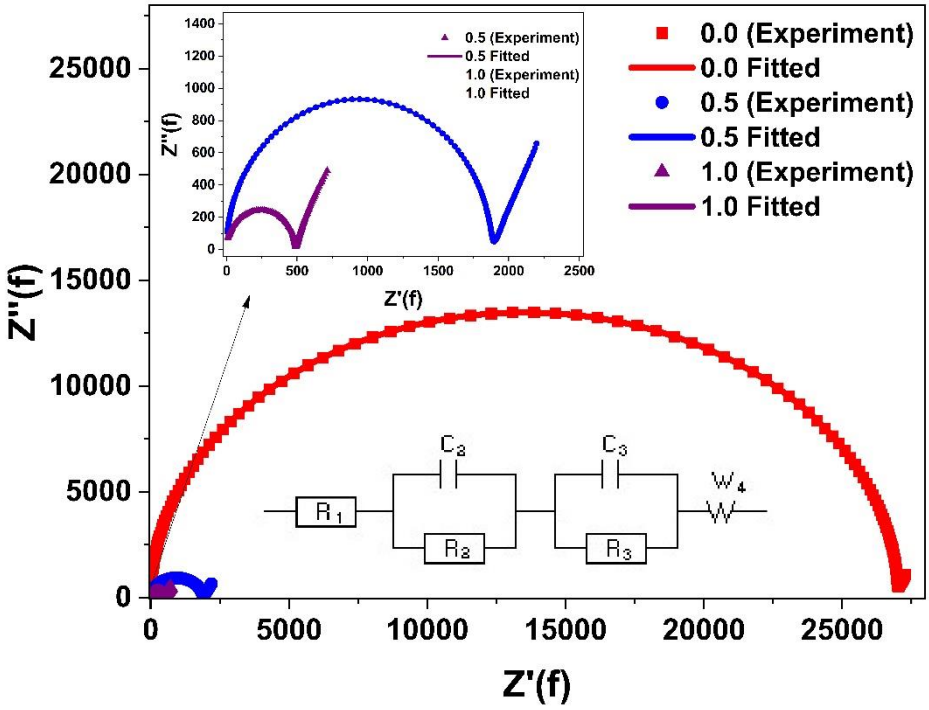

Fig.4.15 The graphical representation of experimental data points along with fitted data points of complex impedance spectra plot (Z″ vs Z′) using an equivalent RC circuit. The concentrations represented are X_A=0.0, X_A=0.5, and X_A=1.0 at 303.15 K.

Table 4.5 Fitted parameters of four element equivalent RC circuit for all concentration (0.0→1.0) double layer relaxation time constant (τ_{EDL}) and geometric relaxation time (τ_g) at 303.15 K.

X_A	R_{dc} (Ω)	R_1 (Ω)	C_2 (μF)	R_2 (Ω)	C_3 (nF)	R_3 (Ω)	σ_4 ($\Omega\ s^{-1/2}$)	τ_σ (μsec)	τ_{EDL} (s)
0.0	27034.89	0.522	6.82	4281	0.402	26982	965.5	10.84	0.0292
0.1	4705.09	0.307	9.32	1791	0.435	4699	4462	2.04	0.0167
0.2	2249.55	0.940	18.30	625	0.505	3525	4088	1.78	0.0114
0.3	3586.68	0.745	17.44	2220	0.579	1311	2453	0.75	0.0387
0.4	2137.64	0.913	17.71	2103	0.662	1188	3075	0.78	0.0372
0.5	1336.69	0.957	17.57	1865	0.749	1760	2780	1.31	0.0328
0.6	1261.91	1.049	15.71	1813	0.829	2038	2876	1.68	0.0285
0.7	1129.81	0.741	18.51	1326	0.911	1107	2432	1.00	0.0245
0.8	933.78	0.803	18.27	915	1.091	1797	2080	1.96	0.0167
0.9	534.74	1.369	18.03	1347	0.991	521.1	2271	0.51	0.0243
1.0	491.50	1.109	19.10	1474	1.167	480.8	1661	0.56	0.0282

It can be observed from Table 4.5 that the volume fraction of DMF increase with a decrease in bulk resistance values (Rdc). It is clearly observed that the R_3 value and bulk resistance for all concentrations are nearly equal and observed geometric relaxation time (τ_g) and ionic conduction relaxation time (τ_σ) (In Table 4.3) for all the concentrations are almost equal. The value of electric double layer formation time constant (τ_{EDL}) and the geometric relaxation time constant (τ_g) anomalous behavior for all concentrations.

Figure 4.16 indicates the tan δ, Z"(Imaginary part of impedance), M"(Imaginary part of modulus), σ"(Imaginary part of conductivity) on the same frequency scale for both pure n-Hexanol+DMF and volume fraction X_A=0.0, X_A=0.5 and X_A=1.0 at different temperatures. This master plot is important because it helps us understand the various relaxation processes in dipolar liquids. It also guides us in choosing the right spectrum to study a particular relaxation process effectively [10]. Vertical dotted lines in the master curve mark the locations of Electric Double Layers (EDLs) and conductivity relaxation processes. In the Z″ spectra, we see both relaxation processes clearly with peaks and valleys, while the other spectra only show one of the two relaxation

processes. This analysis suggests that when studying the relaxation processes caused by ionic charge impurities in pure dipolar liquids and their mixtures, impedance spectroscopy is more useful than dielectric and modulus spectroscopies [44]. Figures 4.16 collectively illustrate a concentration-dependent shift of the EDL and conductivity peaks toward higher frequency ranges, consistently observed across various temperatures. This shift is linked to the relaxation process of the EDL, resulting in a reduction in the σ" and tanδ spectra. In contrast, the peak observed in the M" spectrum is specifically attributed to the ionic relaxation process.

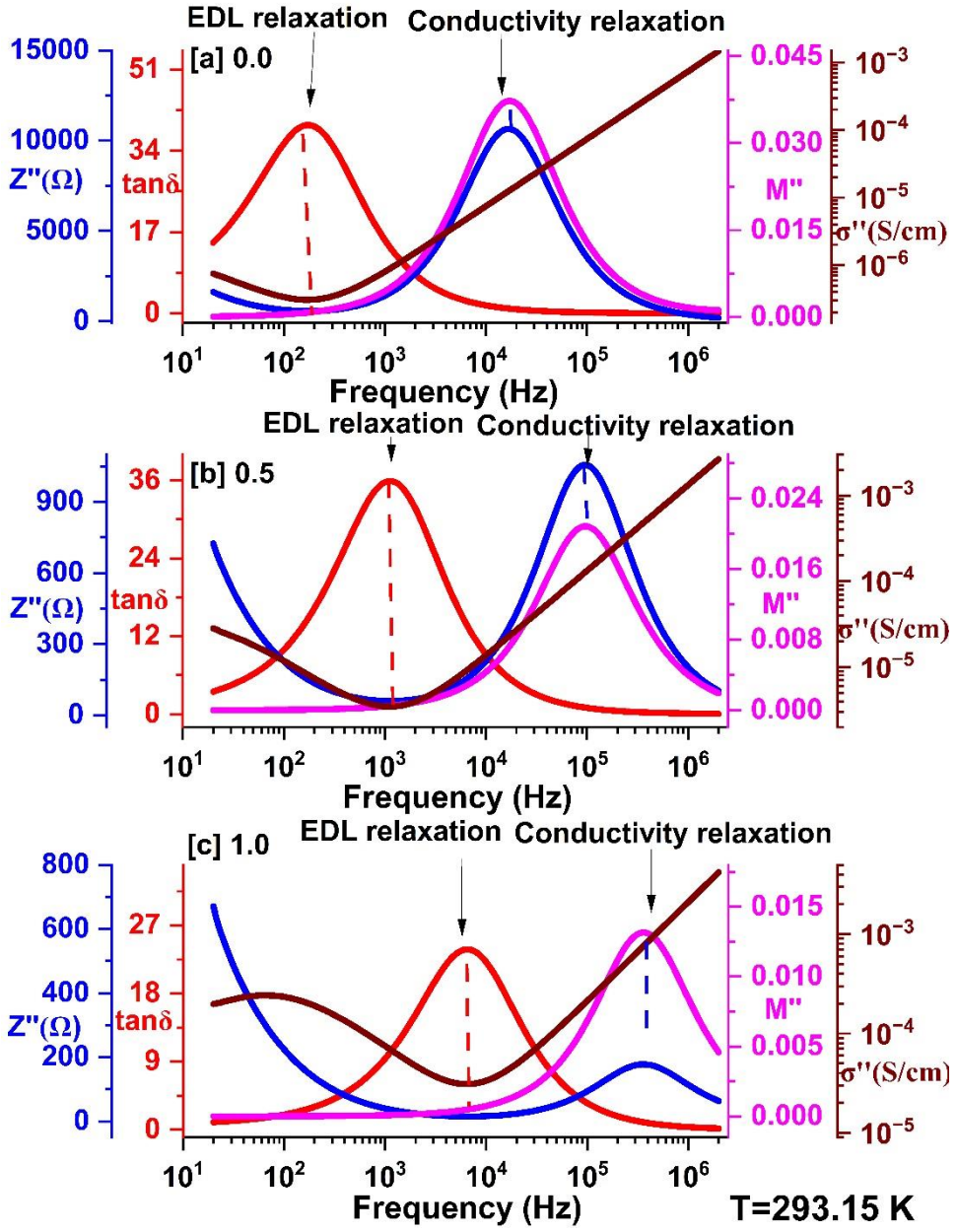

Fig.4.16. (A) Master curves showing EDL and conductivity relaxation processes for X_A=0.0, X_A=0.5, and X_A=1.0 at 293.15 K.

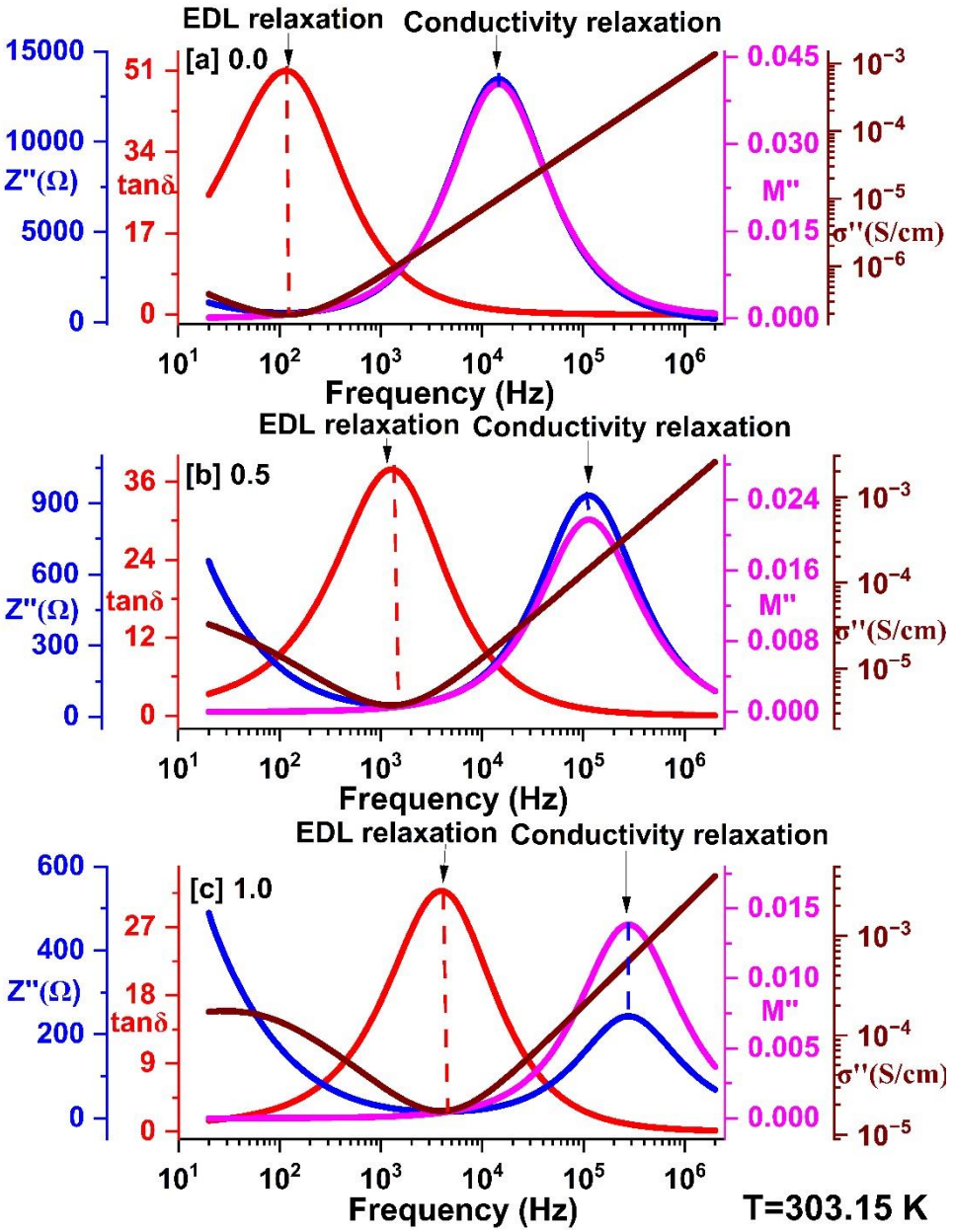

Fig.4.16. (B) Master curves showing EDL and conductivity relaxation processes for X_A=0.0, X_A=0.5, and X_A=1.0 at 303.15 K.

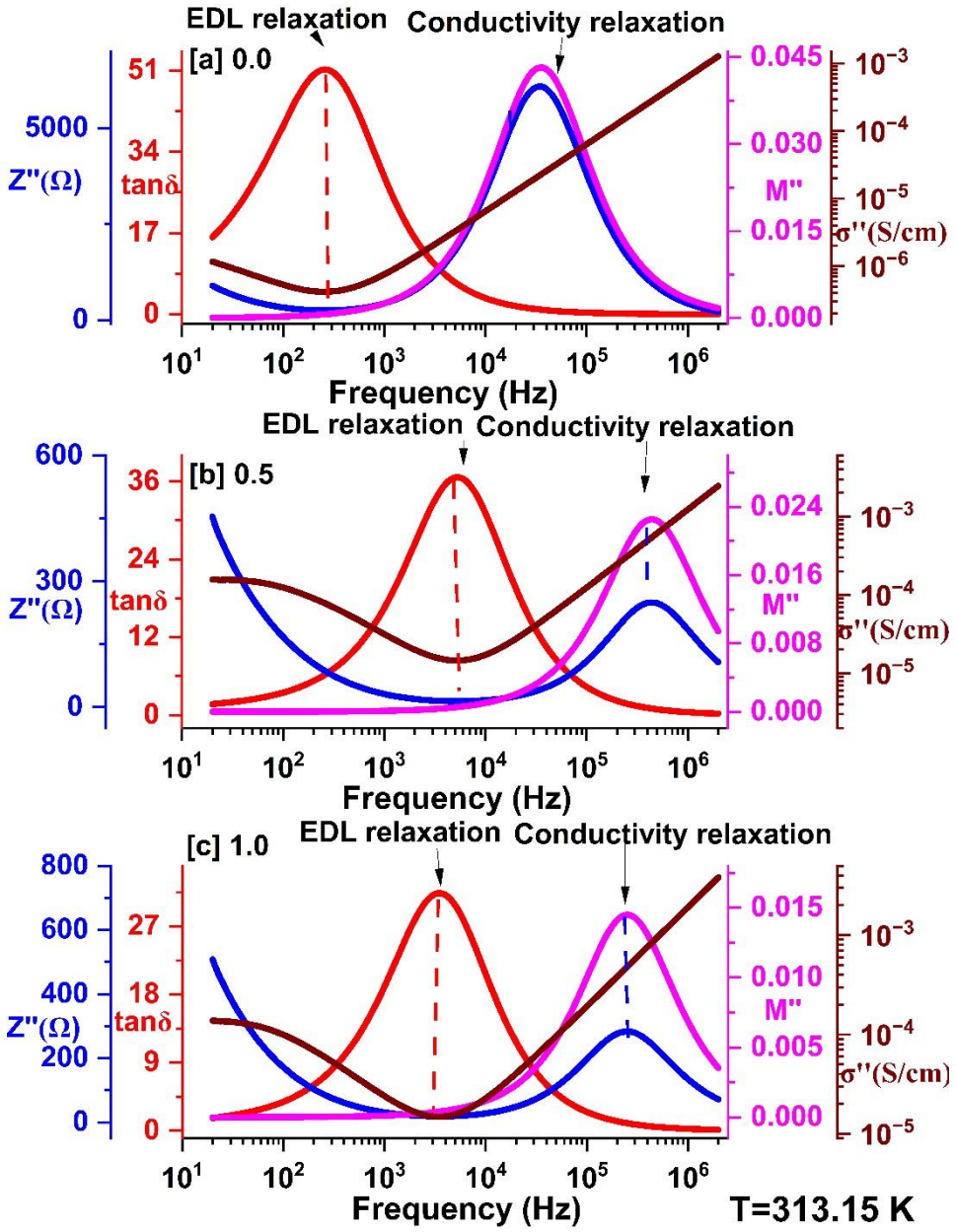

Fig.4.16. (C) Master curves showing EDL and conductivity relaxation processes for X_A=0.0, X_A=0.5, and X_A=1.0 at 313.15 K.

4.3.2 Dielectric relaxation spectroscopy in the Higher Frequency Range 200 MHz to 20 GHz

4.3.2.1 Complex dielectric permittivity spectra

Figures 4.17 illustrate the frequency-dependent spectra of the dielectric constant *(ε′)* across the frequency range of 200 MHz to 20 GHz for the complete mole fraction (0.0 →1.0) of n-Hexanol at different temperatures (293.15 K, 303.15 K, 313.15 K). The figures clearly demonstrate a monotonic decrease in the dielectric constant *(ε′)* values

with increasing temperatures as the concentration of n-Hexanol increases in the binary mixtures.

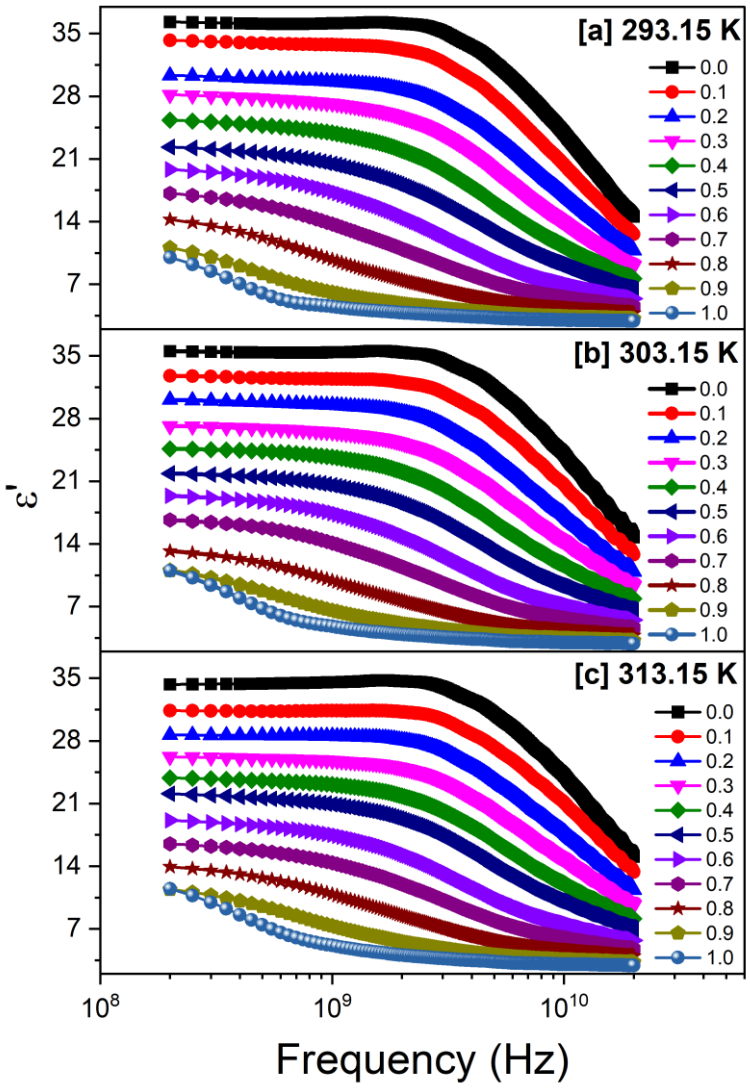

Fig. 4.17 Frequency dependent dielectric constant (ε′) spectra of (n-Hexanol+DMF) binary mixtures in frequency span 200 MHz to 20 GHz frequency at different temperatures.

Similarly, Figure 4.18 showcase the frequency-dependent spectra of the dielectric loss (ε″) across the entire concentration range (0.0 → 1.0) within the frequency span of 200 MHz to 20 GHz at various temperatures. The figures reveal that the dielectric loss (ε″) values decrease with both increasing temperatures and frequency. Moreover, the peak values of dielectric loss (ε″) decrease and shift towards the lower frequency side as the concentration of n-Hexanol increases in the binary mixtures. The experimental complex dielectric data were fitted to different asymmetry and broadness dependent dielectric relaxation models by the CNLS method [40]. The general form of dielectric relaxation

model, including asymmetric and broadening of dielectric relaxation, is given by Havriliak–Negami (HN) [35] using Eq.4.1.

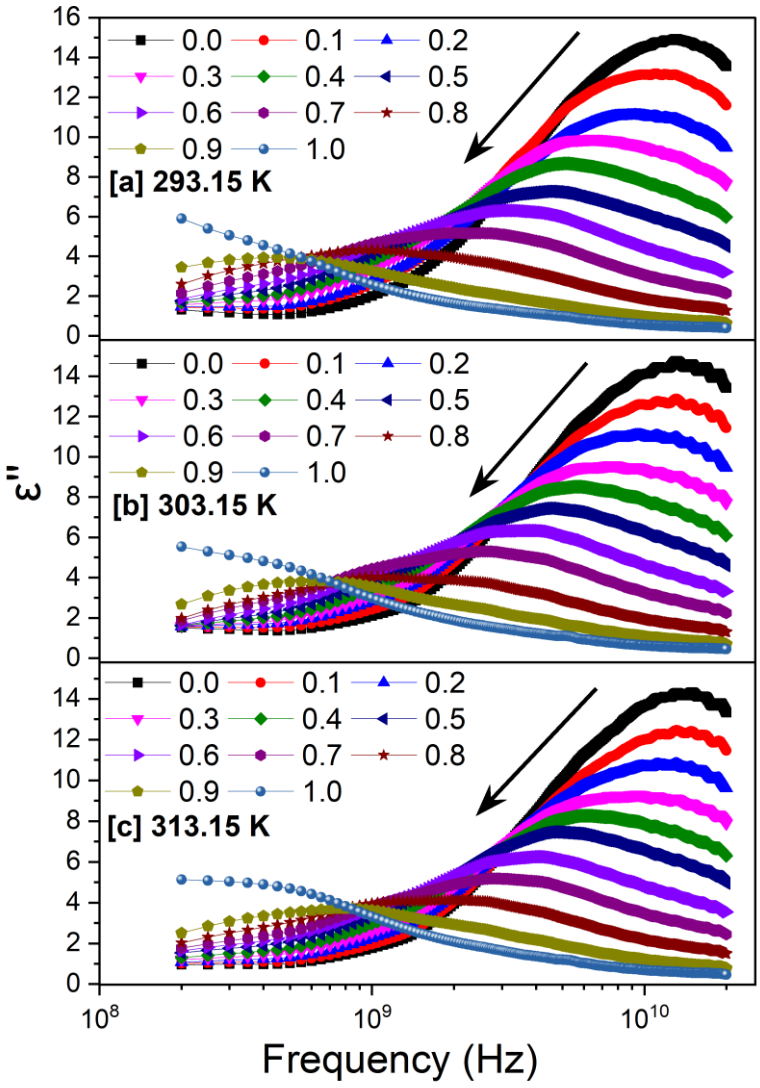

Fig.4.18 Frequency dependent dielectric loss (ε′′) spectra of (n-Hexanol+DMF) binary mixtures in frequency span 200 MHz to 20 GHz frequency at different temperatures.

Using Eq.4.1 in this study, the complex permittivity at angular frequency ω, is analyzed. The algebraic difference between a static dielectric constant (ε_0) and an optical dielectric constant (ε_∞) is defined as dielectric strength ($\Delta\varepsilon = \varepsilon_0 - \varepsilon_\infty$), while τ_0 represents the relaxation time of the mixture concentration. Two shape parameters, α and β, play a crucial role in selecting dielectric relaxation models. Specifically, the Cole-Davidson (CD) model, characterized by α = 1, and the Cole-Cole (CC) model, characterized by β = 1, represent symmetrical and asymmetric relaxation curves, respectively. The real and imaginary parts of the complex permittivity spectra of binary mixtures at different

concentrations are fitted into the dielectric models (Cole-Davidson (CD) / Cole-Cole (CC)) using a CNLS fitting program. Evaluated parameters such as high-frequency limiting dielectric constant (ε_∞), dielectric relaxation strength ($\Delta\varepsilon$), relaxation time (τ), the values of α and β are tabulated in Table 4.6 at various temperatures. Figure 4.19 shows typical model-fitted data plots for representative mole fractions (X_1 = 0, 0.3805, 0.8468, and 1.0) at a temperature of 293.15 K. While none of the models achieved a perfect fit to the experimental data across the entire frequency range, upon critical evaluation, it was observed that the Cole-Cole (CC) model (for $0 \leq X_1 \leq 0.8468$) and the Cole-Davidson (CD) model ($X_1 = 1$) exhibited superior agreement with the real (ε') and imaginary parts (ε'') of the experimental complex permittivity data compared to other models.

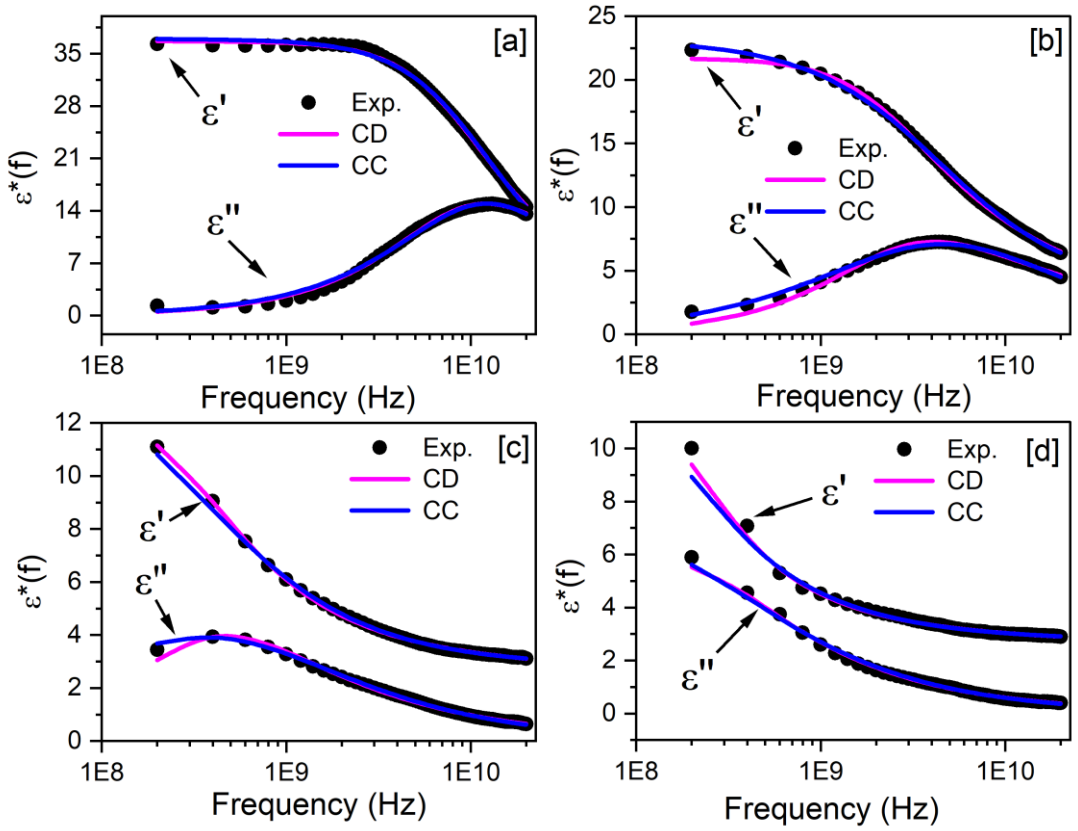

Fig. 4.19 Plots of complex permittivity vs frequency for different concentration of (a) X_1 = 0.0, (b) X_1 = 0.3805, (c) X_1 = 0.8468, and (d) X_1 = 1.0. for the binary liquid system at 293.15K temperature. The solid line (–) shows the CNLS fitted dielectric relaxation models for CD-Cole Davidson, and CC-Cole Cole.

Table 4.6 Values of optical dielectric constant ($\varepsilon_{\infty 0}$), CNLS fitting parameters high frequency limiting dielectric constant ($\varepsilon_{\infty 1}$), dielectric relaxation strength ($\Delta\varepsilon$), relaxation time (τ_0) and shape parameter (α,β) of binary mixtures of n-Hexanol + DMF at different temperatures.

X_A	$\varepsilon_{\infty 0}$	$\varepsilon_{\infty 1}$	$\Delta\varepsilon$	τ_0 (ps)	α	Model
T = 293.15 K						
0.0000	2.046	5.11 (2.53)	31.88 (0.53)	12.93 (0.45)	0.95 (0.37)	C-C
0.0639	2.041	4.40 (2.41)	30.46 (0.49)	14.88 (0.43)	0.91 (0.37)	C-C
0.1331	2.037	4.06 (1.98)	26.76 (0.45)	16.43 (0.40)	0.88 (0.35)	C-C
0.2084	2.033	3.89 (1.88)	24.99 (0.52)	21.12 (0.50)	0.85 (0.42)	C-C
0.2905	2.031	3.68 (1.54)	23.47 (0.53)	26.64 (0.59)	0.82 (0.44)	C-C
0.3805	2.026	3.32 (1.22)	20.01 (0.52)	35.04 (0.69)	0.78 (0.42)	C-C
0.4795	2.023	3.50 (0.89)	17.45 (0.65)	51.43 (1.02)	0.78 (0.47)	C-C
0.5890	2.019	3.33 (0.68)	15.27 (0.80)	81.97 (1.46)	0.76 (0.51)	C-C
0.7107	2.014	3.05 (0.42)	13.32 (0.92)	157.42 (1.87)	0.73 (0.47)	C-C
0.8468	2.011	2.77 (0.25)	12.50 (1.30)	438.56 (2.79)	0.71 (0.46)	C-C
1.0000	2.008	2.73 (0.40)	11.91 (2.10)	985.18 (4.16)	0.69 (0.78)	C-D
T = 303.15 K						
0.0000	2.041	5.79 (8.00)	30.01 (1.30)	12.47 (2.09)	0.98 (0.82)	C-C
0.0639	2.038	4.64 (7.90)	28.41 (1.14)	13.60 (1.90)	0.93 (0.81)	C-C
0.1331	2.032	4.01 (6.45)	26.47 (0.92)	15.83 (1.56)	0.89 (0.75)	C-C
0.2084	2.028	3.70 (4.75)	24.07 (0.74)	18.80 (1.23)	0.85 (0.68)	C-C
0.2905	2.025	3.67 (2.86)	21.79 (0.56)	23.99 (0.87)	0.83 (0.56)	C-C
0.3805	2.022	3.56 (1.63)	19.30 (0.42)	32.16 (0.64)	0.81 (0.44)	C-C
0.4795	2.019	3.49 (0.90)	16.97 (0.35)	45.41 (0.56)	0.79 (0.35)	C-C
0.5890	2.015	3.32 (0.63)	14.79 (0.40)	69.12 (0.72)	0.77 (0.35)	C-C
0.7107	2.012	2.99 (0.48)	11.89 (0.57)	118.93 (1.17)	0.75 (0.41)	C-C
0.8468	2.010	2.79 (0.33)	11.46 (1.37)	304.02 (2.81)	0.73 (0.55)	C-C
1.0000	2.007	2.71 (0.40)	11.39 (1.45)	708.87 (2.96)	0.72 (0.73)	C-D
T = 313.15 K						
0.0000	2.029	6.78 (0.57)	27.97 (1.14)	12.25 (1.78)	1.00 (0.68)	C-C
0.0639	2.027	5.43 (6.14)	26.29 (1.08)	12.66 (1.78)	0.96 (0.69)	C-C
0.1331	2.022	4.55 (5.37)	24.59 (0.88)	14.30 (1.51)	0.92 (0.65)	C-C
0.2084	2.017	4.02 (4.38)	22.68 (0.74)	16.85 (1.27)	0.88 (0.63)	C-C
0.2905	2.014	3.78 (2.99)	20.65 (0.58)	21.01 (0.94)	0.85 (0.56)	C-C
0.3805	2.011	3.71 (2.22)	19.00 (0.54)	27.55 (0.83)	0.82 (0.56)	C-C
0.4795	2.007	3.45 (1.40)	16.48 (0.48)	38.64 (0.73)	0.79 (0.49)	C-C
0.5890	2.005	3.28 (0.92)	14.23 (0.49)	56.68 (0.83)	0.77 (0.47)	C-C
0.7107	2.001	3.05 (0.57)	12.26 (0.57)	100.76 (1.14)	0.75 (0.44)	C-C
0.8468	1.998	2.81 (0.37)	10.84 (0.85)	252.29 (1.84)	0.74 (0.43)	C-C

1.0000	1.995	2.74 (0.36)	10.53 (0.91)	621.33 (1.99)	0.72 (0.59)	C-D

*Number in brackets denote relative standard deviation in percentage as obtained by CNLS fitting, e.g., 31.88 (0.53) means 31.88 ± 0.53%.

4.3.2.2 Static dielectric constant and relaxation time

The change of the static dielectric constant is significantly influenced by temperature, the molecular structure of the material and hydrogen bonding in the liquid [21,36,47-50]. It is apparent from table 4.6 that the concentration of n-Hexanol increases in the mixture the dielectric relaxation strength (Δε) decreases. This trend remains unaltered at 293.15, 303.15 and 313.15 K temperatures. Furthermore, it has been observed that as the mole fraction of n-Hexanol increases in the mixture, the static dielectric constant values decrease systematically in a non-linear manner at different temperatures shown in Fig.4.20. The most plausible explanation for decrease in static dielectric constant (ε_0) values with the increase in temperature is due to (i) rapid fall in orientation polarization because the increased thermal motion reduces the alignment of the permanent dipoles [51-53].

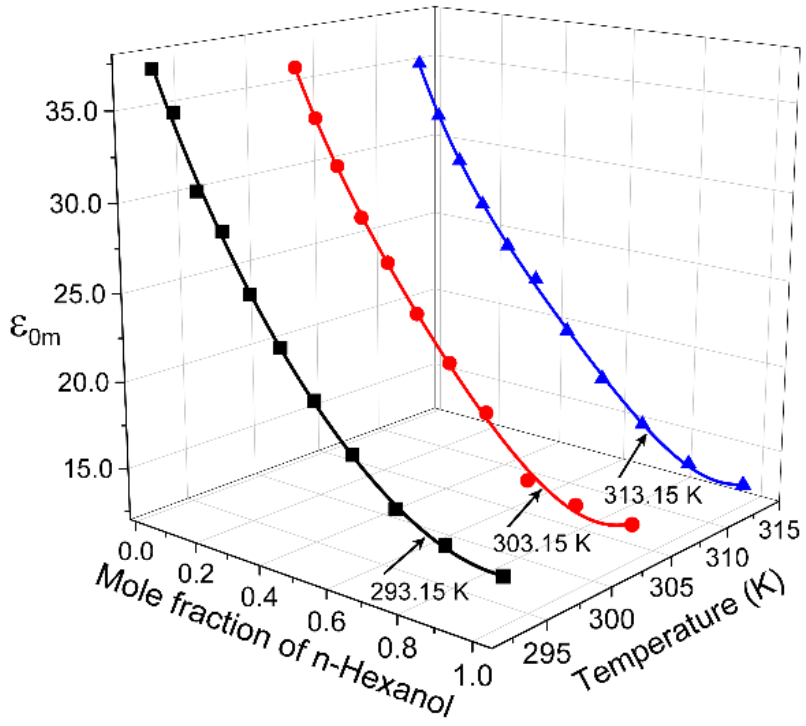

Fig.4.20 The variation of static dielectric constant (ε_{0m}) against mole fraction of n-Hexanol at different temperatures.

Table 4.6 shows the variation of relaxation time (τ) against mole fraction of n- Hexanol in the binary mixture at different temperatures. The relaxation time values increase with increases in mole fraction of n-Hexanol and decreases with increases in temperature

shown in fig.4.21. It has been observed that in the mole fraction range ($0 \leq X_1 \leq 0.5890$) the values of relaxation time increase moderately as the concentration of n-Hexanol increases in the mixture, this suggests that in the DMF rich region, the self-associated H- bonds of n-Hexanol disrupt and forms new weak H-bonds with DMF molecules due to highly polar nature of DMF. While $X1 \geq 0.5890$ the relaxation time increases rapidly due to large number n-Hexanol molecules present in the mixture moiety which unaltered the self-associated H-bonds of n-Hexanol. Similar inferences were drawn by Sengwa et al, Patil et al, Kumbharkhane et al and Ramchandran et al in their study [54-57].

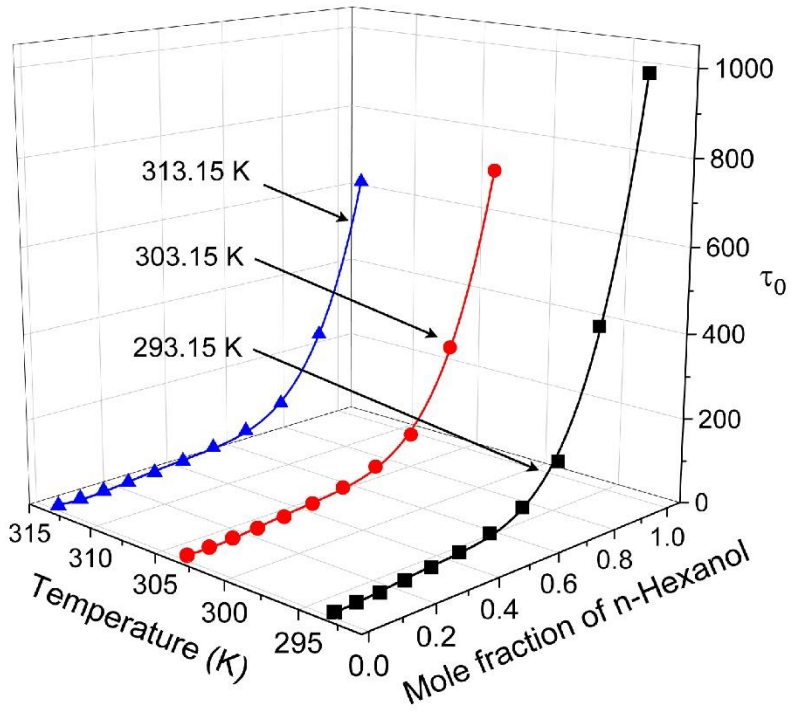

Fig.4.21 The variation of Relaxation time (τ_0) against mole fraction of n-Hexanol at different temperatures.

The excess static permittivity $(\varepsilon_0)^E$ values of the binary mixtures provide experimental evidence of the formation of complexes through H-bonds. The excess static permittivity, excess inverse relaxation time $(1/\tau)^E$ and excess high frequency limiting dielectric constant $(\varepsilon_\infty)^E$ is determined through the relation (3.20), (3.21) and (4.6) [58]. The excess high frequency limiting dielectric constant $(\varepsilon_\infty)^E$ are computed using the following relations [30]. The excess static permittivity and excess, inverse relaxation time, excess high frequency limiting dielectric constant was fitted to the Redlich-Kister equation (3.22) [59].

$$(\varepsilon_\infty)^E = (\varepsilon_\infty)_m - [(\varepsilon_\infty)_1 X_1 + (\varepsilon_\infty)_2 X_2] \quad (4.6)$$

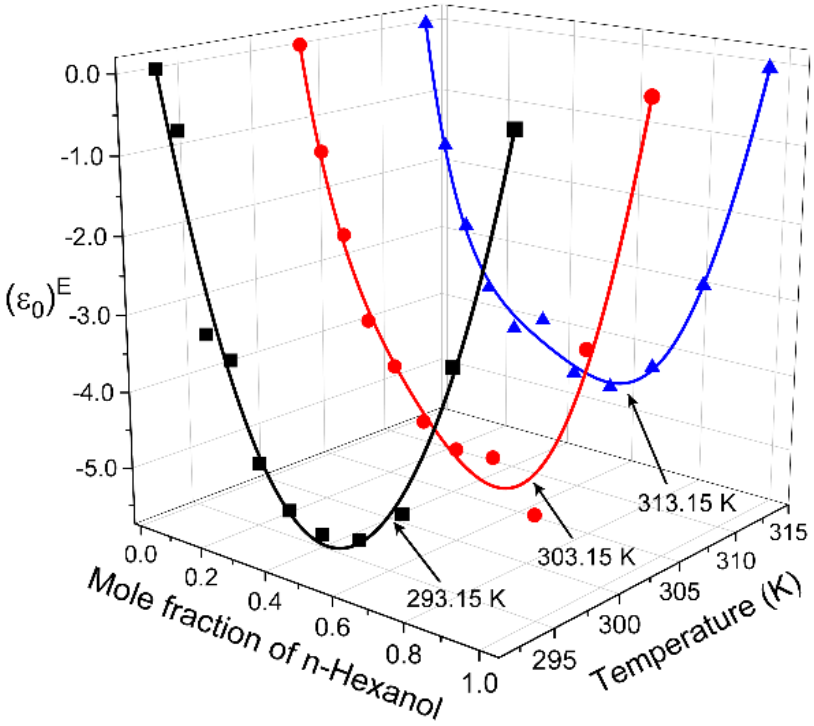

Fig. 4.22 Plot of excess dielectric constant $(\varepsilon_0)^E$ against mole fraction of n-Hexanol in binary mixtures at different temperatures.

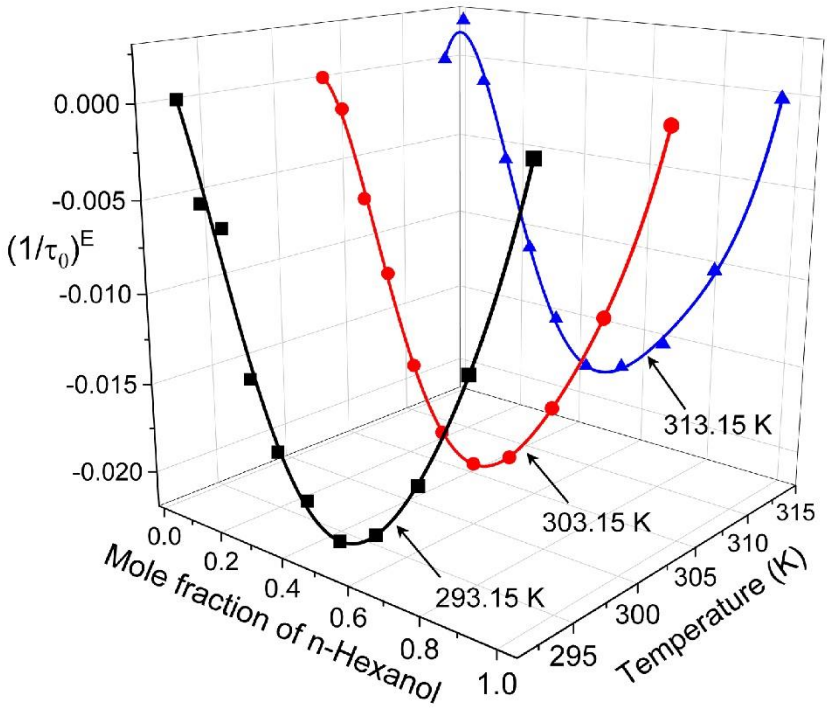

Fig. 4.23 Plot of excess inverse relaxation time $(1/\tau_0)^E$ against mole fraction of n-Hexanol in binary mixtures at different temperatures.

Figure 4.22 Shows the excess dielectric constant $(\varepsilon_0)^E$ against mole fraction of n-Hexanol in DMF binary mixtures at different temperatures. The observed that the $(\varepsilon_0)^E$ values show negative deviation over the entire mixture range, which suggests that one of the mixture constituents molecules act as 'structure-breaker' and hence there is decrease in the total number of aligned effective dipoles that contributed to the mixture dielectric polarization [21,47,48,54,60-63]. The pronounced maxima for $(\varepsilon_0)^E$ values were observed at intermediate concentration for all temperatures with different magnitudes. Further it has been observed that the pronounced maxima values $(\varepsilon_0)^E$ systematically decreases as the temperatures increases. The spectral line broadening analogy for inverse relaxation time is obtained from resonant spectroscopy, which is the inverse of relaxation time [51,64]. Figure 4.23 shows the variation of $(1/\tau_0)^E$ against mole fraction of n-Hexanol for all three temperatures. The observed excess inverse relaxation time $(1/\tau_0)^E$ values are found negative over the entire concentration range, which denotes the formation of a linear structure that rotate slowly under the influence of an external applied field [51,64,65].

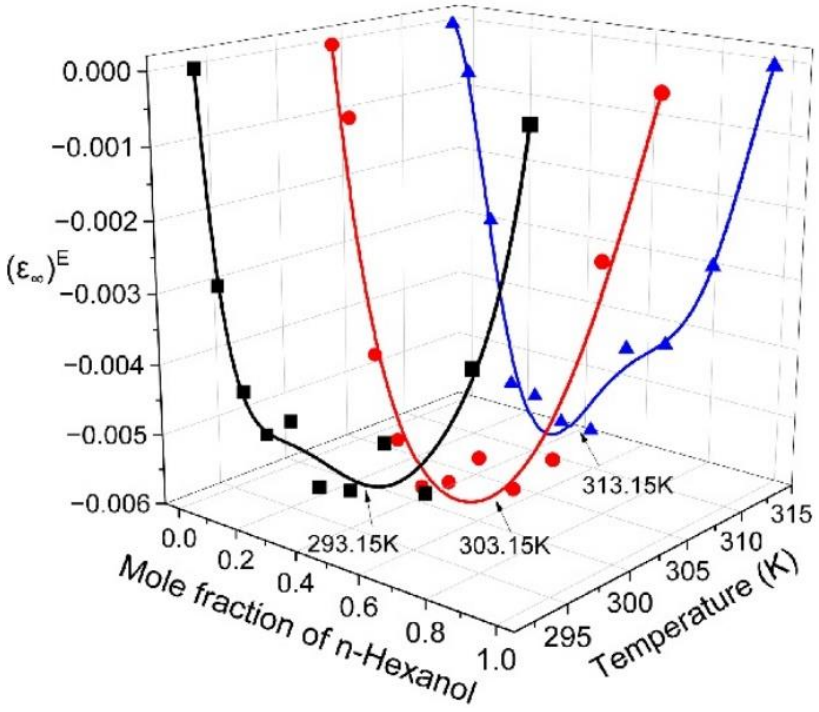

Fig. 4.24 Plot of excess high-frequency limiting dielectric constant $(\varepsilon_\infty)^E$ against mole fraction of n-Hexanol in binary mixtures at different temperatures.

Figure 4.24 illustrates the excess high-frequency limiting dielectric constant $(\varepsilon_\infty)^E$ as a function of the mole fraction of n-Hexanol at different temperatures. The negative

values of $(\varepsilon_\infty)^E$ across the entire concentration range for DMF and n-Hexanol mixtures indicate weak molecular interactions. The hydrogen-bond formation between the −OH group of n-Hexanol (proton donor) and $-CONH_2$ group of DMF (proton acceptor) alters electronic distribution within the molecules in such a way that polarization is hindered [33,34]. The experimental values of excess parameters ($(\varepsilon_0)^E$, $(1/\tau_0)^E$, $(\varepsilon_\infty)^E$) were fitted to the Redlich-Kister polynomial equation and determined values of the coefficients, correlation coefficient (R^2) and standard deviation (δ) are tabulated in table 4.7.

Table 4.7 Value of coefficients of R. K. Polynomial, correlation coefficient (R) and standard deviation (δ) for excess dielectric constant $(\varepsilon_0)^E$, excess inverse relaxation time $(1/\tau)^E$ and excess high frequency limiting dielectric constant $(\varepsilon_\infty)^E$ at different temperatures.

Excess properties	Temp. (K)	a_0	a_1	a_2	a_3	R	δ
$(\varepsilon_0)^E$	293.15	-21.8144	0.4719	-1.3697	-1.2945	0.9894	0.3634
	303.15	-20.4415	-6.5671	-7.3932	6.1362	0.9923	0.2901
	313.15	-17.8099	-3.2884	-10.6475	8.5283	0.9971	0.1510
$(1/\tau)^E$	293.15	-0.0849	-0.0074	0.0745	-0.0024	0.9940	0.0010
	303.15	-0.0815	0.0069	0.0295	-0.0482	0.9995	0.0002
	313.15	-0.0699	-0.0067	0.0503	-0.0827	0.9990	0.0003
$(\varepsilon_\infty)^E$	293.15	-0.0196	-0.0014	-0.0201	0.0184	0.9883	0.0003
	303.15	-0.0243	0.0072	-0.0060	0.0029	0.9742	0.0006
	313.15	-0.0218	0.0169	-0.0073	-0.0318	0.9862	0.0004

4.3.2.3 Kirkwood correlation factor and Bruggeman factor

Some valuable insights into dipole-dipole correlation and the orientation of electric dipoles in polar liquids can be gained using the Kirkwood correlation factor (g) [60-64]. The Kirkwood correlation parameters such as effective Kirkwood correlation factor (g^{eff}) and corrective Kirkwood correlation factor (g^f) are determined from equations (3.16) and (3.17) [47,60-64]. To determine the effective Kirkwood correlation factor (g^{eff}) and corrective Kirkwood correlation factor (g^f), the dipole moment for n-Hexanol and N,N-Dimethylformamide (DMF) are taken as 1.60 D [33] and 3.86 D [33], respectively. The determined values of effective Kirkwood correlation factor (g^{eff}) and Corrective Kirkwood correlation factor (g^f) over the entire concentration range of DMF

(0.0→1.0) at different temperatures are tabulated in Table 4.8. The temperature and concentration dependence of g^{eff} and g^{f} for the system (n-Hexanol+DMF) is shown in Fig. 4.25 and Fig. 4.26, respectively.

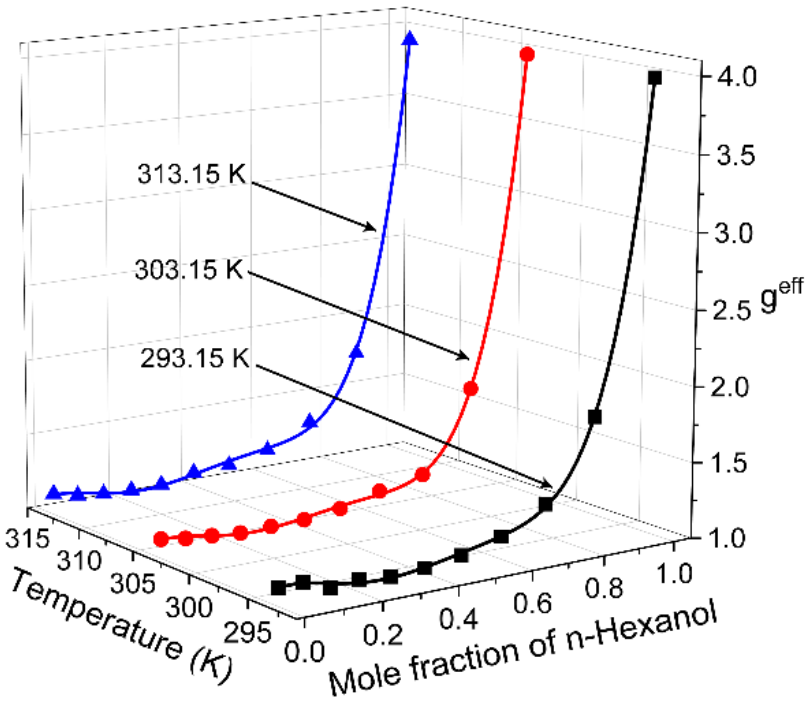

Fig. 4.25 Variation of effective Kirkwood correlation factor (g^{eff}) versus mole fraction of n-Hexanol in binary mixtures at different temperatures**.**

Figure 4.25 illustrates a non-linear relation between g^{eff} and the concentration of the n-Hexanol at all temperatures, concluding an increment in the parallel alignment of the dipoles and the formation of H-bonded structures. Furthermore, the stabilization of the active structures is achieved upon increasing the temperature due to the coordination among the electrical dipoles. The value of g^{eff} is unchanged upon addition of n-Hexanol into DMF until the mole fraction X reaches to 0.5890 in the mixture; A rapid increment in g^{eff} is observed at $X_1 \geq 0.7107$. This suggests that the number of parallel-aligned dipoles increases in the mixture with the addition of n-Hexanol to DMF. More parallel-aligned dipoles are compensated by the anti-parallel-aligned dipoles beyond the mole fraction $X_1 = 0.7107$. This trend is found to be consistent for the entire temperature range considered in the current study. The corrective Kirkwood correlation factor g^{F} is '1' for pure liquids. The dipole-dipole interaction between the two hetero molecules causes a deviation in the value of g^{F} from unity. The evaluated values of g^{F} for the liquid mixtures are observed to be less than unity at all concentrations as mentioned in the Table 4.8.

Table 4.8 Determined values of effective kirkwood correlation factor (g^{eff}) and corrective kirkwood correlation factor (g^{f}) of mixtures of n-Hexanol and DMF at various temperatures.

X_A	293.15 K	303.15 K	313.15 K
Effective Kirkwood correlation factor (g^{eff})			
0.0000	1.117	1.125	1.139
0.0639	1.117	1.101	1.100
0.1331	1.054	1.086	1.081
0.2084	1.069	1.069	1.071
0.2905	1.046	1.075	1.074
0.3805	1.057	1.078	1.118
0.4795	1.091	1.108	1.127
0.5890	1.161	1.176	1.185
0.7107	1.317	1.235	1.333
0.8468	1.830	1.765	1.766
1.0000	3.971	3.966	3.915
Corrective Kirkwood correlation factor (g^{f})			
0.0000	1.000	1.000	1.000
0.0639	0.982	0.960	0.949
0.1331	0.906	0.927	0.913
0.2084	0.894	0.888	0.882
0.2905	0.845	0.863	0.856
0.3805	0.817	0.828	0.854
0.4795	0.794	0.802	0.812
0.5890	0.775	0.782	0.787
0.7107	0.768	0.718	0.778
0.8468	0.839	0.808	0.815
1.0000	1.000	1.000	1.000

The variation of the g^F as a function of the mole fraction of n-Hexanol at different temperatures is presented in Figure 4.26. The maximum deviation of g^F from unity is observed at X_1 = 0.7107, showing high molecular interaction among the hetero molecules within the mixture at this concentration. The root of this phenomenon maybe explained with the following reasoning: there are a large number of alcohol molecules (n-Hexanol) at high concentrations which surround the DMF molecules. Thus, the voids of the clusters of alcohol molecules are occupied by these DMF molecules. And the hydrogen bonding between the two hetero molecules is enabled due to the role of alcohol molecules as proton donors. As a result, owing to the formation of multimers

and the reduction of the parallel-aligned electric dipoles there is a large dipole-dipole interaction in the binary mixtures.

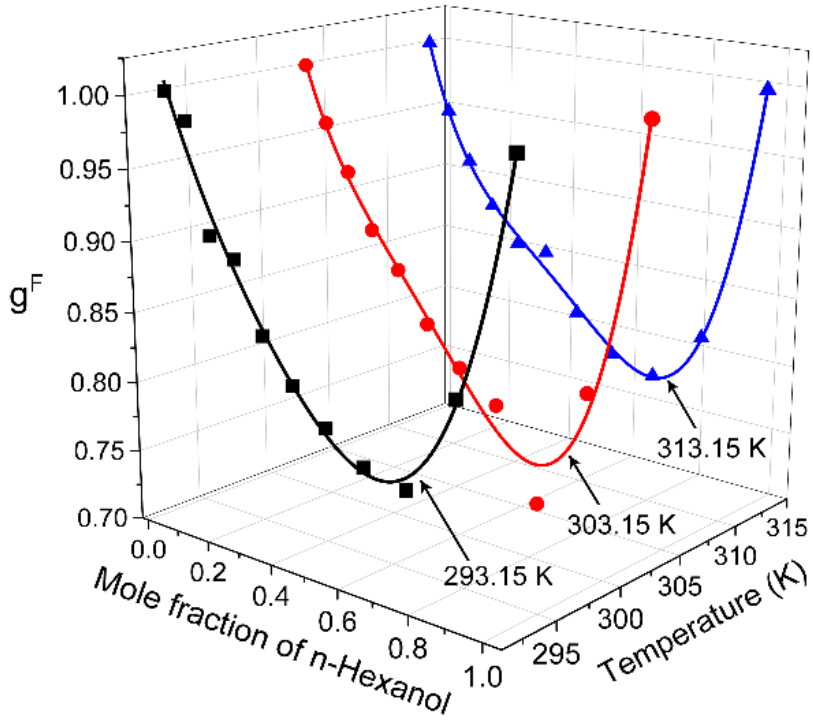

Fig. 4.26 Variation of corrective Kirkwood correlation factor (g^f) versus mole fraction of n-Hexanol in binary mixtures at different temperatures.

The Bruggeman parameter (f_B), provides information on the interaction that occurs between the participating components of the mixture [36,47,67,68]. The Bruggeman parameter (f_B) and modified are determined from equations (3.18) [68]. Despite the linear relationship expected by Equation 3.18, the experimental f_B values for the binary system display deviations. Hence, to accurately account for these deviations, the experimental data underwent fitting using a modified Bruggeman model [68].

$$f_B = 1 - [a - (a - 1)\Phi_2]\Phi_2 \quad (4.7)$$

where a is a numerical fitting parameter that represents a change in molecular orientation and quantifies the degree to which the binary mixture's polar liquid components interact through dipoles in terms of molecular size and volume. The value A numerical fitting parameter of a = 1 indicates the ideal Bruggeman mixture formula, while deviations from linearity suggest molecular interactions among the components. Figure 4.27 illustrates the plot of the Bruggeman factor (f_B) against the volume fraction of n-Hexanol at varying temperatures, highlighting the influence of temperature on molecular interactions within the system. It has been observed that the values of 'a" founds to be greater than unity at all temperatures and ('a' = 1.2295, a= 1.2182 and a=

1.1376 at 293.15 K, 303.15K, 313.15K respectively). This suggests that the as the concentration of n-Hexanol increase while mixing the effective volume of the binary mixture (n-Hexanol + DMF) increases. Similar inference was drawn by many researches in their study.

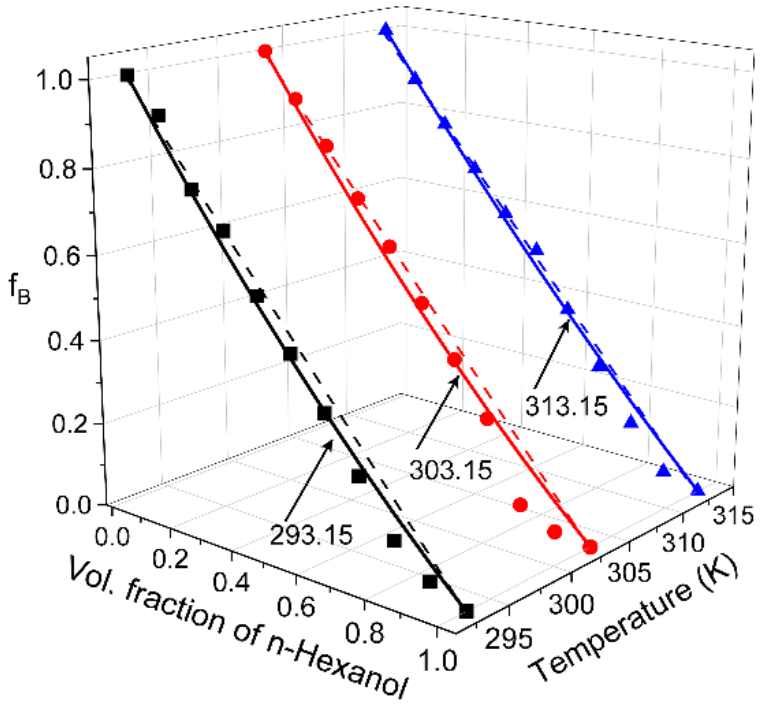

Fig. 4.27 Plot of Bruggeman factor (f_B) against mole fraction of n-Hexanol in binary mixtures at different temperatures.

4.3.2.4. Thermodynamical parameters

To analyze the orientational dynamics using thermodynamic parameters, the dipolar relaxation process is approached as a chemical rate process [69,70]. In this process, it is assumed that molecules transition between equilibrium states based on: (I) the frequency of collisions between neighboring molecules, (II) the local structural arrangement of the medium during dipole orientation, and (III) the potential energy barrier between two equilibrium positions [71]. Dielectric relaxation process can be understood of as the dipole rotating between two equilibrium positions separated by a potential barrier. The dielectric relaxation time (τ_0), depends on the height of the potential barrier, a constant that changes with temperature, and the average time it takes for an excited molecule to move from one equilibrium position to the other [72]. According to Eyring dielectric relaxation is related to the chemical rate theory using determined change in activation energy (ΔFe, ΔHe, ΔSe) eq. (3.24) and (3.25) [73-76].

Table 4.9 The table shows the values of the thermodynamic parameters for mixtures of n-Hexanol and N, N-Dimethylformamide (DMF).

X_1	ΔFe (K. J. mol^{-1})			ΔSe (J. K^{-1}.mol^{-1})			ΔHe (K. J. mol^{-1})
	293.15 K	303.15 K	313.15 K	293.15 K	303.15 K	313.15 K	
0.0000	10.649	11.006	11.407	-37.861	-37.788	-37.863	-0.450
0.0639	10.992	11.225	11.493	-34.517	-34.146	-33.912	0.873
0.1331	11.233	11.607	11.810	-36.076	-36.119	-35.613	0.658
0.2084	11.845	12.041	12.237	-35.432	-34.908	-34.421	1.458
0.2905	12.411	12.655	12.812	-37.015	-36.599	-35.930	1.560
0.3805	13.079	13.394	13.517	-39.212	-38.956	-38.107	1.584
0.4795	14.015	14.263	14.398	-40.978	-40.447	-39.586	2.002
0.5890	15.151	15.322	15.396	-42.269	-41.440	-40.351	2.760
0.7107	16.741	16.690	16.893	-45.242	-43.582	-42.839	3.478
0.8468	19.238	19.056	19.283	-50.418	-48.152	-47.341	4.458
1.0000	21.211	21.189	21.630	-60.001	-57.951	-57.506	3.621

Using the eq. 3.24 and 3.25 the determined values of activation energy ((ΔFe), enthalpy of activation (ΔHe) and entropy of activation (ΔSe) over the entire concentration range of DMF (0.0→1.0) at different temperatures are tabulated in Table 4.9. Observations from table 4.9 suggest that the activation energy (ΔFe) decreases with increasing mole fraction of n-Hexanol, indicating a trend where higher concentrations of n-Hexanol promote the formation of hydrogen-bonded networks between DMF and n-Hexanol. This results in larger effective sizes of rotating dipoles and heightened dielectric frictional force between them. Negative values of entropy of activation (ΔSe) are observed, which stem from cooperative molecular orientation likely caused by steric forces or parallel alignment of dipoles involved in dipole–dipole interactions. Positive values of enthalpy of activation (ΔHe), especially noticeable at higher mole fractions of n-Hexanol (X1 ≥ 0.0639), indicate an endoergic reaction involving heat absorption. This absorption of energy is attributed to the formation of hydrogen bonds, leading to the conversion of monomers into multimers and increased orderliness within the system, consequently resulting in cooperative molecular orientation.

4.3.2.5. Microwave heating parameters

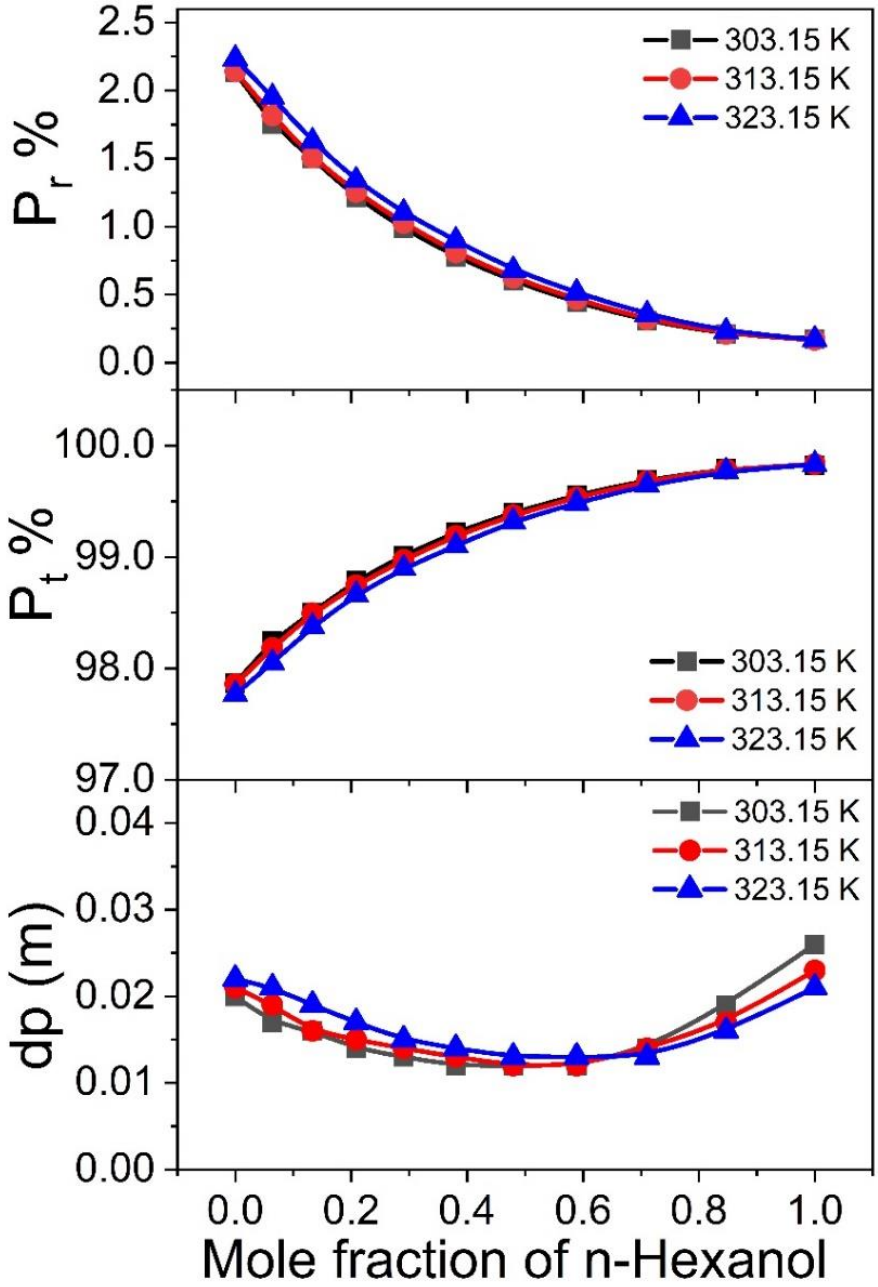

Fig. 4.28 Variation of power reflected (P_r), power transmitted (P_t) and penetration depth (d_p) against mole fraction of n-Hexanol in binary mixtures at different temperatures.

The microwave frequency 2.45 GHz is chosen for industrial use to prevent interference with frequencies crucial for telecommunications, military, and navigation applications. The microwave heating parameters like penetration depth (dp), power reflected (Pr) and power transmitted (Pt) are determined from the observed values of dielectric constant (ε′) and dielectric loss (ε′′) at 2.45 GHz frequency using determined eq. (3.26), (3.27), (3.28) [77,78].

Penetration depth (dp) is a critical parameter that defines the extent to which heat is uniformly dissipated within a material [79]. When electromagnetic radiation interacts with a material's surface, a portion of the energy is reflected, while the remaining energy is transmitted into the material. The ability of the electromagnetic field to penetrate the material depends on its properties, with the field potentially extending deep into the material. Penetration depth characterizes the rate at which the electromagnetic wave diminishes inside the material. For effective electromagnetic heating, it is essential that the energy penetrates deeply; otherwise, heating remains confined to the surface, leading to uneven drying [80]. The variation of power reflected, power transmitted and penetration depth at different temperature against mole fraction of n-Hexanol are shown in fig. 4.28 (a), (b), (c). It has been observed that there is no appreciable change in power reflected and power transmitted values at different temperatures. The penetration depth shows significant change against temperatures and concentration of n-Hexanol in the binary mixtures. The penetration depth (d_p) at the intermediate concentration is lower than its average values.

4.4 Conclusion

- This study explores the concentration-dependent dielectric and electrical properties of n-Hexanol, N, N-Dimethylformamide (DMF), and their binary mixtures within the frequency range of 20 Hz to 2 MHz at different temperatures (293.15K, 303.15 K, 313.15K).
- The lower frequency complex dielectric behavior is mainly governed by ionic conduction and electrode polarization phenomena of concentration dependent behavior are observed in the ionic conduction and electrode polarization processes within the studied binary mixtures.
- In the low frequency region, ionic conduction and electrode polarization have a dominant influence, leading to the large values of dielectric constant (ε') and dielectric loss (ε'') in the mixtures.
- The loss tangent peak systematically shift for all the binary mixtures.
- Experimentally determined values of complex permittivity of mixtures of n-Hexanol+1-DMF can very well be fitted into the Cole–Cole model (with α values ≈ 1) for all concentration, in which EP is represented by a simple Debye relaxation.
- The experimental complex permittivity values align well with the Cole-Cole model. Evaluated values of Electrode polarization relaxation time (τ_{EP}),

relaxation time (τ'_{EP}) and ionic relaxation time (τ_σ) are using various formalisms to demonstrate good agreement with experimental values of ε''.

- The M′ spectra show a dispersion in the frequency region between f_{EP}' and fσ frequencies.
- M" spectra show a peak in the intermediate frequency region and peak is shifted to the lower frequency as the concentration of DMF increases.
- Complex modulus spectra show a Debye tyle semicircular arc for all the concentration range.
- Complex impedance data is fitted to the equivalent circuit model to obtain six different components. Equivalent circuit elements signify various electrical processes in the bulk sample as well as at the electrode surface and are confirmed by the Bode plot analysis of the complex impedance data.
- Z″ spectra exhibit EDL and ionic relaxation processes in the considered frequency region while tan δ, M" and σ" exhibit either EDL process or ionic relaxation process.
- The complex permittivity data of n-Hexanol, DMF and their mixtures have been obtained for different concentration (0.0→1.0) and temperature (293.15 K, 303.15K, 313.15K) in frequency 200 MHz and 20 GHz.
- The complex permittivity spectra in the frequency range 200 MHz to 20 kHz could be well fitted to Cole-Cole/Debye model for all binary mixtures of n-Hexanol and DMF at different temperatures.
- The study evaluates a range of dielectric properties, including static dielectric constant, high frequency dielectric constant, relaxation time, Kirkwood correlation factor, Bruggeman factor, and excess dielectric properties such as excess static permittivity and excess inverse relaxation time, across various temperatures and mole fractions of n-Hexanol for the binary mixtures.
- The formation and strength of complexes in the mixtures, attributed to heteromolecular interactions between participating molecules, are revealed through changes in these parameters with varying concentrations of n-Hexanol.
- Nonlinear trends in static dielectric constant, high-frequency dielectric constant, and relaxation time with increasing mole fraction of n-Hexanol suggest significant intermolecular interactions.

- In DMF-rich mixtures, the effective dipole moments rotate slowly, while in n-Hexanol-rich regions, dipole rotation occurs rapidly. In the studied binary system (n-Hexanol + DMF) show deviation in Bruggeman parameter from linearity indicating deviation in the static dielectric constant value at different concentrations from normal mixture values resulting molecular interaction between dissimilar molecular species.
- Activation energy, enthalpy of activation, and entropy of activation have been calculated and reported for n-Hexanol, DMF, and their binary mixtures across the range of studied temperatures, providing insights into the energy requirements and thermodynamic aspects of the systems.
- Microwave heating parameters, namely reflected power (Pr), transmitted power (Pt), and penetration depth (Dp), have been determined, offering valuable information for understanding the efficiency and behavior of microwave heating in these mixtures.

References

[1] H. P. Vankar, V. A. Rana, Electrode polarization and ionic conduction relaxation in mixtures of 3-bromoanisole and 1-propanol in the frequency range of 20 Hz to 2 MHz at different temperatures. J. Mol. Liq. 254 (2018) 216-225.

[2] J. Swiergiel, J. Jadzyn, Conductivity Dynamics and Static Dielectric Permittivity of Highly Conducting Molecular Liquids Studied with Impedance Spectroscopy. Formamides. J. Phys. Chem. B 113 (2009)14225-14228.

[3] V. A. Rana, T. R. Pandit, Dielectric spectroscopic and molecular dynamic study of aqueous solutions of paracetamol. J. Mol. Liq. 290 (2019) 111203.

[4] R. J. Sengwa, S. Sankhla, Dielectric Dispersion Study of Poly (vinyl Pyrrolidone)–Polar Solvent Solutions in the Frequency Range 20 Hz–1 MHz. J. Macromol. Sci. Phys 46 (2007) 717-747.

[5] R. J. Sengwa, S. Sankhla, Characterization of solvent effect on low-frequency dielectric dispersion and relaxation behaviour of ethylene glycol oligomers. J. Mol. Liq. 141 (2008) 73-93.

[6] N. Shinyashiki, R. J. Sengwa, S. Tsubotani, H. Nakamura, S. Sudo, S. Yagihara, Broadband Dielectric Study of Dynamics of Poly (vinyl pyrrolidone)-Ethylene Glycol Oligomer Blends. J. Phys. Chem 110 (2006) 4953-4957.

[7] R. J. Sengwa, S. Choudhary, A. Bald, Dielectric dispersion and electric relaxation processes induced by ionic conduction in formamide, 2-aminoethanol and their binary mixtures. J. Solut. Chem 42 (2013)1960-1975.

[8] A. N. Prajapati, V. A. Rana, A. D. Vyas, S. P. Bhatanagar, D. H. Gadani, Dielectric studies of binary mixtures of 1-propanol and fluorobenzene. Solid State Phenom 209 (2014) 203-206.

[9] J. Jadzyn, J. Swiergiel On intermolecular dipolar coupling in two strongly polar liquids: dimethyl sulfoxide and acetonitrile. J. Phys. Chem. B 115 (2011) 6623-6628.

[10] R. J. Sengwa, S. Choudhary, P. Dhatarwal, Characterization of relaxation processes over static permittivity frequency regime and compliance of the Stokes-Einstein Nernst relation in propylene carbonate. J. Mol. Liq. 225 (2017) 42-49.

[11] H. A. Chaube, V. A. Rana, Dielectric and electrical properties of binary mixtures of anisole and some primary alcohols in the frequency range 20 Hz to 2 MHz. Adv. Mater. Res 665 (2013) 194-201.

[12] S. Choudhary, P. Dhatarwal, R. J. Sengwa, Characterization of conductivity relaxation processes induced by charge dynamics and hydrogen-bond molecular interactions in binary mixtures of propylene carbonate with acetonitrile. J. Mol. Liq. 231 (2017) 491- 498.

[13] W. G. Scaife, The natural electrical conductivity of organic liquids subjected to hydrostatic pressures. J. Phys. D Appl. Phys. 7(4) (1974) 647.

[14] S. Choudhary, R. J. Sengwa, Characterization of dielectric dispersion and ionic conduction behaviour of acetonitrile at low frequencies. Indian J. Pure Appl. Phys. 50 (2012) 411-414.

[15] A. Marchetti, C. Preti, M. Tagliazucchi, L. Tassi, G. Tosi, The N, N-dimethylformamide + ethane-1,2-diol solvent system. Dielectric constant, refractive index, and related properties at various temperatures. J. Chem. Eng. Data 36(4) (1991) 365–368.

[16] C. M. Trivedi, V. A. Rana, Static permittivity, refractive index, density and related properties of binary mixtures of pyridine and 1-propanol at different temperatures. Indian J. Pure Appl. Phys. 52 (2014) 183-191.

[17] F. Corradini, L. Marcheselli, L. Tassi, G. Tosi, Static dielectric constants of the N, N-dimethylformamide/2-methoxyethanol solvent system at various temperatures. Can. J. Chem 70 (1992) 2895-2899.

[18] H. Yaman, B. Dogan, M. K. Yesilyurt, D. Erol, Application of Higher-Order Alcohols (1-Hexanol-C6 and 1-Heptanol-C7) in a Spark-Ignition Engine: Analysis and Assessment. Arab. J. Sci. Eng 46(12) (2021) 11937-11961.

[19] R. J. Sengwa, V. Khatri, S. Sankhla, Static Dielectric Constants and Kirkwood Correlation Factor of the Binary Mixtures of N-Methylformamide with Formamide, N, N-Dimethylformamide and N, N-Dimethylacetamide. J. Sol. Chem 38 (2009) 763-769.

[20] H. N. Thorat, A. Murugkar, Thermo-acoustical properties of carbamide and N, N-dimethylformamide binary mixture at different temperatures. Indian J. Pure Appl. Phys 58 (2020) 141-146.

[21] A. N. Prajapati, S.P. Patel, V.A. Rana, Study of short range and long range molecular interactions in binary liquid mixtures of N, N-dimethylformamide (DMF) and 1-propanol, J. Mol. Liq. 354 (2022) 118832-118839.

[22] J. Bao, M. L. Swicord, C. C. Davis, Microwave dielectric characterization of binary mixtures of water, methanol, and ethanol, J. Chem. Phys. 104 (1996) 4441-4450.

[23] M. N. Afsar, J. R. Birch, R. N. Clarke, G.W. Chantry, The measurement of the properties of materials, Proc. IEEE. 74 (1986) 183–199.

[24] R. J. Sengwa, S. Choudhary, P. Dhatarwal, Dielectric and electrical behaviour over the static permittivity frequency regime, the refractive indices and viscosities of PC– PEG binary mixtures, J. Mol. Liq. 252 (2018) 339–350

[25] S.B. Kolhe, P.B. Undre, V.P. Deshpande, P.W. Khirade, Dielectric characterization and molecular interaction behaviour in binary mixtures of methyl acetate with 1- butanol and 1-pentanol, (2019).

[26] A. Mohan, M. Malathi, Dielectric Relaxation and Thermodynamic Studies of Binary Mixtures of 2-Nitrotoluene with Primary and Secondary Alcohols at Different Temperatures, J. Solution Chem. 47 (2018) 667–683.

[27] H. A. Chaube, V.A. Rana, P. Hudge, A.C. Kumbharkhane, Dielectric relaxation studies of binary mixture of diethylene glycol mono phenyl ether and methanol by Time Domain Reflectometry, J. Mol. Liq. 211 (2015) 346–352.

[28] L. S. Gabrielyan, S. A. Markarian, H. Weingärtner, Dielectric spectroscopy of dimethylsulfone solutions in water and dimethylsulfoxide, J. Mol. Liq. 194 (2014) 37–40.

[29] R. Hilfer, Fitting the excess wing in the dielectric α-relaxation of propylene carbonate, J. Phys. Condens. Matter. 14 (2002) 2297–2301.

[30] V. A. Rana, H. A. Chaube, Static permittivity, density, viscosity and refractive index of binary mixtures of anisole with 1-butanol and 1-heptanol at different temperatures, J. Mol. Liq. 173 (2012) 71–76.

[31] S. Manual, Agilent 16452A Liquid Test Fixture Operation and Service Manual, ReVision. 2015 (2007) 1–29.

[32] SPEAG, Dielectric Assessment Kit (DAK) Professional Handbook, 2.2 (2017).

[33] D. R. Lide. CRC Handbook of Chemistry and Physics 90th Edition CD-ROM. CRC Press 2009-2010.

[34] V. A. Rana, H. A. Chaube, Relative permittivity, density, viscosity, refractive index and ultrasonic velocity of binary mixture of ethylene glycol monophenyl ether and 1-hexanol at different temperatures, J. Mol. Liq. 187 (2013) 66-73.

[35] C. Wohlfarth, Static Dielectric Constants of Pure Liquids and Binary Liquid Mixtures, Supplement to Volume IV/17,book (2015).

[36] A. V. Navarkhele, R. S. Sakhare, S. M. Vijayendraswamy, V. V. Navarkhele, Dielectric Constant, Density, and Refractive Index in Binary Mixtures of Ethanol with N, N- imethylformamide at 293.15 K, Russian Journal of Physical Chemistry A 96 (5) (2022) 945-953.

[37] I. Płowass, J. Swiergiel, J. Jadzyn, Relative static permittivity of dimethyl sulfoxide+ water mixtures, J. Chem. Eng. Data. 58 (2013) 1741–1746.

[38] K. S. Cole, R. H. Cole, Dispersion and absorption in dielectrics I. Alternating current characteristics. J. Chem. Phys. 9 (1941) 341–351.

[39] S. Havriliak, S. Negami, A complex plane analysis of α-dispersions in some polymer systems, in: J. Polym. Sci. Part C Polym. Symp., Wiley Online Library.14 (1966) 99-117.

[40] H. P. Vankar, V. A. Rana, S. Dey, H. D. Patel, V. K. Jain, Molecular interaction in binary mixtures of 3-Bromoanisole and methanol: A microwave dielectric relaxation spectroscopy and molecular dynamic simulation study. J Mol Liq 325 (2021) 115186.

[41] R. J. Sengwa, S. Sankhla, Characterization of ionic conduction and electrode polarization relaxation processes in ethylene glycol oligomers, Polym. Bull. 60 (2008) 689–700.

[42] R. J. Sengwa, S. Choudhary, S. Sankhla, Low frequency dielectric relaxation processes and ionic conductivity of montmorillonite clay nanoparticles colloidal suspension in poly (vinyl pyrrolidone)-ethylene glycol blends, Express Polym. Lett. 2 (2008) 800–809.

[43] K. N. Shah, V. A. Rana, Dielectric spectroscopic study of solutions of amino silicone oil in the polar solvent mixtures of methyl ethyl ketone and methyl iso butyl ketone. J Mol Liq. 288 (2019) 111078.

[44] V. A. Rana, K. N. Shah, H. P. Vankar, C. M. Trivedi, Dielectric spectroscopic study of the binary mixtures of amino silicone oil and methyl ethyl ketone in the frequency range of 100Hz to 2MHz at 298.15K temperature. J Mol Liq. 271 (2018) 686-695.

[45] S. Ramesh, A. K. Arof, Ionic conductivity studies of plasticized poly (vinyl chloride) polymer electrolytes. Mater. Sci. Eng. B. 85(2001) 11-15.

[46] M. Mozurkewich, S.W. Benson, Negative activation energies and curved Arrhenius plots. 1. Theory of reactions over potential wells, J. Phys. Chem. 88 (1984) 6429– 6435.

[47] A. N. Prajapati, V. A. Rana, A. D. Vyas, S. P. Bhatnagar, Study of heterogeneous interaction through dielectric properties of binary mixtures of fluorobenzene with methanol, In. J. of Pure and Appl. Phys. 49 (2011) 478–482.

[48] R. J. Sengwa, V. Khatri, S. Sankhla, Dielectric properties and hydrogen bonding interaction behaviour in binary mixtures of glycerol with amides and amines, Fluid Phase Equilb. 266 (2008) 54-58.

[49] R. J. Sengwa, V. Khatri, S. Sankhla, Static dielectric constant, excess dielectric properties, and Kirkwood correlation factor of water-amides and water -amines binary mixtures, Proc. Indian Nat. Sci. Acad. 74 (2008) 67-72.

[50] A. N. Prajapati, Dielectric study of binary mixtures of 1-butanol with N, N Dimethylformamide, AIP Conf. Proc. 2220 (2020) 0400301-400304.

[51] C. V. V. Ramana, A. B. V. Kiran Kumar, A. Satya Kumar, M. Ashok Kumar, M.K. Moodley, Dielectric and excess dielectric constants in non-polar + polar binary liquid mixtures of toluene with alcohols at 303, 313 and 323 K, Thermochim. Acta 566 (2013) 130-136.

[52] A. Rodrıguez, J. Canosa, J. Tojo, Physical Properties of Binary Mixtures (Dimethyl Carbonate + Alcohols) at Several Temperatures, J. Chem. Eng. Data 46 (2001) 1476-1486.

[53] K. Ramachandran, P. Sivagurunathan, K. Dharmalingam, S. Mehrotra, Dielectric Relaxation Study of Amide-Alcohol Mixtures by Using Time Domain Reflectometry, Acta Phys. Chim. Sin. 23 (10) (2007) 1508-1515.

[54] R. J. Sengwa, S. Choudhary, V. Khatri, Microwave dielectric spectra and molecular relaxation in formamide-N, N-dimethylformamide binary mixtures, Spectrochimica Acta Part A: Molecular and Biomolecular Spectroscopy 82 (2011) 279-282.

[55] D. Balamurugan, S. Kumar, Krishnan, S. Dielectric relaxation studies of higher order alcohol complexes with amines using time domain reflectometry, J. Mol. Liq. 122 (2005) 11-14.

[56] F. A. Saif, P. B. Undre, S.A. Yaseen, A.S. Alameen, S. S. Patil, P.W. Khirade, Hydrogen Bonding Interaction between Amide and Alcohols: Dielectric Relaxation and FTIR Study, Integrated Ferroelectrics 202 (1) (2019) 79-88.

[57] S. P. Patel, A.N. Prajapati, Dielectric properties of binary liquid mixtures Winkelmann-Quitzsch approach, AIP Conf. Proc. 2220 (2020) 0400181-400184.

[58] R.J. Sengwa, V. Khatri, S. Sankhla, Dielectric behaviour and hydrogen bond molecular interaction study of formamide-dipolar solvents binary mixtures, J. Mol. Liq. 144 (2009) 89–96.

[59] O. Redlich, A.T. Kister, Algebraic representation of thermodynamic properties and the classification of solutions, Ind. Eng. Chem. 40 (1948) 345–348.

[60] R. J. Sengwa, Madhvi, S. Sankhla, S. Sharma, Characterization of heterogeneous interaction behaviour in ternary mixtures by a dielectric analysis: equi-molar H-bonded binary polar mixtures in aqueous solutions, Journal of Solution Chem. 35 (2006) 1037-1055.

[61] R. J. Sengwa, S. Sankhla, Dielectric properties of binary and ternary mixtures of alcohols: analysis of H-bonded interaction in complex systems, J. Non Cryst. Solids. 353 (2007) 4570-4574.

[62] R. J. Sengwa, S. Sankhla, N. Shinyashiki, Dielectric parameters and hydrogen bond interaction study of binary alcohol mixtures, J. Sol. Chem. 37 (2008) 137-153.

[63] V. P. Pawar, Dielectric relaxation of propanol with chlorobenzene, 1,2-dichloroethane, and dimethyl chloride at (288, 298, 308, and 318) K using time-domain reflectometry technique, J. Chem. Eng. Data 51 (2006) 882-885.

[64] R. J. Sengwa, V. Khatri, S. Sankhla, Static dielectric constant, excess dielectric properties, and Kirkwood correlation factor of water-amides and water -amines binary mixtures, Proc. Indian Nat. Sci. Acad. 74 (2008) 67-72.

[65] X. Liao, G. S. V. Raghavan, V. A. Yaylayan, Dielectric properties of alcohols (C1-C5) at 2450 MHz and 915 MHz, J. Mol. Liq. 94 (2001) 51-60.

[66] R. J. Sengwa, Madhvi, S. Sankhla, H-bonded molecular interaction study on binary mixtures of mono alkyl ethers of ethylene glycol with different polar solvents by concentration dependent dielectric analysis, Phys. Chem. Liq. 44 (2006) 637–653.

[67] S. A. Ingole, A.R. Deshmukh, R.V. Shinde, A. C. Kumbharkhane, Dielectric relaxation study of aqueous tetraethylene glycol using time domain reflectometry technique in the frequency range 10 MHz to 50 GHz, J. Mol. Liq. 272 (2018) 450-455.

[68] A. N. Prajapati, A. D. Vyas, V. A. Rana and S. P. Bhatnagar, Dielectric relaxation and dispersion studies of mixtures of 1-propanol and benzonitrile in pure liquid state at radio and microwave frequencies, J. Mol. Liq. 151 (2010) 12-16.

[69] S. Glasstone, K.J. Laidler, H. Eyring, The theory of rate processes, McGraw-Chapter 4 Department of Physics, Gujarat University 166 hill, 1941.

[70] J. Lou, A.K. Paravastu, P.E. Laibinis, T.A. Hatton, Effect of temperature on the dielectric relaxation in solvent mixtures at microwave frequencies, J. Phys. Chem. A. 101 (1997) 9892–9899.

[71] A. Mohan, M. Malathi, A.C. Kumbharkhane, Microwave dielectric relaxation spectroscopy studies on associative polar binary mixtures of nitrobenzene with primary alcohols, J. Mol. Liq. 222 (2016) 640–647.

[72] M. T. Hosamani, N. H. Ayachit, D.K. Deshpande, Activation energy (DG), enthalpy (DH), and entropy (DS) of some indoles and certain of their binary mixtures, J. of Ther. Anal. and Cal. 107 (2012) 1301-1306.

[73] S. S. Birajdar, A. C. Kumbharkhane, S. N. Hallambe, P. G. Hudge, D. B. Suryawanshi, Thermodynamic and Dielectric Properties of Cyclohexanol-Xylene Binary Mixtures Using Dielectric Spectroscopy, Poly. Aro. Comp. 43 (2022) 1619-1627.

[74] C. V. Maridevarmath, G. H. Malimath, Studies on the effect of temperature on dielectric relaxation, activation energy (ΔG*), enthalpy (ΔH*), entropy (ΔS*) and molecular interactions of some anilines, phenol and their binary mixtures using X-band microwave bench, J. Chem. Therm. 144 (2020) 166068-166074.

[75] G. Parthipan, P. Anandan, An investigation on molecular dynamics of binary mixtures of anisole and isobutanol in benzene at 303, 313 and 323 K, J. Non-Crys. Sol. 356 (2010) 1721–1724.

[76] A. N. Prajapati, A. D. Vyas and V. A. Rana, Dielectric dispersion studies of mixtures of aniline and benzonitrile in benzene solutions, J. Mol. Liq. 144 (2009) 1- 4.

[77] V. A. Rana, T. R. Pandit, Microwave dielectric relaxation spectroscopy of paracetamol and its aqueous solutions, J. Mol. Liq. 314 (2020) 113673.

[78] Y. Tao, B. Yan, D. Fan, N. Zhang, S. Ma, L. Wang, Y. Wu, M. Wang, J. Zhao, H. Zhang, Structural changes of starch subjected to microwave heating: A review from the perspective of dielectric properties, Tren. in Food Sci. & Tech., 99 (2020) 593-607.

[79] M. K. Ndife, G. Şumnu, L. Bayindirli, Dielectric properties of six different species of starch at 2450 MHz, Food Res. Int. 31 (1998) 43-52.

[80] G. M. Walker, T. R. A. Magee, C. R. Holland, M. N. Ahmad, J. N. Fox, N. A. Moffatt, A. G. Kells, Caking processes in granular NPK fertilizer, Ind. Eng. Chem. Res. 37 (1998) 435-438.